Development of smart vibration shaker plate instrumented with piezoelectric patches where some of the vibration modes are simultaneously tracked

Final report

Submitted to the

UGC

2019

by

Professor Manu Sharma

UNIVERSITY INSTITUTE OF ENGINEERING & TECHNOLOGY
PANJAB UNIVERSITY, CHANDIGARH –160014
INDIA

Acknowledgements

I would like to hereby thank University Grants Commision for providing financial support to this project. Support given by UIET Panjab University Chandigarh for carrying out this project is also deeply acknowledged. My PhD student Dr. Behrouj Kheiri (Iranian national) has actually executed this project under joint supervision of me and Dr. Damanjeet Kaur. Would like this opportunity to thank Dr. Behrouj Kheiri for completing this project successfully.

Dr. Manu Sharma

I dedicate this work to my Nation.

Abstract

The area of vibration control is evolving rapidly primarily due to high demand of low weight structures in automobile sector. To ensure that vibration control happens efficiently when the product is in field, vibration testing of product is required in a laboratory in an environment that resembles that of field. In this study, a novel technique is presented for generating desired transient vibrations in a test plate structure.

For this, first three vibration modes of a cantilevered plate have been simultaneously made to track reference curves. Cantilevered plate structure is instrumented with one piezoelectric sensor patch and one piezoelectric actuator patch. Quadrilateral plate finite element having three degrees of freedom at each node (two rotations and one flexural displacement) is employed to divide the plate into finite elements. Thereafter, Hamilton's principle is used to derive equations of motion of the smart plate. In Hamilton's principle kinetic energy, potential energy and work expressions of a single finite element of smart plate are substituted. Variations with respect to displacement vector are taken to derive mass matrix, stiffness matrix and force vector of finite element model. Finite element model of structure is reduced to first three modes using orthonormal modal truncation and subsequently the reduced finite element model is converted into a state-space model. Optimal tracking control is then applied on the state-space model of the smart plate. Optimal control law optimizes a performance index which results in minimization of difference between actual trajectories and reference trajectories using minimal control effort. Feedback gain and feedforward gains of controller are calculated offline by solving a Riccati equation. Using this optimal controller, cantilevered plate is made to vibrate as per desired decay curves of first three modes.

Simulation results show that presented optimal control strategy is very effective in simultaneously tracking first three vibration modes of the smart plate. Theoretical findings are verified by conducting experiments. For experimentation, Kalman observer is used to estimate first three modes and Labview software is used for

interfacing intelligent plate to the host PC. Presented strategy can be used to do dynamic vibration testing of a product by forcing the product to experience same transient vibrations that it is expected to experience while in field.

List of publications

A. **Journal papers:**

1. B. Kheiri, M. Sharma & D. Kaur, "Simulation of a New Technique for Vibration Tests, Based upon Active Vibration Control", *IETE journal of research (Taylor & Francis)*, Vol. 62, No. 5, 2016, **(SCI indexed journal)**
2. B. Kheiri, M. Sharma, D. Kaur & N. Kumar, "A novel technique for generating desired vibrations in structure", Integrated Ferroelectrics, Vol. 176, No. 1, 2016, **(SCI indexed journal)**
3. B. Kheiri, M. Sharma, D. Kaur & N. Kumar, "An optimal control based technique for generating desired vibrations in a structure", Iranian Journal of Science and Technology, Transactions of Electrical Engineering, Vol. 41, No. 3, 2017, **(SCI indexed journal)**
4. B. Kheiri, M. Sharma & D. Kaur, "A novel technique for active vibration control based on optimal tracking control", Pramana, 2017 **(SCI indexed journal)**

B. Conference papers

1. Kheiri.B, Sharma.M, Kaur.D, "Techniques for creating mathematical model of structures for active vibration control", *IEEE conference*, 2014, **(Scopus Index)**.

Table of contents

List of figures

List of tables

Abbreviations

symbol	description
AVC	Active vibration control
ACLD	Active Constrained Layer Damping
DOF	Degree of Freedom
D/A	Digital/ Analog
DRE	Difference Riccati Equation
ERA	Eigen system Realization Algorithm
FEM	Finite Element Method
FSDT	First order Shear Deformation Theory
FLC	Fuzzy Logic Control
IPMC	Ionic Polymer Metal Composite
IL	Iterative Learning
HST	Higher order Shear deformation Theory
LQG	Linear Quadratic Gaussian
LQR	Linear Quadratic Regulator
LQT	Linear Quadratic Tracking
LPA	Laminated Piezoelectric Actuator
MIMO	Multi-Input and Multi-Output

MIMSC	Modified Independent Modal Space Control
OKID	Observer/Kalman filter Identification
PVC	Passive Vibration Control
PVDF	Poly Vinylidene Fluoride
PZT	Lead Zirconate Titanate
PFRC	Piezoelectric Fiber Reinforced Composite
PID	Proportional-Integral-Derivative
PSO	Particle Swarm Optimization
PDE	Partial Differential Equation
SISO	single-input single-output

Chapter 1: Introduction

Our vocal cords vibrate so that we can articulate our feelings via our speech. Vibrations of our vocal cords sets the air surrounding us into vibrations (contractions and rarefactions). Our speech travels through air to ears of a listener and his/her ear-drums are in turn set into vibrations. Vibrations of the ear drum are marvellously deciphered by the brain of the listener and our speech gets communicated to him/her. We owe our existence to incessant vibrations of our heart and our lungs. A physician gets a good idea of our condition by sensing vibrations of our heart through a stethoscope or by sensing our pulse around our wrist. When Nature decides to recreate, vibrations of an earthquake help in creating a blank canvas for mother Nature. So, importance of vibrations to mankind can just not be over emphasized.

In this material world, one can appreciate role of mechanical vibrations by comparing a ride on 'Delhi Metro' and 'Indian railway train' or ride on a 'state transport bus' and 'Volvo luxury bus'. Vibrations generated by an I.C engine on a bumpy road profile, if not isolated sufficiently can result in acute inconvenience of the passengers travelling in an automobile. Compressor of a household refrigerator can be major source of noise if shell of the compressor is poorly designed. There have been instances when mighty bridges have been damaged by vibrations generated by march of soldiers or by a specific flow of wind. Mechanical machines having rotating parts such as pumps, turbines, fans, compressors etc have to be meticulously designed, properly aligned and sufficiently balanced so as to keep low vibration levels while in operation. Structure of an aeroplane particularly its wings are prone to flow induced vibrations and therefore special materials having high structural damping & high strength are needed. Material for construction of an aeroplane should also have low density to save fuel cost. Sometimes vibrations are required but mostly vibrations are cause of discomfort, unwanted noise and wastage of energy.

Vibrations may occur due to external excitation, unbalanced force, friction etc. There are three types of vibrations viz. free vibration, forced vibration and self-excited vibration. Vibrations generated in a structure due to some initial displacement or/and velocity or/and acceleration are called free vibrations. Forced vibrations occur

when the structure is continuously excited by some harmonic or random force. In case of self-excited vibration exciting force is a function of motion of the vibrating body. Since time immemorial man has been trying to dissipate undesirable vibrations occurring in structures and machines. Several ways have been developed to control vibrations and newer techniques are being developed. Passive Vibration Control (PVC), Active Vibration Control (AVC) and semi-active vibration control are main ways to control vibrations. In passive control mass and/or stiffness and/or damping of the structure are changed so as to control structural vibrations, this may increase overall mass of the system. On the other hand, in active vibration control, an external source of energy is used to control structural vibrations. An actively controlled structure essentially consists of sensors to sense structural vibrations, a controller to manipulate sensed vibrations and actuators to deform the structure as per orders of the controller. Such a structure is also called "intelligent structure" because it exhibits desired dynamic characteristics even in the presence of an external load and disturbances in the environment. In semi-active vibration control technique, passive as well as active techniques are simultaneously used. Active vibration control may fail if an external source of energy gets exhausted or sensing mechanism ill performs or actuating mechanism ill performs or controller malfunctions. Therefore, semi-active control has found importance as in this technique passive technique can still control the vibrations if active technique fails. AVC is suited for applications where stringent weight restrictions are present e.g. aerospace, nanotechnology, robotics etc. In situations where low-frequency vibrations are present, AVC is more effective than PVC.

In AVC different type of sensors can be used e.g. strain gauge [1], piezoelectric accelerometer [2], piezoelectric patch [3], Piezoelectric Fibre Reinforced Composite (PFRC) [4], Poly Vinylidene Fluoride (PVDF) [5] etc. Similarly different type of actuators can be used e.g. magneto-rheological damper [6], electro-rheological damper [7], piezoelectric patch [8], piezoelectric stack [9] etc. Piezoelectric patches have been extensively used in AVC both as sensors as well as actuators. Piezoelectric materials have coupled electromechanical properties. Piezoelectric material layers can be pasted on the base structure [10] or segmented piezoelectric patches can be pasted on the surface [11], piezoelectric layer can be sandwiched between two layers of

structure [12], segmented piezoelectric patches can be embedded in the composite structure [13], wires of piezoelectric material can be embedded in the composite structure [14] etc.

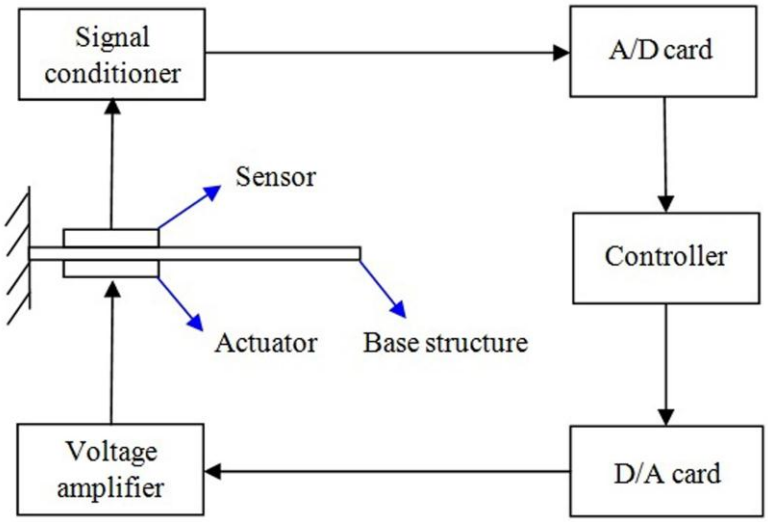

Figure 1.1 Schematic diagram of an intelligent structure

In figure (1.1), one piezoelectric sensor and one piezoelectric actuator are instrumented on a cantilevered plate. Signal sensed by the sensor is conditioned by signal conditioner and then fed to host PC through A/D card. Control voltage generated by host PC is converted into an analog voltage, suitably amplified and then applied on the piezoelectric actuator. Following steps have to be followed for implementing active vibration control on a typical structure:

- Create mathematical model of structure instrumented with sensors and actuators
- Find optimal locations of sensors and actuators
- Design a suitable controller

Numerous simulations have to be performed using the mathematical model of the structure so as to evaluate performance of an AVC scheme under various loads. Following sections briefly discuss typical steps that need to be followed while actively controlling a structure.

1.1. Mathematical model of a structure

First step in AVC is to capture the physics of the system in mathematical form. For creating mathematical model of an intelligent structure, governing equations of

motion of the base structure and relation for electro-mechanics of sensors & actuators are required [15]. Governing equations of motion of the structure can be written using experimental tests [16], finite element techniques [17] and Hamilton's principle [18]. Finite element technique is powerful and widely accepted technique for analysing an intelligent structure. Generally, to derive equations of motion of a structure, following steps can be followed:

- Define the structure using an appropriate coordinate system and draw its schematic diagram
- Draw free body diagrams of the structure
- Write equilibrium relations using free body diagrams

1.2. Optimal placement of sensors and actuators

Placement of sensors and actuators at appropriate locations over a base structure using an optimization technique is called an optimal placement. One important issue in active vibration control is to find the optimal position and size of sensors/actuators. Limited number of sensors and actuators can be placed over a structure in many ways. Effective optimal placement of sensors/actuators over a structure increases the performance of an AVC scheme. Usually to find optimal locations of sensors/actuators, a criterion is exterimized which is called an optimization criterion. Then a suitable optimization technique is employed to search optimal locations of sensors and actuators over the base structure.

1.2.1. Optimization criteria

The process of optimal placement of sensors/actuators over a structure aims at maximizing the efficiency of an AVC scheme. Some criterion is fixed based upon end application and is subsequently extremized so as to obtain locations of sensors/actuators. Some of the possible optimization criteria which can be used in AVC are:

- Maximizing force applied by actuators

In AVC, actuators are desired to be placed over the structure in such a way that forces applied by actuators on the base structure are large. For instance, in case of a cantilevered plate, force applied by actuators can be maximized when actuators are placed near the root of the cantilevered plate. Hence, output force by an actuator can be considered as a criterion for optimal placement of actuators.

- Maximizing deflection of the base structure:

In AVC, actuators are desired to be placed over the structure in such a way that maximum deflection of the base structure is obtained. Therefore, deflection of base structure can be considered as a criterion for optimal placement of actuators.

- Maximizing degree of controllability/observability

One of the necessary conditions in any control process is controllability and observability. Effective and stable AVC depends on the degree of controllability/ observability of the system. Controllability and observability can be checked by using rank test. Optimal placement of actuators/sensors can be determined by using degree of controllability/observability as optimization criterion.

- Minimizing the control effort

With ever increasing cost of energy, a very natural criterion for optimal placement of sensors and actuators over a structure is amount of control effort. Also, it is to be appreciated that limited supply of external energy is usually available to suppress the structural vibrations. Therefore, minimizing the control energy can be considered as a criterion for optimal placement of sensors/actuators.

- Minimizing the spillover effects

A continuous structure has infinite natural frequencies or modes. Usually first few modes of vibration have most of vibrational energy. Therefore in AVC, controller is designed to control first few modes only and not all the modes. Uncontrolled residual modes can make the system unstable and reduce the control effectiveness. This phenomenon is called as spillover effect. Therefore, placement of sensors/actuators can be selected that minimizes the spillover effects.

1.2.2. Optimization techniques

A large number of optimization methods are available and still new techniques are continuously coming [19]. Optimization is an art of finding the best convergent mathematical solution that extremizes an objective function. Best mathematical solution is calculated by maximizing the efficiency function or/and minimizing the cost function of the system. Optimization techniques can be classified as classical techniques (single variable function & multivariable function with no constraints), numerical methods for optimization (linear programming [20], nonlinear programming [21], integer programming [22] and quadratic programming [23]) and advanced optimization methods (univariate search method [24], swarm intelligence algorithm [25], simulated annealing algorithm [26], genetic algorithms [27], Tabu search [28]).

1.3. Control law

Finally, a control technique has to be used to generate a suitable control signal in an AVC application. Control strategies which have been applied in AVC so far, can be classified as: classical control, modern control and intelligent control.

1.3.1. Classical control

Classical control techniques are described using system transfer functions. Feedback controller, feedforward controller and PID controller have been frequently used in active vibration control. In feedback control, manipulated signal is calculated using error between setpoint and dynamic output signal. In feed-forward controller, control signal is based on error signal and disturbance signal. The feedback control [29], feed forward control [30], Proportional-Integral-Derivative (PID) [31] are the very famous control techniques which have been used practically in AVC.

1.3.2. Modern control

Classical control methods are limited to single-input single-output (SISO) control configurations and being used for linear time-invariant systems only. To solve multi-input and multi-output (MIMO) systems, modern control techniques are used.

Governing equations of the plant are converted into a state-space format. In optimal control, control gains are derived by extremizing a performance index. In eigenvalue assignment method, those control gains are used which give desired eigen values of the plant in closed loop. Control gains can also be calculated by satisfying Lyapunov stability criterion. Many times an observer is used to estimate states of the plant and these estimated states are used in the control law. Adaptive control [32], optimal control [33], robust control [34], sliding mode control [35], μ-control [36] etc have been frequently used in active vibration control.

1.3.3. Intelligent control

Classical and modern control theories find it difficult to control uncertain and nonlinear systems effectively. Therefore, most of nonlinear systems are stabilized using controllers based on intelligent control. Intelligent control exhibits intelligent behaviour, rather than using purely mathematical method to keep the system under control. Intelligent control is most suited for applications where mathematical model of a plant is not available or it is difficult to develop mathematical model of a plant. It is based on qualitative expressions and experiences of people working with the process. Neural network based control techniques require a set of inputs and outputs for training the neural network by a training algorithm. Once neural network has been trained for specific purpose, the network gives useful outputs even for unknown/unforeseen inputs. No mathematical model of the plant is required for neural network based control. Fuzzy logic is based on simple human reasoning. Fuzzy logic involves: fuzzification, rule base generation and defuzzification. Simple if-then rules specify the control law. Input variables are fuzzified using fuzzy sets in step called fuzzification. Crisp output is obtained by defuzzifying output variables in step called defuzziification. Mamdani fuzzy controllers [37] and Takagi-Sugeno fuzzy controllers [38] are extensively used techniques in fuzzy logic.

1.4. Illustration of principle of active vibration control

Let us understand the principle of active vibration control through an example of a two degrees of freedom spring-mass-damper system shown in figure (1.2).

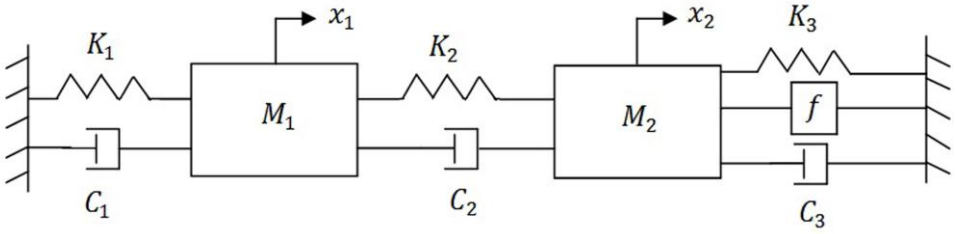

Figure 1.2 Schematic diagram of two degrees of freedom spring-mass-damper system

Mass $'M_1'$ is connected to mass $'M_2'$ through spring of stiffness $'K_2'$ and damper with damping coefficient $'C_2'$. Mass $'M_1'$ is connected to a boundary through a spring of stiffness $'K_1'$ and a damper with damping coefficient $'C_1'$. Mass $'M_2'$ is connected to a boundary through a spring of stiffness $'K_3'$ and a damper with damping coefficient $'C_3'$. Actuator $'f'$ is capable of exerting force $'f'$ on mass $'M_2'$. Free body diagrams of the two masses are drawn in figure (1.3).

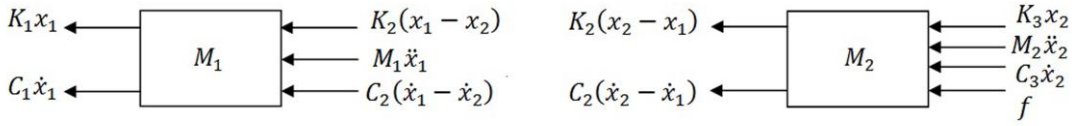

Figure 1.3 Free body diagrams of the two masses

Equations of motion are written from free body diagrams as:

$$\begin{aligned} M_1\ddot{x}_1 + K_2(x_1 - x_2) + C_2(\dot{x}_1 - \dot{x}_2) + K_1x_1 + C_1\dot{x}_1 = 0 \\ M_2\ddot{x}_2 + C_3\dot{x}_2 + K_3x_2 + f + K_2(x_2 - x_1) + C_2(\dot{x}_2 - \dot{x}_1) = 0 \end{aligned} \quad (1.1)$$

So we have a system of two second order ordinary differential equations which are coupled with each other. These equations can be converted into a state-space format by taking:

$$x_3 = \dot{x}_1 \quad \text{and} \quad x_4 = \dot{x}_2$$

now equations (1.1) can be rewritten as:

$$\begin{aligned} M_1\dot{x}_3 + K_2(x_1 - x_2) + C_2(x_3 - x_4) + K_1x_1 + C_1x_3 = 0 \\ M_2\dot{x}_2 + C_3x_4 + K_3x_2 + f + K_2(x_2 - x_1) + C_2(x_3 - x_4) = 0 \end{aligned} \quad (1.2)$$

These equations can be expressed as matrix equation of motion as:

$$\{\dot{x}\}_{4\times1} = [A]_{4\times4}\{x\}_{4\times1} + [B]_{4\times1}\{f\}_{1\times1} \quad (1.3)$$

where

$$\{x\} = \begin{Bmatrix} x_1 \\ x_2 \\ x_3 \\ x_4 \end{Bmatrix}$$

$$[A] = \begin{bmatrix} 0 & 0 & 1 & 0 \\ 0 & 0 & 0 & 1 \\ \frac{-K_1 - K_2}{M_1} & \frac{K_2}{M_1} & \frac{-C_1 - C_2}{M_1} & \frac{-C_2}{M_1} \\ \frac{-K_2}{M_2} & \frac{-K_2 - K_3}{M_2} & \frac{C_2}{M_2} & \frac{-C_2 - C_3}{M_2} \end{bmatrix}$$

$$[B] = \begin{Bmatrix} 0 \\ 0 \\ 0 \\ -1 \end{Bmatrix}$$

Control law for this system can be expressed as:

$$f_{1\times1} = -\{k\}_{1\times4}\{x\}_{4\times1} \tag{1.4}$$

where $\{k\}_{1\times4}$ is vector of control gains. This vector of control gains can be easily obtained using optimal control, pole-placement technique, Lyapunov control etc. State-space equations can be solved using following algebraic equation:

$$x_{4\times1}(n+1) = \bar{A}_{4\times4}x_{4\times1}(n) + \bar{B}_{4\times1}f(n) \tag{1.5}$$

where $\bar{A}_{4\times4}$ and $\bar{B}_{4\times1}$ are discretised forms of A and B matrices discretised using a small sampling time interval. Alternatively, second order coupled differential equations of motion of the system in closed loop can be solved using suitable numerical technique like Newmark-β method. Simulink software of MATLAB can also be employed to solve this system. Simulink model for this system is produced in figure (1.4).

For $M_1 = 2M_2 = 10kg, K_1 = 2K_2 = 3K_3 = 1000\ N/m, C_1 = C_2 = C_3 = 0.8, Nsec/m$ optimal gains can be obtained using LQR command in MATLAB as:

$$K = [1.2347 \quad -0.3189 \quad -0.5925 \quad -1.7024]$$

If at time = 0 second, $x^T = [0.1\ 0\ 0\ 0]$ then controlled and uncontrolled responses of both the masses are as plotted in figures (1.5) and (1.6). It can be observed that application of optimal control has successfully suppressed vibration of both the masses.

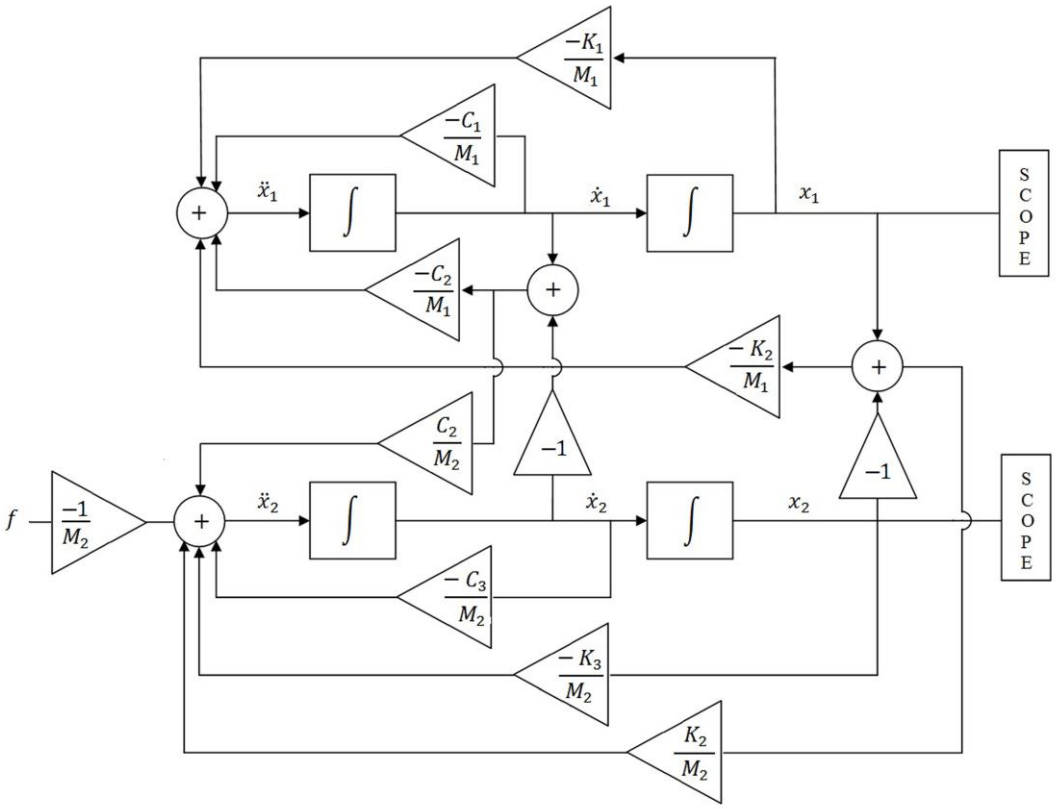

Figure 1.4 Simulink model of two degree of freedom system

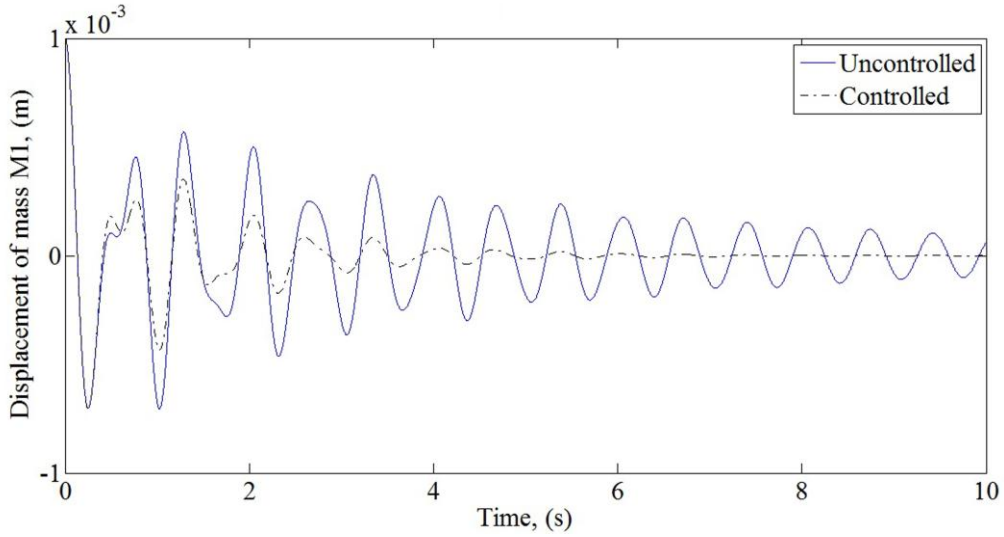

Figure 1.5 Controlled/uncontrolled time responses of a two degree of freedom system, mass M1

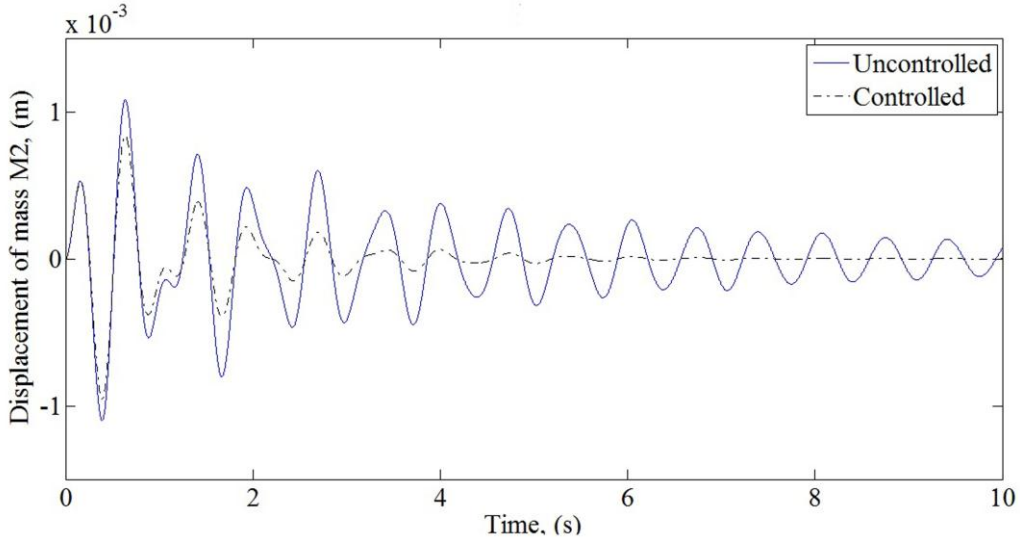

Figure 1.6 Controlled/uncontrolled time responses of a two degrees of freedom system, mass M2

Chapter 2: Literature review

2.1. Introduction

Active Vibration Control (AVC) has attracted lot of interest during last few decades. Numerous researches have been published and still new researches are required to fill the research gaps in AVC. Not many applications are visible in real world in which concept of AVC has been applied. This field is thoroughly interdisciplinary involving knowledge of physics, mechanics, instrumentation, control, signal processing, programming and electronics. Therefore project on actively controlled structure would require a cross-functional team with members coming from diverse backgrounds. Application of an AVC scheme on a structure requires:

- mathematical model of intelligent structure
- optimal placement of sensors/actuators over the structure
- usage of suitable control law

These vital aspects of AVC are discussed in following sections.

2.2. Mathematical model

Mechanical structures can be broadly classified as beams, plates and shells. Numerous mathematical models of these structures are available. A researcher working in AVC selects a suitable model, uses it to model his/her intelligent structure and applies suitable control law. In this section a comprehensive review of mathematical models is done.

2.2.1. Mathematical model of beam-like structure

A cantilever beam can be divided into discrete elements of same length that are modelled using rigid-body dynamics to get lumped parameter model. Equation of motion of lumped parameter model can be obtained using Lagrange's equation:

$$\frac{d}{dt}\left(\frac{\partial T}{\partial \dot{y}_n}\right) - \frac{\partial T}{\partial y_n} + \frac{\partial U}{\partial y_n} = 0 \qquad n = 1,2,3 \dots, N \qquad (2.1)$$

where T is kinetic energy of system, U is potential energy of system, t is time variable and y_n is vertical coordinate of n^{th} lumped mass. Potential energy and kinetic energy of the cantilever beam as a continuum replaced by lumped masses can be expressed as:

$$U = \sum_{n=0}^{N-1} \frac{1}{2} K_\delta (\Delta\delta_n)^2 + \sum_{n=1}^{N} \Delta m g \, Y_n$$
$$T = \sum_{n=1}^{N} [\frac{1}{2} \Delta m \left(\frac{dY_n}{dt}\right)^2 + \frac{1}{2} J_x \left(\frac{d\delta_n}{dt}\right)^2] \tag{2.2}$$

where K_δ is bending stiffness, Δm is mass, δ_n is change in angular displacement, J_x is moment of inertia about x axis perpendicular to the centre line of the beam and g is acceleration due to gravity [39].

Finite element model of isotropic as well as orthotropic fiber reinforced composite beam with distributed piezoelectric actuator subjected to both electrical and mechanical loads can be developed using simple higher order shear deformation theory. The displacement fields for the beam instrumented with piezoelectrics using higher order shear deformation theory at any point through the thickness are:

$$\begin{aligned} u(x, y, z) &= u_0(x) + z\phi_x - \frac{4}{3h^2} z^3 [\phi_x + \frac{\partial w}{\partial x}] \\ v(x, y, z) &= 0 \\ w(x, y, z) &= w_0(x) \end{aligned} \tag{2.3}$$

where u, v & w are displacements in x, y & z directions respectively, u_0 is displacement in midplane in x direction, w_0 is displacement in midplane in z direction, ϕ_x is rotation about y axis and h is beam thickness. The kinetic energy of the structure with mass density ρ and volume q, can be written as:

$$T = \frac{1}{2} \int_q \rho [\dot{u}^2 + \dot{w}^2] \, dq \tag{2.4}$$

Work done due to external mechanical and electrical loads can be written as:

$$W = \int_0^l f_a u\, dx + \int_0^l f_t w\, dx + f_{t_i} w_i + \int_s \sigma\phi\, ds \qquad (2.5)$$

where l is length of beam element, f_a & f_t are axial & transverse mechanical forces respectively, σ is surface charge density on the actuator surface, ϕ is electrical potential on the piezoelectric surface area s, f_{t_i} is i^{th} point force and w_i is i^{th} point displacement. Potential energy in case of isotropic beam and orthotropic beam can be expressed as:

$$\begin{aligned} &\text{isotropic beam} \quad U = \tfrac{1}{2}\textstyle\int_v [E\epsilon_{xx}^2 + G\gamma_{xz}^2 - 2\tilde{e}_{31}E_z\epsilon_{xx} - \tilde{\epsilon}_{zz}^s E_x^2]dv \\ &\text{orthotropic beam} \quad U = \tfrac{1}{2}\textstyle\int_v [\tilde{Q}_{11}\epsilon_{xx}^2 + \tilde{Q}_{55}\gamma_{xz}^2 - 2\tilde{e}_{31}E_z\epsilon_{xx} - \tilde{\epsilon}_{zz}^s E_x^2]dv \end{aligned} \qquad (2.6)$$

where ϵ_{xx} is strain in x direction, γ_{xz} is shear strain in x-z direction, E is Young's modulus of elasticity, $\tilde{e}_{31}$& $\tilde{\epsilon}_{zz}^s$ are modified piezoelectric coefficients, G is modulus of rigidity, $e_{31}$is a piezoelectric coefficient, ϵ_{zz} is a piezoelectric coefficient and $\tilde{Q}_{11}$ & $\tilde{Q}_{55}$ are reduced stiffness coefficients. Two node beam element with four mechanical degrees of freedom and one electrical freedom at each node can be used to find out equations of motion. Expressions of potential energy, kinetic energy and work done can be substituted into Hamilton's principle to obtain equations of motion [40].

Dynamic model of a piezolaminated composite beam can be developed with first order shear deformation theory, where displacements of beam are assumed to be as:

$$\begin{aligned} U(x,y,t) &= u(x,t) + z\psi(x,t) \\ W(x,y,t) &= w(x,t) \end{aligned} \qquad (2.7)$$

where $U(x,y,t)$ & $W(x,y,t)$ are the axial & lateral displacements of a point on the midline and ψ is the bending rotation of the normal to the midline. Voltage on a piezoelectric layer mounted on the piezoelectric slender beam is given by:

$$\phi^k = \frac{(z_k + 0.5h)V^k}{h} + [z_k^2 - (\frac{h}{2})^2]\frac{e_{31}}{2\alpha_{33}}\psi' \qquad (2.8)$$

where z_k is z-coordinate of k^{th} layer, V is potential difference across k^{th} piezoelectric layer, ψ is the bending rotation of the normal to the midline, h is thickness of the piezoelectric layer and e_{31} & α_{33} are constants which are dependent on properties of material. In case of closed electrode $V^k = 0$, additional stiffness is

introduced due to direct piezoelectric effect resulting in increase in eigenvalue by about 3% for zero electric field in x-direction [41].

A laminated hygrothermopiezoelectric plate subjected to coupled effect of mechanical, electrical, thermal and moisture fields needs to satisfy following governing equations:

$$\begin{aligned} &\text{conservation of momentum} && \sigma_{ij,j} = \rho\ddot{u}_i \\ &\text{conservation of charge} && D_{i,i} = 0 \\ &\text{heat condition equation} && p_{i,i} = -T_o\dot{\eta} \\ &\text{moisture diffusion equation} && q_{i,i} = -\dot{\gamma} \end{aligned} \tag{2.9}$$

where D_i is electrical displacement, σ_{ij} is component of stress tensor, u_i is component of displacement, ρ is mass density, p_i is heat flux component, T_o is stress-free reference temperature, η is entropy density, q_i is moisture flux component and γ is change of moisture concentration. The weak form of these equations, can be formulated using the method of weighted residuals as:

$$\int_s \left[\delta u_i\left(\sigma_{ij,j} - \rho\ddot{u}_i\right) + \delta\emptyset D_{i,i} + \delta\theta\left(\rho_{i,i} + T_0\dot{\eta}\right) + \delta\gamma(q_{i,i} + \dot{\gamma})\right] ds = 0 \tag{2.10}$$

where $\delta u_i, \delta\emptyset, \delta\theta$ and $\delta\gamma$ are arbitrary and independent weight functions. Constitutive equations and assumed solutions can now be substituted into this weak form equation (2.10) to solve the coupled system [42].

A viscoelastic layer can be sandwiched between the host and the constraining layer for damping vibrations by way of shear deformation of the viscoelastic layer. In Active Constrained Layer Damping (ACLD), the passive constrained layer is replaced by an active piezoelectric material layer to extend and actively control the shear deformation of the viscoelastic layer. ACLD can be applied for controlling geometrically nonlinear vibrations of rotating composite beams. A nonlinear FE model can be made using First order Shear Deformation Theory (FSDT) and Von-Karman type non-linear strain-displacement relations. Constitutive relation for the vicoelastic material can be used in following form as:

$$\{\sigma_{xz}^k\} = \int_0^t G(t-\tau)\frac{d\varepsilon}{d\tau}d\tau \tag{2.11}$$

where τ is time delay, t is time instant, $G(t)$ is the relaxation function of the viscoelastic material, ε is strain and $\{\sigma_{xz}^k\}$ is the stress vector for k^{th} layer. Hamilton's principle can be used to write equations of motion of rotating composite beam subjected to ACLD treatment. Potential energy of the typical element of the ACLD beam system due to rotation of beam can be expressed as:

$$T_p = \frac{1}{2}\int_0^{l_e} F_{cen}(x)(\frac{dw}{dx})^2 dx \tag{2.12}$$

where l_e is length of the element and $F_{cen}(x)$ is the centrifugal load due to rotation of the beam [43].

In an efficient finite element model quadratic variation of electric potential ϕ across the thickness of piezoelectric layer is incorporated by approximating ϕ piecewise between n_ϕ points at z_ϕ^j, $j = 1, 2, \ldots, n_\phi$ across the thickness.

$$\phi(x,z,t) = \psi_\phi^j(z)\phi^j(x,t) + \psi_c^l(z)\phi_c^l(x,t) \tag{2.13}$$

where $\phi^j(x,t) = \phi\left(x, z_\phi^j, t\right)$ denotes the potential at piezoelectric layer surface/ interface, $\phi_c^l(x,t)$ denotes quadratic component of electric potential at $(z_\phi^l + z_\phi^{l+1})/2$ and $l = 1,2,3,\ldots, n_\phi^l$ with $n_\phi^l = n_\phi - 1$. Also $\psi_\phi^j(z), \psi_c^l(z)$ are piecewise linear and quadratic interpolation functions as:

$$\psi_c^l(z) = \begin{cases} \dfrac{4\left(z_\phi^{l+1} - z\right)\left(z - z_\phi^l\right)}{(z_\phi^{l+1} - z_\phi^l)^2} & if\ z_\phi^l \le z \le z_\phi^{l+1} \\ 0 & otherwise \end{cases} \tag{2.14}$$

The axial displacement u can be approximated as:

$$u(x,z,t) = u_0(x,t) - zw_{0,x} + R^k(z)\psi_0(x,t) \tag{2.15}$$

where $R^k(z)$ is a layerwise function of z of the form:

$$R^k(z) = R_1^k + zR_2^k + z^2R_3 + z^3R_4 \tag{2.16}$$

where the coefficients R_1^k, R_2^k, R_3 & R_4 are dependent on the lay-up & material properties of the layers and k is number of layer [44].

Free vibration of a flexible beam can be modelled using partial differential Euler-Bernoulli equation as:

$$\hat{m}(x)\frac{\partial^2}{\partial t^2}w(x,t) + \hat{c}(x)\frac{\partial}{\partial t}w(x,t) + \frac{\partial^2}{\partial x^2}\left[\hat{k}(x)\frac{\partial^2}{\partial x^2}w(x,t)\right] = 0 \qquad (2.17)$$

where $\hat{m}(x)$, $\hat{c}(x)$ and $\hat{k}(x)$ are the mass, damping and stiffness per unit length respectively. Solution of the following form can be assumed for this equation:

$$w(x,t) = \phi(x)e^{st} \qquad (2.18)$$

where ϕ is a spatial function of x variable and s is an eigenvalue of the system. Substituting assumed solution in equation of motion gives a differential eigenvalue problem as:

$$\frac{\partial \phi_i^4}{\partial x^4} = -\sigma_i \phi_i \qquad (2.19)$$

where $\sigma_i = (\hat{m}s^2\hat{c}s)/\hat{k}$. A clamped-free Euler-Bernoulli beam with perfectly bonded piezoelectric patches has regions where both piezoelectric and base structure are present and regions where only base structure is present. Equation (2.18) can be written for both these regions separately [45]. A single piezoelectric patch has very less stroke and can apply very less actuation force. Stroke length as well as actuation force can be appreciably increased if piezoelectric patches are stacked so as to have a more powerful actuator called Piezo Stack Actuator (PSA). PSA can be instrumented along links of macro-manipulator for controlling vibration of the macro-manipulator. Each flexible link can be considered as an Euler-Bernoulli beam and following partial differential equation can be written for transverse motion y:

$$\frac{\partial^2}{\partial x^2}\left(EI\frac{\partial^2 y(x,t)}{\partial x^2}\right) + \rho A\frac{\partial^2 y(x,t)}{\partial t^2} = 0 \qquad (2.20)$$

where EI is the flexural rigidity of the beam and ρA is the mass per unit length of the beam. Equation of motion of the link can be obtained by multiplying equation (2.20) by each mode shape and integrating over length [46].

The dynamic motion of flexible beam in transverse vibrations can be formulated by using fourth order Partial Differential Equation (PDE) as:

$$\mu^2 \frac{\partial^4 y(x,t)}{\partial x^4} + \frac{\partial^2 y(x,t)}{\partial x^2} = \frac{1}{m} u(x,t) \tag{2.21}$$

where μ is beam constant represented by $\mu^2 = \frac{EI}{\rho A}$, with E, I, ρ, A and m representing Young's modulus, moment of inertia, mass density, cross-sectional area and mass of the beam respectively. The beam can be discretized into a finite number of equal length segments and then by using first-order central Finite Difference (FD) method equation of motion (2.21) becomes:

$$Y_{j+1} = -Y_{j-1} - \lambda^2 S Y_j + \frac{\Delta t^2}{m} U(x,t) \tag{2.22}$$

where $U(x,t)$ is $n \times 1$ matrix which represents the actuating force applied on the beam, $0 < \lambda^2 \leq 0.25$, Δt is constant time interval, Y_k $(k = j-1, j, j+1)$ is $n \times 1$ matrix which is the deflection of the beam at segments 1 to n at time step k and S is stiffness matrix [47].

Consider a cantilever beam instrumented with piezoelectric patches as shown in figure (2.1). By using the assumed modes method, the flexural deflection can be expressed as:

$$w(x,t) = \sum_{j=1}^{\infty} \phi_j(x) q_j(t) \tag{2.23}$$

where ϕ_j & q_j denote the j^{th} mode shape & the corresponding generalized coordinate respectively.

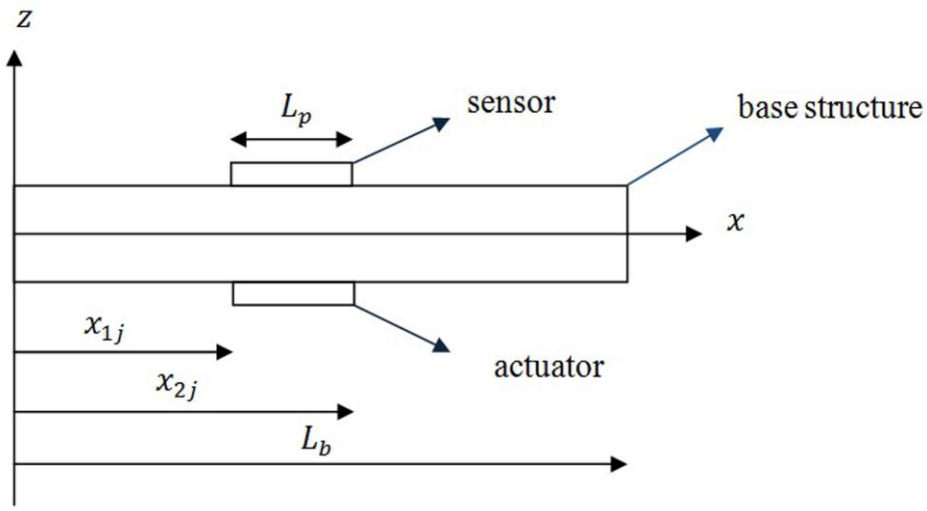

Figure 2.1 Cantilever beam instrumented with piezoelectric patches

The charge generated by piezoelectric sensor is expressed as:

$$q_i(t) = -e_{31i} b_{si} \int_{x_{i1}}^{x_{i2}} r_i \frac{\partial^2 w(x,t)}{\partial x^2}\, dx\,, \qquad i = 1,2,\dots,N_s \qquad (2.24)$$

where e_{31i} is the piezoelectric stress constant of the i^{th} piezoelectric sensor, b_{si} is the width of i^{th} piezoelectric sensor, x_{i1} & x_{i2} are the locations of the left & right edges of the i^{th} piezoelectric sensor, r_i is the distance from the middle of piezoelectric patch to the middle of the beam and N_s is the number of PZT sensors. Using flexural deflection as defined in (2.23), the equation of motion of piezoelectric driven beam becomes:

$$\ddot{q}_i + 2\xi_i \omega_i \dot{q}_i + \omega_i^2 q_i = \frac{1}{\rho_b A_b} \sum_{j=1}^{N_a} C_0 \varepsilon_{pe}^{j} \left[\acute{\phi}_i(x_{2j}) - \acute{\phi}_i(x_{1j})\right] \qquad (2.25)$$

where ξ_i is damping ratio, ω_i is natural frequency, C_0 is a constant, N_a is number of PZT actuators, x_{1j} & x_{2j} are the locations of the edges of the j^{th} actuator, ρ_b is the mass density, A_b is cross sectional area of the beam and ε_{pe} is piezoelectric strain [48].

Equation of motion with respect to y direction of a beam carrying a moving mass can be expressed as:

$$\begin{aligned} &E_b I \frac{\partial^4 y(x,y)}{\partial x^4} + \acute{m} \frac{\partial^2 y(x,t)}{\partial t^2} \\ &= mg\delta(x - vt) - m\left(\frac{\partial^2 y(x,t)}{\partial t^2} + 2v \frac{\partial^2 y(x,t)}{\partial x \partial t} + v^2 \frac{\partial^2 y(x,t)}{\partial x^2}\right) \\ &\qquad \delta(x - vt) + \sum_{i=1}^{N} K_i V_{ai}(t) \frac{\partial^2 F_i(x)}{\partial^2 x} \end{aligned} \qquad (2.26)$$

where E_b is Young's modulus, I is second moment of area of the beam cross-section, ḿ is mass per unit length, m is moving mass, $\delta(\dots)$ is Dirac delta function, v is velocity of moving mass, g is acceleration due to gravity, $F_i(x)$ is the position distributed function for the i^{th} piezoelectric patch, K_i is constant dependent on the piezoelectric elements & the cantilever beam's structural parameters and V_{ai} is the voltage applied on the i^{th} piezoelctric patch [49].

Ionic Polymer Metal Composite (IPMC) actuator can also be used for structural vibration control. IPMCs are generally made of nafion, a perfluorinated polymer electrolyte, sandwiched in between platinum (or gold) electrodes on both sides. IPMC produces large bending moment upon application of relatively low voltage. Governing equation of motion of vibratory flexible link instrumented with IPMC actuators can be expressed as:

$$\frac{\partial^2}{\partial x^2}\{M(x) - m(x)\} + \rho_b \frac{\partial^2}{\partial t^2} w(x,t) = T \tag{2.27}$$

where $w(x,t)$ is the transverse displacement of the flexible link, $M(x)$ is the beam internal bending moment, $m(x)$ is the externally applied distributed bending moment from IPMC actuator, T is the motor torque supplied at the hub and ρ_b is mass per unit length of the flexible link [50].

Piezoelectric sandwich beams subjected to large amplitude vibrations can be modelled by Partial Deferential Equation (PDE) including non linearity effect of large amplitudes. For beam structure transversally excited by harmonic force and neglecting the axial displacement, the equation of motion can be expressed as nonlinear partial differential equation as:

$$\begin{aligned} \propto_1 \ddot{w} + \propto_2 w_{,xxxx} + N(t) w_{,xx} + \propto_3 \left(w^2{}_{,xx} - w_{,x} w_{,xxx}\right) - \propto_4 \dot{w}_{,x} w_{,xxx} \\ + \propto_5 \dot{w}_{,xx} w_{,xxx} + \propto_6 w_{,x} \dot{w}_{,xxx} - \propto_7 \dot{w}_{,xxxx} = F_z \end{aligned} \tag{2.28}$$

where $\propto$ are constants dependent on the intelligent structure, $N(t)$ is the resulting axial force, w is transverse displacement and F_z is harmonic force. Using Galerkin's approximation, transverse deflection can be assumed as:

$$w(x,t) = \sum_{k=1}^{n} q_k(t) \phi_k(x) \tag{2.29}$$

where $\phi_k(x)$ are the free vibration modes of the sandwich beam and $q_k(t)$ are the associated time dependent amplitudes. Based on the one mode assumption and using the method of multiple scales, time response of deflection can be obtained [51].

Magnetically mounted piezoelectric elements can be used to sense and control vibrations of a pinned-free beam subjected to excitation at the base. The equations of

axial & lateral motion of the beam and control moments can be derived using Hamilton's principle for coupled electromechanical system as:

$$\int_{t_1}^{t_2} [\delta(T_b + T_c - U_b - U_c + W_e + W_N + W_f) - \delta V q_a] dt = 0 \qquad (2.30)$$

where T_b is kinetic energy of the beam, T_c is kinetic energy of the magnetic-piezoelectric control mounts, U_b is beam's stored energy, U_c is potential energy stored in control mounts, W_e is work performed by piezoelectric field on piezoelectric element, W_N is work due to interfacial normal forces, W_f is work due to interfacial tangential forces, $\delta V q_a$ is virtual work due to applied charge q_a on piezoelectric elements and V is the voltage measured across the electrodes [52].

When a sensor-actuator pair is not collocated then the system tends to become unstable as it has non-minimum-phase zeros. This problem can be addressed if control input u is taken proportional to delayed acceleration signal and a low pass filter is used to filter out high frequency noise of the sensor signal as in:

$$u = -K_a \ddot{w}(t - \Delta t) \frac{a}{s + a} \frac{b}{s + b} \qquad (2.31)$$

where w is transverse displacement which is obtained by an experimental identification method, t is time interval, Δt is phase tuning time, s is Laplace operator, a & b are the corner frequencies of first order low pass filter and $K_a > 0$ is the proportional gain of acceleration feedback control [53].

Piezoelectric fibre with metal core can be embedded in CFRP composite beam for sensing as well as controlling the vibrations. If a voltage V is applied to the piezoelectric fiber, the strain developed is:

$$\varepsilon = \frac{d_{31} V}{r - r_c} \qquad (2.32)$$

where r is radius of the piezoelectric fibre, r_c is the radius of the metal core and d_{31} is piezoelectric coefficient. When the piezoelectric fiber is strained, the sensor voltage V_s is given as:

$$V_s = \frac{2\pi E_a h d_{31} r_c \acute{y}(l)}{C_p} \tag{2.33}$$

where $\acute{y}$ is the spatial derivative of y, h is distance between neutral axis & centre of piezoelectric fibre, l is length of beam, E_a is modulus of elasticity of the beam and C_p is capacitance of piezoelectric fibre [54].

2.2.2. Mathematical model of plate-like structures

Consider a plate which has two piezoelectric sheets symmetrically attached to both sides of the plate in the centre position. As shown in figure (2.2(a)), this system can act as an absorber consisting of piezoelectric material, an inductance and a resistance. Where $L_a = \frac{h_p}{S_p \varepsilon_{33} \omega_a^2}$, $R_a = 2\xi_a \omega_a L_a$, S_p is the area of piezoelectric material, h_p is thickness of piezoelectric material, ξ_a is damping ratio of the absorber, C_p is capacitance of piezoelectric sheet, ε_{33} is dielectric constant, ω_a is natural frequency, V_a is sensor voltage, i_a is current in the absorber and ϕ^* is voltage at the location of the piezo patch.

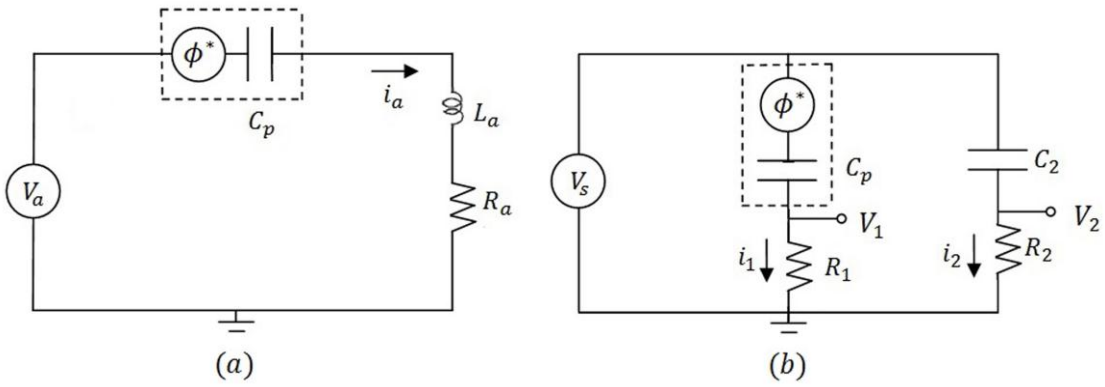

Figure 2.2 The active absorber and sensor

Velocity feedback of the main system depresses the frequency sensitivity of the absorber and displacement feedback of the main system has insignificant effect. A piezoelectric patch instrumented on a host plate can act as a sensor with signal conditioning as shown in figure (2.2(b)). The governing equation of the sensor is given as:

$$\frac{d(R_1 i_1)}{dt} + \frac{1}{C_p} i_1 = \frac{dV_s}{dt} + \frac{d\phi_1^*}{dt}$$
$$\frac{d(R_2 i_2)}{dt} + \frac{1}{C_2} i_1 = \frac{dV_s}{dt} \quad (2.34)$$

The output voltage $V_o = V_2 - V_1$ of the sensor can be expressed in the following form in the frequency domain:

$$V_o(s) = \frac{R_1 C_p s}{1 + R_1 C_p s} \phi^*(s) + [\frac{R_1 C_p s}{1 + R_1 C_p s} - \frac{R_2 C_2 s}{1 + R_2 C_2 s}] V_s \quad (2.35)$$

where R_1 & R_2 are the additional resistances, i_1 & i_2 are currents, C_2 is capacitance proportional to C_p and V_s is sensor voltage [55].

Following three easily realizable design constraints are sufficient to guarantee the asymptotic stability of a piezoelectrically active laminated anisotropic rectangular plate: (1) for each piezoelectric actuator laminate above the composite structure mid-plane there must exist a corresponding identically polarized sensor laminate located above the mid-plane, (2) input to the actuator should be proportional to the negative of current induced in the corresponding sensor and (3) for each conjugate pair above the mid-plane there must exist an identical pair below the mid-plane [56].

The dynamic balance equation of a stiffened plate instrumented with Laminated Piezoelectric Actuator (LPA) can be written as:

$$\rho h_e \frac{\partial^2 w}{\partial t^2} + D_x \frac{\partial^2 w}{\partial x^4} + 2B \frac{\partial^2 w}{\partial x^2 \partial y^2} + D_y \frac{\partial^4 w}{\partial y^4} = \rho_z(x, y, z) + m_{ax} \frac{\partial^2 R}{\partial x^2} + m_{ay} \frac{\partial^2 R}{\partial y^2} \quad (2.36)$$

where ρ is density of material, h_e is the equivalent thickness of the smart plate, D_x & D_y are equivalent stiffness in x & y directions, R is function related to force induced by actuator, B is effective torsional rigidity, $\rho_z(x, y, z)$ is external force and m_{ax} & m_{ay} are magnitudes of actuation moments per unit voltage. Displacement can be written as:

$$w = \sum_{j=1}^{\infty} \sum_{k=1}^{\infty} W_{ij}(x, y) q_{jk}(t) \quad (2.37)$$

where W_{ij} is mode shape and q_{jk} is transient displacement. Optimal position of LPA can be found by optimizing modal control force induced by LPA [57]. Mathematical model of cantilevered plate can be derived using finite element technique based on Hamilton's principle. The properties of piezoelectric patches get changed at elevated temperature. Therefore new equations containing updated coefficients can be used to control vibrations using negative velocity feedback [58].

Based on the hypothesis of Kirchhoff's law the free vibration equation of two-dimensional rectangular plate is:

$$D_p\left(\frac{\partial^4}{\partial x^4}+2\frac{\partial^4}{\partial x^2\partial y^2}+\frac{\partial^4}{\partial y^4}\right)w(x,y,t)+\rho_p h\frac{\partial^2 w(x,y,t)}{\partial t^2}=0 \qquad (2.38)$$

where $w(x,y,t)$ is transverse modal displacement, $D_p=\frac{E_p h^3}{12(1-v_p^2)}$ is flexural rigidity, E_p is Young's modulus, v_p is Poisson's ratio, h is thicknes of the plate, ρ_p is density of plate material, x & y are the coordinate variables of the plate and t is time variable. According to Rayleigh-Ritz method transverse displacement can be written as:

$$w=\sum_{m=1}^{\infty}\sum_{n=1}^{\infty}w_{mn}(x,y)\eta_{mn}(t) \qquad (2.39)$$

where the subscripts m & n denote the $(m,n)^{th}$ mode of vibration, $w_{mn}(x,y)$ denotes the modal function of the plate and $\eta_{mn}(t)$ denotes the modal coordinate [59].

For better closed loop performance of smart plate structure it is essential to obtain more exact system parameters such as natural modes, damping ratios and modal actuation forces. The in-plane displacement through the thickness of composite plate with piezoelectric actuators can be estimated better using layerwise plate theory. Using layerwise plate theory, displacement fields can be expressed as:

$$\begin{aligned} u(x,y,z,t)&=\sum_{J=1}^{N}U^J(x,y,t)\phi^J(z)\\ v(x,y,z,t)&=\sum_{J=1}^{N}V^J(x,y,t)\phi^J(z)\\ w(x,y,z,t)&=W(x,y,t)\end{aligned} \qquad (2.40)$$

where U^J & V^J are undetermined coefficients, $\phi^J(z)$ is the Lagrangian interpolation function through the thickness and N is the number of degrees of freedom for in-plane displacement along the thickness. Thereafter refined FE model can be made using Hamilton's principle [60].

Functionally Graded Materials (FGM) are microscopically inhomogeneous composite materials which exhibit smooth and continuous change of material properties along the thickness direction. The effective material properties for a FGM plate using power law are given by:

$$\begin{aligned} E_f &= E_{m1}V_{m1} + E_{m2}V_{m2} \\ V_{m1} + V_{m2} &= 1 \\ V_{m1} &= \left(\frac{2z+h}{2h}\right)^n \end{aligned} \tag{2.41}$$

where E_{m1} & E_{m2} are elastic moduli of constituent materials (aluminium & stainless steel), V_{m1} & V_{m2} are volume functions of constituent materials, n is power law index and z is thickness co-ordinate variable. Free vibration analysis of functionally graded plate integrated with a piezoelectric layer at the top and bottom faces can be done based on finite element method by considering Higher Order Shear deformation Theory (HOST) and Van-Karman's hypothesis [61].

Finite element method can be used to model a smart plate instrumented with piezoelectric patches and stiffened with stiffener. Stiffeners of varying forms need not pass along the nodal lines of the finite element mesh and for this stiffener has to be expressed in terms of the local coordinates tangential to the stiffener at that point. The relationship between the global and local coordinates is as follows:

$$\begin{Bmatrix} u'_o \\ \theta_{\acute{x}} \\ \theta_{\acute{y}} \end{Bmatrix} = \begin{bmatrix} cos\phi & sin\phi & 0 & 0 \\ 0 & 0 & cos\phi & sin\phi \\ 0 & 0 & -sin\,\phi & cos\phi \end{bmatrix}_{3\times4} \begin{Bmatrix} u_0 \\ v_0 \\ \theta_x \\ \theta_y \end{Bmatrix}_{4\times1} \tag{2.42}$$

$$\begin{Bmatrix} x \\ y \end{Bmatrix} = \begin{Bmatrix} u'_o\, cos\phi - v'_o\, sin\phi \\ u'_o\, sin\phi - v'_o\, cos\phi \end{Bmatrix}$$

where ϕ is angle between x and $\acute{x}$ axis, u_0, v_0 & w_0 are the displacements in global coordinates along x, y & z axis respectively, u'_o is displacement along ẋ axis of local coordinate, v'_o is displacement along $\acute{y}$ axis of local coordinate and θ_x, θ_y, $\theta_{\acute{x}}$ & $\theta_{\acute{y}}$ are rotations about x axis of global frame, y axis of global frame, ẋ axis of local frame & ẏ axis of local frame respectively [62].

According to layerwise theory, electric potential is assumed to follow a quadratic variation across layers. The electric potential ϕ can be described in terms of surface potential ϕ^j at $z = z_\phi^j$ and internal quadratic component ϕ_c^l at $z = (z_\phi^l + z_\phi^{l+1})/2$ as:

$$\phi(x, y, z, t) = \psi_\phi^j(z)\phi^j(x, y, t) + \psi_c^l(z)\phi_c^l(x, y, t) \tag{2.43}$$

where $j = 1,2, \dots, n_\phi$ and $l = 1,2, \dots, n_\phi - 1$. $\psi_\phi^j(z)$ and $\psi_c^l(z)$ are the piecewise linear and quadratic functions, given by:

$$\psi_\phi^j(z) = \begin{cases} 0 & if\ z \le z_\phi^{j-1} \quad or \quad z \ge z_\phi^{j+1} \\ (z - z_\phi^{j-1})/(z_\phi^j - z_\phi^{j-1}) & if\ z_\phi^{j-1} < z < z_\phi^j \\ (z_\phi^{j+1} - z)/(z_\phi^{j+1} - z_\phi^j) & if\ z_\phi^j < z < z_\phi^{j+1} \end{cases} \tag{2.44}$$

where

$$\psi_c^l(z) = \begin{cases} 4(z_\phi^{l+1} - z)(z - z_\phi^l)/(z_\phi^{l+1} - z_\phi^l)^2 & if \quad z_\phi^l < z < z_\phi^{l+1} \\ 0 & otherwise \end{cases} \tag{2.45}$$

Piezoelectric Fiber Reinforced Composite (PFRC) materials have high strength, toughness, good operating range (-1500 to 2800 V), long life (200 million cycles) and conformability to curved surfaces. FE method based on fully coupled efficient layer wise theory can be used to model laminated plates equipped with electrode monolithic piezoelectric and PFRC sensors & actuators. Electric potential can be assumed to follow a quadratic variation across the piezoelectric [63].

The equation of motion of lamina n, of an N-layers piezoelectric laminated rectangular plate in the absence of body forces and free charges is given by.

$$\sigma_{ij,j}^{(n)} = \rho^{(n)}\ddot{u}_i^{(n)}, \quad D_{j,j}^{(n)} = 0 \qquad (i, j = 1,2,3) \tag{2.46}$$

where $\sigma_{ij}, u_i,\ \rho$ and D_i are the components of the Cauchy's stress tensor, displacement vector, mass density and electric displacement vector respectively. A semi inverse solution can be assumed for displacement and electric potential as:

$$\begin{aligned} u_1^n &= U_1^n(x_3)e^{j\omega t}\cos px_1 \\ u_2^n &= U_2^n(x_3)e^{j\omega t}\cos px_1 \\ u_3^n &= U_3^n(x_3)e^{j\omega t}\sin px_1 \\ \phi^n &= \phi^n(x_3)e^{j\omega t}\cos px_1 \end{aligned} \tag{2.47}$$

where x_1 is position in x direction, ω is angular frequency, t is time instant, x_3 is position of material surface in vertical direction, U_i are coefficients, ϕ is electrical potential, n is a particular layer, $p = \frac{k\pi}{L}$ is a constant, L is length of piezoelectric plate and k is a non negative integer. Substituting in constitutive equation of piezoelectricity we get four coupled second-order ordinary differential equations for $U_j^n(x_3)$ and $\phi^n(x_3)$. A power series solution can be assumed for $U_j^n(x_3)$ and $\phi^n(x_3)$ [64].

2.2.3. Mathematical model of shells and complex structures

Usually isoparametric hexahedron solid element is used in the finite element modelling and analysis of smart piezoelectric plate structures. When the piezoelectric patch is two to three order thinner than the master structure it is inefficient to use the conventional isoparametric hexahedron solid element because excessive shear strain energy gets stored in the element and in the stiffness coefficients in the thickness direction. This problem can be overcome by introducing internal Degree of Freedoms (DOFs) in the enthalpy equation while applying Hamilton's principle. Displacement interpolation now becomes:

$$\{q\} = [N_q]\{q_i\} + [X]\{a_j\} \tag{2.48}$$

where $[X]$ is the extra mode shape function matrix for the added internal DOFs $\{a_j\}$, $[N_q]$ is the shape function matrix and $\{q_i\}$ is the nodal displacement vector. Guyan reduction scheme can then be used to condense internal DOFs [65].

Multi-layer piezoelectric actuator (MPA) consists of N identical piezoelectric patches polarized along the normal direction and bonded together through the surfaces with the same polarity. Each piezoelectric patch of MPA is applied with identical control voltage. MPA generates greater actuation forces on controlled structure through in-plane deformations of all piezoelectric patches than a single piezoelectric patch actuator. MPA can be instrumented on a Honeycomb Sandwich Panel (HSP) and the displacement function of this laminated structure can be given as:

$$u(x,y,z,t) = z\phi_x - \frac{z^3}{3\left[h + d + H(x,y,z)N\left(t_p + t_v\right)\right]^2}\left(\phi_x + \frac{\partial w}{\partial x}\right)$$

$$v(x,y,z,t) = -z\phi_y - \frac{z^3}{3\left[h + d + H(x,y,z)N\left(t_p + t_v\right)\right]^2}\left(\phi_y + \frac{\partial w}{\partial y}\right) \qquad (2.49)$$

$$w = w(x,y,t)$$

where u, v & w are the displacements in the x, y & z directions respectively, ϕ_x & ϕ_y are the rotation angles about the y & x axis respectively, N is number of layers, h is half-thickness of the honeycomb core, d is thickness of the faceplates, t_p & t_v are the thickness of single piezoelectric patch of single adhesive layer, t is the time argument and $H(x,y,z)$ is the third-order Heaviside function associated with location of the MPA. Thereafter, Hamilton's principle can be used to yield governing equations of motion [66]. Vibration and radiated sound of a ring-stiffened circular cylindrical shell can be suppressed using piezoelectric sensor and actuator. To derive the mathematical model of the system, mass & stiffness matrices of ring stiffeners needs to be added to the mass & stiffness matrices of the cylindrical shell respectively [67]. A clamped aluminium rectangular plate (length along horizontal axis and width along vertical axis) carrying a cylindrical fluid filled tank, mimics an aircraft wing. Two Polyvinylidene Fluoride (PVDF) sensors and two piezoelectric actuators can be instrumented at clamped end of this plate to control the vibrations of this plate. This system can be modelled using partial defferential equations of the plate, liquid continuity condition and equation of liquid motion. Plate can be modelled using following equation:

$$m_s\frac{\partial^2 w}{\partial t^2} + \xi(w)\frac{\partial w}{\partial t} + YI_s\Delta^2 w = \frac{\partial^2 m_y}{\partial y^2} + \frac{\partial^2 m_z}{\partial z^2} \qquad (2.50)$$

where $w = w(y, z, t)$ is the transverse displacement, $\xi(\omega)$ is an operator quantifying the damping, m_s is the mass per unit plate area, Y is Young's modulus, I is moment of inertia of the plate and m_y & m_z are external moments along y & z axis respectively. Longitudinal movement of the liquid in the tank along the x axis can be modelled using equation of liquid continuity based on Bernoulli's equation of liquid motion as:

$$\frac{\partial \phi}{\partial t} + \frac{p}{\rho} + g(z - h) - C_0 x = 0$$
$$\frac{\partial^2 \phi}{\partial x^2} + \frac{\partial^2 \phi}{\partial y^2} + \frac{\partial^2 \phi}{\partial z^2} = 0 \tag{2.51}$$

where ϕ is the velocity potential, C_0 stands for acceleration along x-axis, g is gravitational acceleration, h is liquid height in the container at rest position, ρ is the density of the liquid and p is the pressure in the liquid [68].

Piezoelectric stack-actuator can be attached along the axis of the columns and at parallel offset. In this configuration, piezostack actuator applies moments on the column when actuated by an electrical voltage. Vibrations of a frame built by columns can be controlled by using stack actuators fixed in the manner as explained [69]. A Stewart platform mechanism is a six DOF parallel manipulator, connected to a fixed base plate and a moving plate. The legs of the platform can be made of piezostack actuator and a collocated force sensor. The equation of the Stewart platform can be written as:

$$M\ddot{x} + Kx = F + Bk\delta \tag{2.52}$$

where M is the inertia matrix, K is the stiffness matrix, F is the disturbance force, x is displacement vector, B is the control influence matrix of the active structure, k is the axial stiffness of the active strut and δ is the unconstrained piezoelectric expansion [70].

2.3. Optimal placement of sensors and actuators over a structure

Depending on desired optimization criterion, different optimization techniques can be suitably employed to find the optimal placement of sensors/actuators over a

structure. A pair of sensor and actuator should be collocated to avoid the risk of hysteresis problem and instability of the system. In collocated arrangement a sensor and an actuator have to be placed in same position but in opposite side of structure. Some of the popular optimal placement methods which have been used in AVC are discussed in subsequent paragraphs.

Genetic algorithms are search procedures based on the mechanics of natural selection, the total number of possible combination of actuator locations, the performance criteria, the number of controlled modes etc. A genetic algorithm is powerful random search method guided by fitness function which may be used to detect efficient location for discrete sensor and actuator location over an intelligent structure for active vibration control. Global optimal sensor and actuator locations can be obtained over a base structure with few generations using a half and quarter chromosome technique. Minimization of the linear quadratic index can be used as an objective function to locate piezoelectric actuators and attenuate first six modes of vibration. This technique gives 99.99% reduction in genetic algorithm search space and 97.8% reduction in computer calculations compared to conventional full-length chromosome [71].

Genetic Algorithm along with developed optimization techniques can be used to find the optimal location of piezoelectric actuator over all clamped edges of plate. Developed optimization technique is employed to find location in such a manner that the performance index is extremized. In order to propose the performance criterion for sensor/actuator locations, the energy spent can be used as:

$$\text{Minimize } E(u) = \int_0^{t_1} u^T(\tau)u(\tau)d\tau \tag{2.53}$$

where u is control effort. Steady state controllability Grammian can be obtained using Lyapuanov's equation as:

$$A\,W(\infty) + W(\infty)A^T + BB^T = 0 \tag{2.54}$$

where A is system matrix, B is control matrix, u is the control input and $W(\infty)$ is steady state controllability grammian. Location of both sensors and actuators can be determined with consideration of controllability, observability and spillover prevention [72].

Following index can be developed based on Frequency Response Function (FRF) of an intelligent structure for controllability assessment in case of a structure with uncertainties.

$$\beta_{ij} = \frac{1}{rp}\sum_{k=1}^{r}\sum_{l=1}^{p}\left\| H_{kl}(\omega_{ij}) + \Delta H_{kl}(\omega_{ij}) + \sum_{i=m+1}^{\infty}\sum_{j=n+1}^{\infty}\Delta R(\omega_{ij})\right\| \sqrt{D_{ij}} \qquad (2.55)$$

$$D_{ij} = 2(\xi_{ij} + \Delta\xi_{ij})(\omega_{ij} + \Delta\omega_{ij})$$

where $H_{kl}(\omega)$ is the transfer function from the k^{th} piezoelectric actuator to l^{th} PVDF sensor response, $\Delta H_{kl}(\omega)$ is residue of FRF caused by parameter variation, $\Delta R(\omega)$ is the residue of FRF caused by higher order modes, ω_{ij} is natural frequency and ξ_{ij} is damping ratio [73].

An optimal placement technique can be developed based on degree of controllability and observability to determine optimal location of piezoelectric patches over the aluminium cantilever plate. By maximizing the degree of controllability and observability based on sensor signal equation and actuator force equation modal vibrations can be controlled. The electrical current for n^{th} sensor can be expressed as:

$$I_n = r_n \iint_s \left(e_{31i}\frac{d^3w}{dx^2dt} + e_{32i}\frac{d^3w}{dy^2dt} + e_{36i}\frac{d^3w}{dxdydt}\right)ds \qquad (2.56)$$

where r_n is distance between the middle plane of the n^{th} sensor & edge of the plate, e_{31i}, e_{32i} & e_{36i} are piezoelectric constants of i^{th} piezoelectric sensor, w is transverse modal displacement, s is area of piezoelectric patch, x & y are coordinates of sensor over the structure and t is time variable. Actuator moments applied by n^{th} piezoelectric actuator in both x & y directions are equal and can be evaluated as:

$$\begin{aligned} m_x &= m_y\,, \\ m_y &= C_o[H(x-x_1) - H(x-x_2)][H(y-y_1) - H(y-y_2)] \end{aligned} \qquad (2.57)$$

where x_1 & y_1 are coordinates of one corner of piezoelectric patch, x_2 & y_2 are coordinates of opposite corner, C_0 is coefficient of n^{th} piezoelectric actuator and H is

Heaviside function. The spillover problem can be solved by passing sensor signal through second order Butterworth filter [59].

Collocated piezoelectric sensor/actuator pair can be optimally placed over the flexible cantilevered steel beam using Linear Quadratic Regulator (LQR) controller. Objective function can be derived based on LQR problem to minimize vibration energy as:

$$\text{Minimize } J(x_i) = tr[P(x_i)] \tag{2.58}$$

where $tr(.)$ denotes trace function of matrix, x_i is optimal location of sensor/actuator pairs among possible x locations and $P(x_i)$ is related to piezoelectric force vector. Then genetic algorithm can be used to find solution for $P(x_i)$ [74].

AVC study can be made on pedestrian structure to find optimal placement of sensors/actuators and control gains simultaneously. The performance index can be developed in such a way that all practical parameters are considered. The objective function is defined as:

$$\text{mimimize } J(K, \Lambda) = \frac{1}{2}\int_0^{t_f} x_{sw}^T(K, \Lambda) Q x_{sw}(K, \Lambda)\ dt \tag{2.59}$$

where K is control gain matrix, Λ represents all possible locations of sensors & actuators, x_{sw} is weight matrix related to state of system, Q is $2n \times 2n$ positive definite matrix and t is simulation time [75].

In AVC, solutions of Generalized Control Algebraic Riccati Equation (GCARE) and Generalized Filtering Algebraic Riccati Equation (GFARE) can be employed to find the optimal location of collocated sensors/actuators pair over the un-damped flexible structure. These two equations are solution of H_∞ controller based on the normalized coprime factorization approach. The optimal location of sensors/actuators will be fulfilled by minimizing close loop H_∞ as:

$$\text{minimize } J = tr(CLC^T) \tag{2.60}$$

where C is output matrix and L is controllability grammian of closed loop system. This approach requires solution of complex Riccati equation [76].

Vibrations can be controlled by dissipating energy of structure using optimal placement of actuators. Piezoelectric sensors/actuators location over a truss can be determined by developing an objective function based on maximization of dissipation energy. In order to determine the optimal placement of sensors and actuators over truss structure total energy dissipated can be formulated as [77]:

$$J = \{x(t)\}^T \int_0^\infty e^{AT} Q e^A dt \{x(t)\} \tag{2.61}$$

where t is time interval, $x(t)$ is structural displacement vector, A is system matrix and Q is described as:

$$Q = \begin{bmatrix} [\bar{Q}] & 0 \\ 0 & [I] \end{bmatrix} \tag{2.62}$$

Objective function can be formulated as:

$$J = tr([K]) \tag{2.63}$$

matrix $[K]$ is a solution of following Lyapunov equation:

$$A^T[K] + [K][A] = [Q] \tag{2.64}$$

2.4. Control techniques for active vibration control

After creating a mathematical model of the smart structure instrumented with optimally placed sensors and actuators, one needs to apply a suitable control law. In following pages some control techniques which have been used in AVC are discussed. Negative velocity feedback can control vibrations of the sandwich beam with flexible core using piezoelectric patches. Using closed loop feedback control, the electric potential applied on the j^{th}electrode actuator can be expressed as:

$$u^{aj} = -g\dot{u}^{sj} \tag{2.65}$$

where u^{sj} is displacement signal of j^{th} sensor and g is control gain [78].

In order to solve the nonlinear differential equations for the dynamic analysis, Newmark direct integration method together with the modified Newton-Raphson

method can be utilized. First, the time derivations are approximated by employing the implicit time integration scheme of Newmark method with $\propto = 0.5$ and $\beta = 0.25$. In the next step, the modified Newton-Raphson method can be used to solve the obtained system of non-linear algebraic equations [79].

A control law using negative feedback can be defined to control the first mode of the cantilevered smart piezoelectric structure. For controlling the first mode using negative first modal velocity feedback, the control voltage is given as:

$$V_{ext} = \frac{k\dot{\eta}}{[U]^T([k_{uv}^e] + [\bar{k}_{uv}^e])} \tag{2.66}$$

where $\dot{\eta}$ is modal velocity and is estimated using a Kalman observer, $[k_{uv}^e]$ is electromechanical interaction matrix and $[\bar{k}_{uv}^e]$ is change in the electromechanical interaction matrix when temperature is other than 'reference temperature'. Piezoelectric coefficient d_{31} and permittivity of PZT-5H piezoelectric change with change in temperature. Vibrations sensed by PZT-5H piezoelectric patch and actuation forces applied by PZT-5H piezoelectric patch would be wrongly predicted if this variation is ignored [80].

In optimal control, control gains are taken such that following performance index is maximized:

$$J = \frac{1}{2}\int_0^\infty [x^T(t)Qx(t) + u^T(t)Ru(t)]dt \tag{2.67}$$

where $x(t)$ is state vector, $u(t)$ is control vector, Q is displacement weighing matrix and R is control weighing matrix. Optimal control law is defined as:

$$u(t) = -kx(t) \tag{2.68}$$

where $k = R^{-1}B^TP$ is gain of controller and P is solution of following Riccati equation:

$$-PA - A^TP + PBR^{-1}B^TP - Q = 0 \tag{2.69}$$

where A & B are system & control matrices of state space model respectively. Compared with Linear Quadratic Gaussian (LQG) control method, robust H_∞ control

has strong robustness to variations in modal parameters. In case full states of system are not available, the states can be estimated by a Kalman filter [81].

Sound radiated from a rectangular plate can be controlled by manipulating line moments applied on the plate. Control voltage obtained by minimizing the radiated sound power is:

$$U = -[\vec{C}^H R \vec{C}]^{-1} \vec{C}^H R \vec{V}_m \tag{2.70}$$

where $\vec{C}$ is the velocity response of unit applied voltage, superscript H denotes Hermitian transpose and R is positive definite matrix. The total velocity of the plate is given by:

$$\vec{V} = \vec{V}_m + \vec{C}U \tag{2.71}$$

where $\vec{V}_m$ is velocity distribution due to line moment and U is control signal. The optimal complex control signal can also be found by setting the value of net complex volume velocity to zero. This gives control voltage as:

$$U = \frac{-S\vec{V}_m}{S\vec{C}} \tag{2.72}$$

where S is the elemental area [82].

Filtered Velocity Feedback (FVF) control can be used to stabilize a control system with non-collocated sensor/moment pair actuator configuration. Since sensor/actuator pair is in non-collocated configuration, the system faces instability at high frequencies. FVF controller can solve the instability problem due to high frequencies by using second order filter characteristics similar to a low pass filter, the FVF equation can be expressed as:-

$$\ddot{q} + 2\xi_c \omega_c \dot{q} + \omega_c^2 q = -q\omega_c^2 V \tag{2.73}$$

where ξ_c is the damping ratio, ω_c is the cut-off frequency of the controller, q is response of the controller and V is output signal of velocity sensor. The control signal is obtained as:

$$T_s = -gH(\omega)V_r \tag{2.74}$$

where g is the feedback gain, $H(\omega)$ is transfer function of FVF controller and V_r is controlled velocity at sensor location [83].

As shown in figure (2.3), feed-forward controller with filtered-X LMS algorithm can be used to control structural vibrations where signal related to disturbance is available.

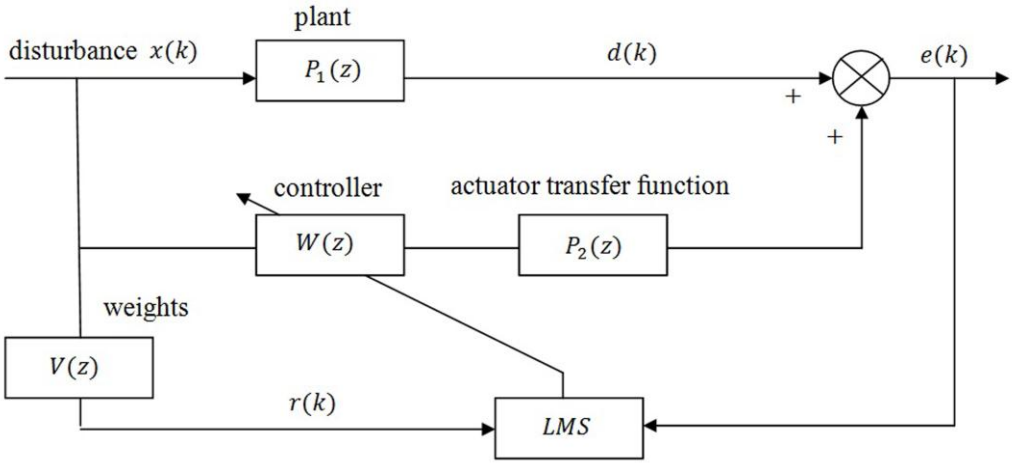

Figure 2.3 Feed forward controller with filtered X-LMS algorithm

$P_1(z)$ & $P_2(z)$ are transfer functions of primary & secondary paths, $V(z)$ is FIR filter, $W(z)$ is controller, $d(k)$ is vibration signal, $x(t)$ is source reference signal, $e(k)$ is an error signal and $r(k) = V(z)x(t)$. The control output $u(k)$ is expressed as:

$$u(k) = \sum_{i=0}^{N-1} w_i x(k-i) \tag{2.75}$$

where w_i are coefficients of the FIR control filter $W(z)$, which are calculated using the gradient descent algorithm. An adaptive controller based on filtered-X Least Mean Square (LMS) algorithm can be used to attenuate vibrations of piezoelectric Stewart platform whose each leg consists of a variable-length piezoelectric actuator and a collocated force sensor [84].

The proportional type Iterative Learning (IL) algorithm is an intelligent strategy through which the performance of a dynamical system becomes better and better as time increases. In proportional type IL algorithm, the input signal $u(k)$ and output signal $y(k)$ are stored in memory each time the system operates. The learning algorithm then evaluates the system performance error $e(k) = \bar{y}(k) - y(k)$, where

$\bar{y}(k)$ is the desired output of the system and $y(k)$ is the actual output. Based on this error signal the learning algorithm then computes a new input signal $u(k+1)$ in such a way that it causes the performance error to be reduced on the next trial or iteration. An intelligent proportional controller based on displacement feedback can be employed to control vibratory response of a flexible plate system [85].

Piezoelectric actuator can be used as an isolator for damping vibrations of a suspended mass. Piezoelectric actuators exhibit non-linear behaviour due to hysteresis. The non linear behaviour can be expressed using Bouc-Wen formula as:

$$V_{Nl} = \frac{q}{C} + k_{\omega} z(t) \tag{2.76}$$

where V_{Nl} is nonlinear voltage developed across piezoelectric patch, q is charge on piezoelectric capacitor, C is capacitance of piezoelectric patch and $k_{\omega} z(t)$ is a perturbation describing the hysteretic behaviour. The piezoelectric actuator can be linearized by using compensated input voltage as:

$$V_e = -g\dot{x} + q\left(\frac{1}{\acute{C}} - \frac{1}{C}\right) \tag{2.77}$$

where g is a positive constant, x is displacement of the platform, $\acute{C}$ is non-linear capacitance of actuator and C is linear capacitance of actuator. A nonlinear compensator can be used for improving the standard skyhook control strategy in a piezoelectric based damper [86].

A general discrete multi variable linear system can be expressed in the state space format as:

$$\begin{aligned} x(i+1) &= Ax(i) + Bu(i) \\ y(i) &= Cx(i) + Du(i) \end{aligned} \tag{2.78}$$

where x is state vector, u is control vector, y is output vector and matrices A, B, C & D are state, control, output & sensor influence matrices respectively. The input-output description of the above system can be written as:

$$y(i) = \sum_{\tau=0}^{i-1} Y_{\tau} u(i-\tau-1) + Du(i) \tag{2.79}$$

where $Y_\tau = CA^\tau B$ together with D are known as the Markov parameters of the system. Markov parameters can be determined by using Observer/Kalman filter Identification technique (OKID). State-space model of the system can be constructed from the system Markov parameters by using Eigenvalue Realization Algorithm (ERA) [87].

Flexible beam can be actively controlled using a mode based digital controller. The input-output description of the system with zero initial condition can be written as:

$$y(k) = \sum_{i=0}^{k-1} Y_i u(k-i-1) DU(k) \tag{2.80}$$

where Y_i & D are the Markov parameters of the system, u is input vector and k is the time interval. A Kalman observer can be created to observe states of the system. A standard recursive least square technique can be used to compute Markov parameters of the observer. Markov parameters of the system can be computed from the Markov parameters of the observer. The state space model of system can be determined using Eigen system Realization Algorithm (ERA). The model can then be used in LQR controller to control modes of vibration [88].

Virtual energy absorption of the piezoelectric patch actuator can define optimal feedback gain where the active damping effect could be maximized. Maximizing the virtual energy absorption is approximately equivalent to minimizing the kinetic energy. Multi-channel robust self-tuning algorithm based on maximizing the virtual energy absorption can update feedback gains of more than one control unit at a time. The energy absorption of each control unit can be written as:

$$\Pi_i = \frac{1}{2} C_o \frac{d_{31}}{h_a} h_i |V_{ci}|^2 \alpha \frac{1}{2} h_i |V_{ci}|^2 \tag{2.81}$$

where d_{31} is piezoelectric material strain constant, h_i is the feedback gain of i^{th} control unit, V_{ci} is the velocity signal at the i^{th} velocity sensor, α is a constant, h_a is thickness of piezoelectric patch actuator and C_o is a constant determined by the characteristics of the piezoelectric patch actuator & size of plate [89].

An online disturbance state-filter can be constructed for the suppression of multiple unknown and time–varying vibrations of variable frequency air-conditioned system.

A state observer estimates the load torque disturbance. Motor torque command of compressor motor can be manipulated to control the structural vibrations of an air conditioner, considering load as disturbance and can be estimated based on motor speed & motor position. Estimated disturbance can be added to the torque command in feed forward manner to control structural vibrations [90].

A structure subjected to a constant follower force may undergo flutter instability. For a parametrically excited system, follower force is given by:

$$P(t) = P_0 + P_1 cos\Omega_{dr} t \tag{2.82}$$

where P_0 & P_1 are forces and Ω_{dr} is driving frequency. The smart plate can be modelled using first-order shear deformation theory and Hamilton's principle. The ratio of the imaginary part to the real part of frequency is called the true damping ratio and the magnitude of that characterizes the intensity of the flutter instability. System is dynamically unstable if ratio of imaginary part of frequency to real part of frequency is less than zero [91].

Noise can be reduced in high speed Switch Reluctance variable Motor (SRM) by using active SRM. Structural vibrations sensed by an accelerometer can be manipulated and used to generate a control signal for two piezoelectric bar actuators located on the stator boundary layer. Typical filter transfer function for this purpose can be taken as:

$$H_{PPF}(s) = k_{PPF} \frac{\frac{s}{\omega_{PPF}}}{1 + 2m_{PPF}\frac{s}{\omega_{PPF}} + \frac{s}{\omega_{PPF}}} \tag{2.83}$$

where ω_{PPF} is resonance ferequency, m_{PPF} is modal mass, k_{PPF} is constant of the filter and s is Laplace operator. Dedicated PPF filter can be designed for increasing damping ratio of a particular mode [92].

Fuzzy logic based Independent Modal Space Control (IMSC) and fuzzy logic based Modified Independent Modal Space Control (MIMSC) can be used to control the vibrations of a plate. First two modal displacements & velocities of the structure can be taken as input and output variables of the fuzzy controller can be taken as the

modal force to be applied by the actuator. According to IMSC the modal force can be obtained as:

$$q_r = \left(-\lambda_r^2 + \lambda_r \sqrt{{\lambda_r}^2 + \frac{1}{R_r}} \right) \eta_r + \left(\sqrt{-2\lambda_r^2 + \frac{1}{R_r} + 2\lambda_r \sqrt{{\lambda_r}^2 + \frac{1}{R_r}}} \right) \dot{\eta}_r \tag{2.84}$$

where η_r, q_r and λ_r represent the modal displacement, modal control force and modal frequency respectively of r^{th} mode. R_r is a factor that weighs the importance of minimizing the vibration with respect to the control forces [93].

To do fuzzification input and output variables of controller have to be designed with relevant range, which each input variable can take and the safe range which each output variable should have. The rules for active vibration control can be generated in the modal domain. Self-tuning fuzzy logic controller can be utilized to control vibrations of a thin walled composite beam integrated with piezoelectric sensor and actuator. In Fuzzy Logic Control (FLC) linguistic rules are used as a base for control by incorporating human expertise into the fuzzy If-Then rules. Commonly used fuzzy control method is the Mamdani method, where i^{th} rule is written as:

$$R^i : \text{if } I_1 = A_i \ \& \ I_2 = B_i \ \text{ then } \ o = C_i \tag{2.85}$$

where I_1 & I_2 present the input variables, o is output variable and A_i, B_i & C_i are the linguistic values of fuzzy variables. In general FLC consists of three principle elements: fuzzification, rules base generation and defuzzification. In fuzzification fuzzy sets are defined over variables and in defuzzification crisp values are obtained from fuzzy output variables. Rule base is a collection of 'if-then' rules based upon human reasoning. Modal displacement η & modal velocity $\dot{\eta}$ can be taken as input variables and output variable can be taken as voltage to be applied on the actuator. Since the universe of discourse of the input variables is in range $[-1\ 1]$, the scaling factors k_d and k_v can be chosen in such a way that they transform the input variables from the sensor to the fuzzy controller to range $[-1\ 1]$. Scaling factors can be taken as:

$$K_d = \frac{1}{|\eta_{max}|}$$
$$K_v = \frac{1}{|\dot{\eta}_{max}|} \tag{2.86}$$

where η_{max} and $\dot{\eta}_{max}$ are maximum amplitudes of modal displacement and modal velocity respectively. Performance and robustness of the FLC controller can be improved by adjusting the scaling factor using peak observer and by optimizing the membership functions using Particle Swarm Optimization (PSO) algorithm [94].

A nonlinear controller based on fuzzy logic controller-Mamdani type can be designed to control vibrations of smart thin elastic rectangular plate. Displacement of a plate structure can be written in the form of a double Fourier's series with the time-dependent coefficients as:

$$W(t,x,y) = \sum_{i,j=1}^{\infty} w^{ij}(t)\omega_{ij}(x,y) \tag{2.87}$$

where w^{ij} are Fourier coefficients and ω_{ij} are the global basis function chosen to match the boundary conditions. Controlling force can be calculated by using a fuzzy logic control with displacement & velocity as input and control force as output [95]. Fuzzy logic meshed with sliding mode can be used to control vibrations of half vehicle model having nonlinearity in actuator and uncertainties in sprung mass of front wheel, un-sprung mass & rear wheel un-sprung mass. Based upon instantaneous values of sprung mass and un-sprung masses, eight state space models of vehicle can be created. Then suitable rule base can be created by using If-Then rules. Thereafter an integral type sliding-surface function can be chosen as:

$$s(t) = G\,x(t) - \int_0^t G\bar{A}\,x(t)dz$$
$$\bar{A} = \sum_{i=1}^{8}\sum_{j=1}^{8} h_i h_j (A_i + B_i k_j) \tag{2.88}$$

where h_i & h_j are the fuzzy weights, A_i & B_i are the system matrices of state space model, G is a constant matrix to be designed satisfying condition that GB_i is non-singular and $k_j \in R^{2\times 8}(j = 1,2,\dots,8)$ is the state feedback gain matrix to be designed. Control law can be taken as:

$$u(t) = \sum_{j=1}^{\infty} h_j K_j x(t) - \hat{\rho}(t) sgn(x(t)) \quad (2.89)$$

where h_j is fuzzy weight function, K_j is the state feedback gain matrix and $\hat{\rho}(t) = 0.5\hat{\delta}\|(x(t))\|$, sgn is sign function, parameter updating law is $\hat{\delta}(t) = 0.1\|s(t)\|\|x(t)\|$ and $s(t)$ is switching function. Takagi-Sugeno (TS) fuzzy approach can be used to compute $u(t)$ [96].

2.5. Gaps in literature

Lot of work has been done to control the vibrations of static and dynamic structures. Different controllers, sensors and actuators have been tested but still they are not that much efficient to control vibrations effectively. Most of the proposed methods in research area are not applicable in practical cases. Following gaps in literature are visible:

i. There is no work in literature in which a time varying non-zero vibration reference signal has been tracked.
ii. Concept of AVC has not been employed for vibration testing.
iii. There is very less work in literature in which concept of active vibration control has been applied on complex structures.
iv. There is limited work in literature in which performance of an actively controlled structure has been checked in complex real life environment.
v. Piezoelectric actuators get fatigued with time. There is no work in literature in which age of piezoelectric sensors and actuators has been considered in the performance of the intelligent structure.
vi. There is no work in which a piezoelectric actuator has been used in shear mode and bending mode simultaneously.
vii. An actively controlled structure is prone to structural changes due to interaction with the environment. To tackle this, the adaptive controller is needed. No research work is available in this direction.
viii. An actively controlled structure may have several sensors and actuators. Some of these sensors or/and actuators may fail while the intelligent structures is in

use. This failure has not been analysed in terms of damage to structure, vibration levels and energy consumption etc.

ix. An actively controlled structure can fail due to several reasons. Therefore the intelligent structure should also be passively controlled in an optimal manner. Such a hybrid structure has not been analysed.

x. Actively controlled structures are projected for use in space structures in which ambient air flows with appreciable speed. This air can charge the piezoelectric patches. This charging of the piezoelectric patch by ambient air has not been analysed in literature.

xi. In many applications, signal proportional to disturbance may be available in the structure and the structure may be experiencing transient disturbances also. Such structure requires feedback as well as feed-forward control. Such a scenario has not been considered.

2.6. Present work

Once a structure has been constructed for desired dynamic characteristics using PVC and/or AVC techniques, the performance of the structure should be thoroughly checked. Only after successful laboratory tests, the structure is fit to be put for its intended use in real life environment. Different types of lab test are available so as to check dynamic characteristics of the test structure. A simple 'Rap test' followed by Fourier transform can be used to find actual natural frequencies and damping ratios. Actual mode shapes of the test-structure can be extracted from an experiment performed using an instrumented hammer. The structure can be mounted on a vibration shaker and subjected to different harmonic excitations so as to check its dynamic strength. The performance of the structure can be observed in the lab by subjecting it to dynamic loads similar to those occurring in real-life environment conditions. In real world environment conditions, a structure may be subjected to several loads simultaneously. Ideally, a test structure should be tested in the lab by subjecting the test structure to these several loads simultaneously. This testing is difficult because: all the loads need to be identified, some of the loads may be complex in nature and simultaneous application of all the loads on a test structure may

require extensive experimental setup. On the other hand, it is very simple to measure actual vibrations being experienced by the structure in a real-life environment.

Present work proposes a novel technique to test a structure in the laboratory before the structure is put to use in the field. There is no work in which test structure has been made to experience transient vibrations in the laboratory which the structure actually experiences in the field. Present work proposes that the test structure should be made to track transient vibrations in the laboratory which it would have experienced in the field. In present work, optimal tracking control strategy has been used successfully to track first three vibration modes of a cantilevered plate instrumented with piezoelectric sensor and actuator patches. Objectives of present work are listed as:

i To create a mathematical model of a smart cantilevered plate instrumented with piezoelectric sensor and actuator patches.
ii To develop an optimal controller to track first three vibration modes of cantilevered plate.
iii To simulate tracking of first three modes of the structure using MATLAB software.
iv Experimentally track first three modes of the structure using Labview software.

2.7. Plan of work

In chapter 3 mathematical model of cantilevered plate instrumented with sensor and actuator patches is developed using MATLAB software. In this chapter mathematical model using finite element technique based on Hamilton's principle is developed for a mild-steel plate instrumented with piezoelectric patches. The model is reduced to first three modes using orthonormal truncation method. Then truncated model is converted to a state space model. In chapter 4 the concept of Kalman filter is explained. Kalman observer is required to estimate states of system during experiments. In chapter 5, optimal tracking control is developed to track modes of vibration. In this chapter optimal control based on Riccati equation has been derived to track first three modes of vibration simultaneously. Then Kalman observer is constructed to estimate all the

states of the state-space model. In chapters 6 & 7 simulation and experimental results of this work are discussed in detail. In these chapters simulation results are obtained using MATLAB software, for tracking first two modes and first three modes of plate. Reference signals of plate are obtained by applying impulse signal on the piezoelectric actuator patch. Then optimal controller is developed to track vibration modes simultaneously. Experiments are conducted to track first three vibration modes of the smart plate simultaneously using LabView software. In chapter 8 conclusions are drawn and future scope of this work are discussed.

2.8. Conclusions:

In this chapter comprehensive review (over 100 papers) has been done of intelligent structures. The literature survey on active vibration control has been classified as: mathematical modelling of structures (beam like, plate-like & shell-like and complex), optimal placement of sensors/actuators and control laws. Based on this comprehensive study, gaps in literature have been identified. Thereafter scope of work and organisation of present work have been discussed in detail.

Chapter 3: Mathematical model of a cantilevered plate structure

3.1. Introduction

Mathematical model of an active structure is required for implementing an Active Vibration Control (AVC) scheme. Finite element techniques [97] and experimental modal analysis [98] have been used frequently in AVC applications. Mathematical equation of beam can be derived using Lagrangian theory [99], Kirchhoff theory [100], Euler-Bernoulli beam theory [101] etc. In active vibration control mathematical model of composite structure, hybrid structure, sandwich structure and multilayer structures can be carried out using Classical theories [102], First order Shear Deformation Theory (FSDT) [103], Third Order Theory (TOT) [104], High order Shear deformation theory [105], layerwise displacement theory [106], Reddy theory [107] etc. Using these methods displacement variables are calculated through the thickness for all the layers, with different material properties of the layers. Equilibrium equations, Von-karman theory, direct numerical integration method also can be utilized while making mathematical model of structures. Finite element techniques have been extensively used to express the mathematical model of structures. Finite element techniques have been used based on Hamilton's principle [108], Galerkin approach [109], Rayleigh-Ritz theory [110] and Hooke's law [111]. After extracting the equations of motion of structures in terms of differential equations, model can be reduced to smaller order using modal truncation. Generally mathematical model of structures are created using physical specifications of structure (mass, stiffness and damping). It has been shown that environment effects also can change the equations of motion. Thermal effect [112], electric-field effect [113], hygro effect [114], magnetic field effect [115] can be incorporated in mathematical model of structures.

In this chapter, mathematical model of a cantilevered plate instrumented with piezoelectric patches is developed. Many real life structures are in the shape of a cantilevered plate such as satellite structures, aircraft wings, wind turbine blades etc.

Piezoelectric patches are used extensively in active vibration control as sensors and actuators. Finite element techniques have emerged as confident techniques to model dynamics of mechanical structures. Finite element method based on Hamilton's principle is used in this work to find the dynamic equations of structure. Application of Hamilton's principle for developing mathematical model of a simple two degree of freedom system is illustrated in section 3.2. In section 3.3, a cantilevered plate is considered and expression is derived for Lagrangian of the system. In section 3.4, equations of motion of the smart plate are derived using Hamilton's principle. Equations of motion are decoupled using modal analysis in section 3.5 and finally in section 3.6 decoupled equations of motion are used to create a state-space model of the system.

3.2. Illustration of Hamilton's principle via a simple two degree of freedom system

Let us try to write equations of motion of a simple two degrees of freedom system as shown in figure (3.1). Mass $'M_1'$ is connected to a boundary through a spring $'K_1'$ and is connected to mass $'M_2'$ through a spring $'K_2'$. Similarly, mass $'M_2'$ is connected to a boundary through a spring $'K_3'$ and is connected to mass $'M_1'$ through a spring $'K_2'$.

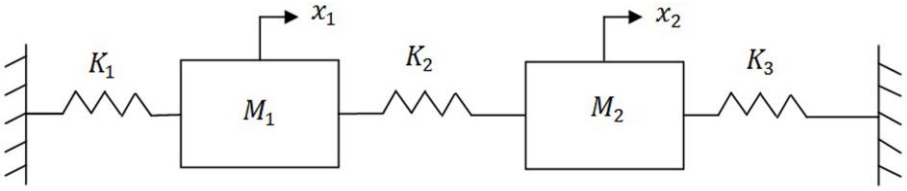

Figure 3.1 Two degrees of freedom spring-mass system

According to Hamilton's principle,

$$\delta \int_{t_0}^{t_1} (T - V)dt = 0 \qquad (3.1)$$

where $'T'$ is kinetic energy and $'V'$ is potential energy of the system at an instant of time. Time instants t_0 and t_1 are arbitrarily chosen. Kinetic energy of the system displayed in figure (3.1) can be expressed as:

$$T = \frac{1}{2}M_1\dot{x}_1^2 + \frac{1}{2}M_2\dot{x}_2^2 \qquad (3.2)$$

potential energy of the system can be expressed as:

$$V = \frac{1}{2}K_1 x_1^2 + \frac{1}{2}K_2(x_1 - x_2)^2 + \frac{1}{2}K_3 x_2^2 \tag{3.3}$$

applying variation operator on the kinetic and potential energy expressions, we have:

$$\begin{aligned} \delta T &= \frac{\partial T}{\partial \dot{x}_1}\delta \dot{x}_1 + \frac{\partial T}{\partial \dot{x}_2}\delta \dot{x}_2 \\ \delta V &= \frac{\partial V}{\partial x_1}\delta x_1 + \frac{\partial V}{\partial x_2}\delta x_2 \end{aligned} \tag{3.4}$$

substituting in equation (3.1),

$$\delta \int_{t_0}^{t_1} (\frac{\partial T}{\partial \dot{x}_1}\delta \dot{x}_1 + \frac{\partial T}{\partial \dot{x}_2}\delta \dot{x}_2 - \frac{\partial V}{\partial x_1}\delta x_1 - \frac{\partial V}{\partial x_2}\delta x_2)dt = 0 \tag{3.5}$$

this can be rewritten as:

$$\begin{aligned} &\frac{\partial T}{\partial \dot{x}_1}\delta x_1|_{t_0}^{t_1} - \int_{t_0}^{t_1} \frac{d}{dt}\left(\frac{\partial T}{\partial \dot{x}_1}\right)\delta x_1 dt + \frac{\partial T}{\partial \dot{x}_2}\delta x_2|_{t_0}^{t_1} \\ &- \int_{t_0}^{t_1} \frac{d}{dt}(\frac{\partial T}{\partial \dot{x}_2})\delta x_2 dt - \int_{t_0}^{t_1} (\frac{\partial V}{\partial x_1}\delta x_1 - \frac{\partial V}{\partial x_2}\delta x_2)dt = 0 \end{aligned} \tag{3.6}$$

at time instants t_0 and t_1 variations in displacement are zero, therefore:

$$\frac{\partial T}{\partial \dot{x}_1}\delta x_1|_{t_0}^{t_1} = \frac{\partial T}{\partial \dot{x}_2}\delta x_2|_{t_0}^{t_1} = 0 \tag{3.7}$$

so now equation (3.5) can be written as:

$$\int_{t_0}^{t_1} \left[\left(-\frac{d}{dt}\left(\frac{\partial T}{\partial \dot{x}_1}\right) - \frac{\partial V}{\partial x_1}\right)\delta x_1 + \left(-\frac{d}{dt}\left(\frac{\partial T}{\partial \dot{x}_2}\right) - \frac{\partial V}{\partial x_2}\right)\delta x_2\right] dt = 0 \tag{3.8}$$

above equation will be satisfied if coefficients of $\delta x_1$and δx_2 are zero, i.e.

$$-\frac{d}{dt}\left(\frac{\partial T}{\partial \dot{x}_1}\right) - \frac{\partial V}{\partial x_1} = 0 \tag{3.9}$$

and

$$-\frac{d}{dt}\left(\frac{\partial T}{\partial \dot{x}_2}\right) - \frac{\partial V}{\partial x_2} = 0 \tag{3.10}$$

again considering equations (3.2) and (3.3), we have:

$$\begin{aligned} \frac{\partial T}{\partial \dot{x}_1} &= M_1 \dot{x}_1 \\ \frac{\partial T}{\partial \dot{x}_2} &= M_2 \dot{x}_2 \end{aligned} \tag{3.11}$$

and

$$\frac{\partial V}{\partial x_1} = K_1 x_1 + K_2(x_1 - x_2)$$
$$\frac{\partial V}{\partial x_2} = K_2(x_1 - x_2) + K_3 x_2 \tag{3.12}$$

equations of motion are finally obtained as under by making these substitution in equations (3.9) and (3.10).

$$-M_1\ddot{x}_1 - K_1 x_1 - K_2(x_1 - x_2) = 0$$
$$-M_2\ddot{x}_2 - K_3 x_2 + K_2(x_1 - x_2) = 0 \tag{3.13}$$

or,

$$-M_1\ddot{x}_1 - (K_1 + K_2)x_1 + K_2 x_2 = 0$$
$$-M_2\ddot{x}_2 + K_2 x_1 - (K_2 + K_3)x_2 = 0 \tag{3.14}$$

These equations can be verified by obtaining equations of motion form free-body diagrams. The free-body diagrams of the two masses can be written as:

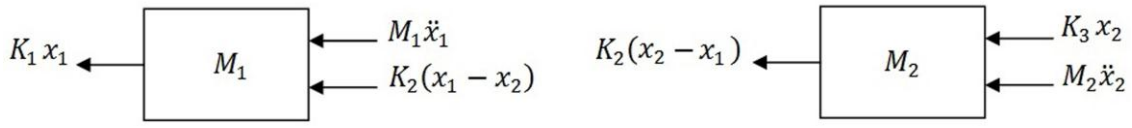

Figure 3.2 Free-body diagrams of two degree of freedom spring-mass system

From these free body diagrams equations of motions are obtained as:

$$M_1\ddot{x}_1 + (K_1 + K_2)x_1 - K_2 x_2 = 0$$
and
$$M_2\ddot{x}_2 - K_2 x_1 + (K_2 + K_3)x_2 = 0 \tag{3.15}$$

Above two equations are same as equations (3.14) which have been derived using Hamilton's principle. So, for deriving equations of motion using Hamilton's principle one has to simply substitute expressions of kinetic energy and potential energy in Hamilton's principle. For deriving equations of motion using free body diagrams one has to draw free-body diagrams and balance forces. Derivation of equations of motion using free-body diagrams is suitable for simple problems and Hamilton's principle approach has been found apt for complex problems & continuous structures. Mathematical modeling technique via Hamilton's principle that has been illustrated here for a simple

discrete system will now be exploited to model a continuous plate structure in following sections.

3.3. Finite element model of a smart plate

Consider a thin cantilevered mild-steel plate of size $16cm \times 16cm$, as shown in figure (3.3). This plate is discretized into $'64'$ equal elements of size $2cm \times 2cm$. One piezoelectric sensor patch is pasted at 11^{th} element and one piezoelectric patch is pasted at 14^{th} element.

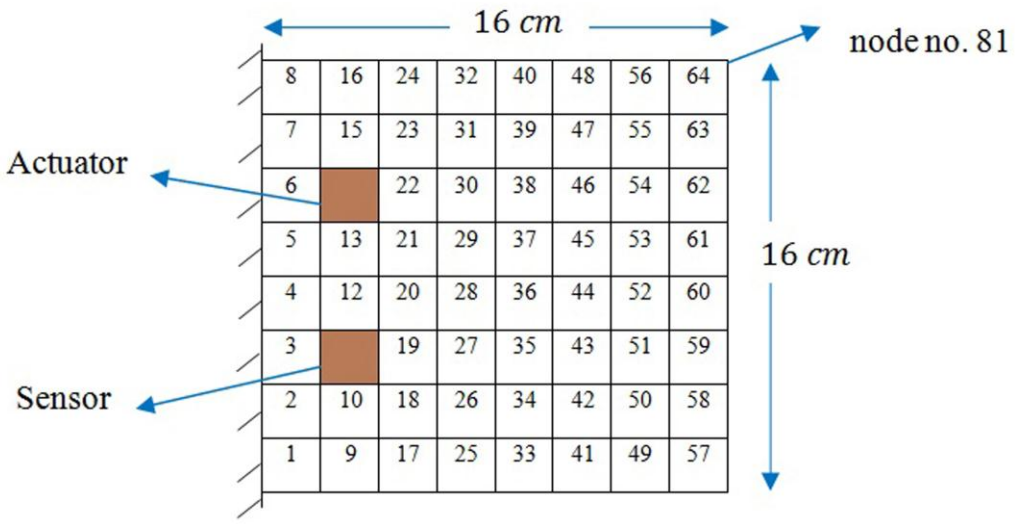

Figure 3.3 Cantilevered plate

Quadrilateral plate element, as shown in figure (3.4), with four node points is used for finite element modeling. Six degrees of freedom are possible at each node. Three degrees of freedom have been considered at each node as:

w displacement normal to the plane of the plate

$\theta_y = -\frac{\partial w}{\partial y}$ rotation about x axis

$\theta_x = \frac{\partial w}{\partial x}$ rotation about y axis

At the piezoelectric patch location, the structure is composite with one layer of mild steel and one piezoelectric layer. Constitutive equations of piezoelectricity can be written as:

$$\{D\} = [e]\{\varepsilon\} + [\zeta]\{E\}$$
$$\{\sigma\} = [D_p]\{\varepsilon\} - [e]^T\{E\} \tag{3.16}$$

where D, E, ε & σ are the electric displacement, electric field, strain and stress vectors respectively. D_p, e and ζ are the elasticity, piezoelectric constant and dielectric constant matrices respectively. For elastic material of the base structure the constitutive equation is:

$$\{\sigma\} = [D_s]\{\varepsilon\} \tag{3.17}$$

where D_s is the elasticity constant matrix of the main structure.

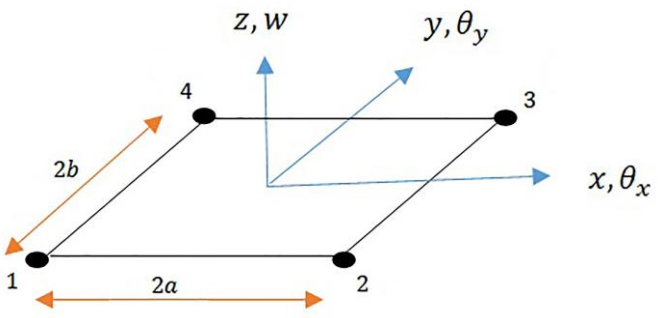

Figure 3.4 Quadrilateral plate element

The normal displacement w can be expressed in terms of nodal displacements as:

$$w = [N_1 N_2 N_3 N_4]\{u^e\}$$
$$= [N]\{u^e\} \tag{3.18}$$

where N_1, N_2, N_3 & N_4 are shape functions and $\{u^e\}$ is a vector of elemental degrees of freedom which is given by:

$$\{u^e\}^T = \left[w_1\ \theta_{x1}\ \theta_{y1}, \dots, w_4\ \theta_{x4}\ \theta_{y4}\right] \tag{3.19}$$

strain vector can be expressed as function of nodal displacements as:

$$\{\varepsilon\} = z\begin{Bmatrix} -\dfrac{\partial^2 w}{\partial x^2} \\ -\dfrac{\partial^2 w}{\partial y^2} \\ -2\dfrac{\partial^2 w}{\partial x \partial y} \end{Bmatrix} \tag{3.20}$$

substituting (3.18) in (3.20) we have:

$$\{\varepsilon\} = z\begin{Bmatrix} -\dfrac{\partial^2}{\partial x^2} \\ -\dfrac{\partial^2}{\partial y^2} \\ -2\dfrac{\partial^2}{\partial x \partial y} \end{Bmatrix}[N]\{u^e\} \tag{3.21}$$

taking

$$[B_u] = \begin{Bmatrix} -\dfrac{\partial^2}{\partial x^2} \\ -\dfrac{\partial^2}{\partial y^2} \\ -2\dfrac{\partial^2}{\partial x \partial y} \end{Bmatrix}[N]$$

we have,

$$\{\varepsilon\} = z[B_u]\{u^e\} \tag{3.22}$$

In present case electric voltage is applied only perpendicular to the plane of the piezoelectric patch, therefore electrical field vector becomes:

$$\{E\} = -\begin{Bmatrix} 0 \\ 0 \\ \dfrac{1}{h_p} \end{Bmatrix}v = -\{B_v\}v \tag{3.23}$$

where v is voltage applied across the piezoelectric patch and h_p is thickness of piezoelectric patch. Total kinetic energy of one finite element can be written as:

$$T_e = \frac{1}{2}\int_{Q_s} \rho_s \dot{w}^2 dQ + \int_{Q_p} \rho_p \dot{w}^2 dQ \tag{3.24}$$

where ρ is density and subscripts s & p refer to main structure & piezoelectric structure respectively. Total potential energy of one finite element can be written as:

$$U_e = \frac{1}{2}\int_{Q_s} \{\varepsilon\}^T\{\sigma\} dQ + \frac{1}{2}\int_{Q_p} \{\varepsilon\}^T\{\sigma\} dQ \tag{3.25}$$

The electrostatic potential energy stored in one element is:

$$W_{elec} = \frac{1}{2}\int_{Q_p} \{E\}^T\{D\} dQ \tag{3.26}$$

Sum of energy stored by the surface force and the energy required to apply surface

electrical charge on piezoelectric is:

$$W_{ext} = \int_{s1} \{w\}^T \{f_s^e\}\, ds - \int_{s2} vq\, ds \tag{3.27}$$

where $\{f_s^e\}$ is the surface force vector, q is applied surface electrical charge density and s_1 & s_2 are surface area of plate & surface area of piezoelectric patch respectively. Lagrangian for one finite element of plate is:

$$L = T_e - U_e + (W_{elec} + W_{ext}) \tag{3.28}$$

after substituting the values of kinetic energy, potential energy and work done by one element the Lagrangian becomes:

$$\begin{aligned} L = &\left(\frac{1}{2}\int_{Q_s} \rho_s \dot{w}^2 dQ + \int_{Q_p} \rho_p \dot{w}^2 dQ\right) \\ &-\left(\frac{1}{2}\int_{Q_s} \{\varepsilon\}^T\{\sigma\} dQ + \frac{1}{2}\int_{Q_p} \{\varepsilon\}^T\{\sigma\} dQ\right) \\ &+\left(\frac{1}{2}\int_{Q_p} \{E\}^T\{D\} dQ + \int_{s1} \{w\}^T\{f_s^e\}\, ds - \int_{s2} vq\, ds\right) \end{aligned} \tag{3.29}$$

substituting w, $\{\varepsilon\}$ and $\{E\}$ in (3.29) we have:

$$\begin{aligned} L = &\left(\frac{1}{2}\,\rho_s \int_{Q_s} \{\dot{u}^e\}^T[N]^T[N]\{\dot{u}^e\} dQ + \frac{1}{2}\,\rho_p \int_{Q_p} \{\dot{u}^e\}^T[N]^T[N]\{\dot{u}^e\} dQ\right) \\ &-\left(\frac{1}{2}\int_{Q_s} (z\,[B_u]\{u^e\})^T\{\sigma\} dQ + \frac{1}{2}\int_{Q_p} (z\,[B_u]\{u^e\})^T\{\sigma\} dQ\right) \\ &+\left(\frac{1}{2}\int_{Q_p} (-[B_v]v)^T\{D\} dQ + \int_{s1} ([N]\{u^e\})^T\{f_s^e\}\, ds - \int_{s2} qv\, ds)\right) \end{aligned} \tag{3.30}$$

or,

$$\begin{aligned} L = &\left(\frac{1}{2}\,\rho_s \int_{Q_s} \{\dot{u}^e\}^T[N]^T[N]\{\dot{u}^e\} dQ\right. \\ &\left. + \frac{1}{2}\,\rho_p \int_{Q_p} \{\dot{u}^e\}^T[N]^T[N]\{\dot{u}^e\} dQ\right) \end{aligned} \tag{3.31}$$

$$-\left(\frac{1}{2}\int_{Q_s} z\,\{u^e\}^T[B_u]^T[\sigma]dQ + \frac{1}{2}\int_{Q_p} z\,\{u^e\}^T[B_u]^T[\sigma]dQ\right)$$
$$+\left(-\frac{1}{2}\int_{Q_p} v[B_v]^T\{D\}dQ + \int_{s1}\{u^e\}^T[N]^T\{f_s^e\}\,ds - \int_{s2} qv\,ds)\right)$$

substituting values of $\{D\}$ and $[\sigma]$ in equation (3.31) we have:

$$\begin{aligned} L = \Bigg(&\frac{1}{2}\,\rho_s\int_{Q_s}\{\dot{u}^e\}^T[N]^T[N]\{\dot{u}^e\}dQ \\ &+\frac{1}{2}\,\rho_p\int_{Q_p}\{\dot{u}^e\}^T[N]^T[N]\{\dot{u}^e\}dQ\Bigg) \\ &-\left(\frac{1}{2}\int_{Q_s} z\,\{u^e\}^T[B_u]^T[D_s]\{\varepsilon\}dQ\right) \\ &-\left(\frac{1}{2}\int_{Q_p} z\{u^e\}^T[B_u]^T(\big[D_p\big]\{\varepsilon\} - [e]^T[E])dQ\right) \\ &-\left(\frac{1}{2}\int_{Q_p} v[B_v]^T([e]\{\varepsilon\} - [\zeta][E])dQ\right) \\ &+\left(\int_{s1}\{u^e\}^T[N]^T\{f_s^e\}\,ds - \int_{s2} qv\,ds)\right) \end{aligned} \tag{3.32}$$

substituting $\{\varepsilon\}$ and $[E]$ from (3.22) and (3.23) in above equation, we have:

$$\begin{aligned} L = \Bigg(&\frac{1}{2}\,\rho_s\int_{Q_s}\{\dot{u}^e\}^T[N]^T[N]\{\dot{u}^e\}dQ + \frac{1}{2}\,\rho_p\int_{Q_p}\{\dot{u}^e\}^T[N]^T[N]\{\dot{u}^e\}dQ\Bigg) \\ &-\left(\frac{1}{2}\int_{Q_s} z\,\{u^e\}^T[B_u]^T(z[D_s][B_u]\{u^e\})dQ\right) \\ &-\left(\frac{1}{2}\int_{Q_p} z\{u^e\}^T[B_u]^T(z\big[D_p\big][B_u]\{u^e\} - [e]^T[B_v]v)dQ\right) \\ &-\left(\frac{1}{2}\int_{Q_p} v[B_v]^T(z[e][B_v]\{u^e\} - [\zeta][B_v]v)dQ\right) \\ &+\left(\int_{s1}\{u^e\}^T[N]^T\{f_s^e\}\,ds - \int_{s2} qv\,ds\right) \end{aligned} \tag{3.33}$$

3.4. Deriving equations of motion using Hamilton's principle

According to Hamilton's principle integration of Lagrangian between any two arbitrarily selected time intervals t_0 and t_1 must satisfy following equation:

$$\delta \int_{t_0}^{t_1} L dt = 0 \tag{3.34}$$

Substituting expression of Lagrangian from equation (3.33) we have:

$$\begin{aligned}
&\delta \int_{t_0}^{t_1} L dt = \\
&\delta \int_{t_0}^{t_1} \left(\frac{1}{2} \rho_s \int_{Q_s} \{\dot{u}^e\}^T [N]^T [N] \{\dot{u}^e\} dQ + \frac{1}{2} \rho_p \int_{Q_p} \{\dot{u}^e\}^T [N]^T [N] \{\dot{u}^e\} dQ \right) \\
&- \left(\frac{1}{2} \int_{Q_s} z^2 \{u^e\}^T [B_u]^T [D_s] [B_u] \{u^e\} dQ \right) \\
&- \left(\frac{1}{2} \int_{Q_p} z^2 \{u^e\}^T [B_u]^T \left[D_p\right] [B_u] \{u^e\} + zv \{u^e\}^T [B_u]^T [e^T]^T [B_v] \, dQ \right) \\
&- \left(\frac{1}{2} \int_{Q_p} vz [B_v]^T [e^T] [B_u] \{u^e\} - v^2 [B_v]^T [\zeta] [B_v] dQ \right) \\
&+ \left(\int_{s1} \{u^e\}^T [N]^T \{f_s^e\} \, ds - \int_{s2} qv \, ds \right) dt = 0
\end{aligned} \tag{3.35}$$

In equation (3.35) we can take variation with respect to both variables $\{u^e\}$ and v one by one, separately. Taking variation with respect to $\{u^e\}$ we have:

$$\begin{aligned}
\int_{t_0}^{t_1} (& \frac{1}{2} \rho_s \int_{Q_s} \{\delta \ddot{u}^e\}^T [N]^T [N] \{\ddot{u}^e\} dQ \\
& + \frac{1}{2} \rho_s \int_{Q_s} \{\ddot{u}^e\}^T [N]^T [N] \{\delta \ddot{u}^e\} dQ \\
& + \frac{1}{2} \rho_p \int_{Q_p} \{\delta \ddot{u}^e\}^T [N]^T [N] \{\ddot{u}^e\} dQ \\
& + \frac{1}{2} \rho_p \int_{Q_p} \{\ddot{u}^e\}^T [N]^T [N] \{\delta \ddot{u}^e\} dQ
\end{aligned} \tag{3.36}$$

$$-\frac{1}{2}\int_{Q_s} z^2\,\{\delta u^e\}^T[B_u]^T[D_s][B_u]\{u^e\}dQ$$

$$-\frac{1}{2}\int_{Q_s} z^2\,\{u^e\}^T[B_u]^T[D_s][B_u]\{\delta u^e\}dQ$$

$$+\frac{1}{2}\int_{Q_p} z^2\{\delta u^e\}^T[B_u]^T\left[D_p\right][B_u]\{u^e\}\,dQ$$

$$+\int_{s1}\{\delta u^e\}^T[N]^T\{f_s\}\;ds) = 0$$

since $\left[D_p\right]$ and $[D_s]$ are symmetric matrices. Therefore equation becomes

$$\begin{aligned}
\int_{t_0}^{t_1}(&\frac{1}{2}\rho_s\int_{Q_s}\{\delta\dot{u}^e\}^T[N]^T[N]\{\dot{u}^e\}dQ+\frac{1}{2}\rho_s\int_{Q_s}\{\delta\dot{u}^e\}^T[N]^T[N]\{\dot{u}^e\}dQ\\
&+\frac{1}{2}\rho_p\int_{Q_p}\{\delta\dot{u}^e\}^T[N]^T[N]\{\dot{u}^e\}dQ\\
&+\frac{1}{2}\rho_p\int_{Q_p}\{\delta\dot{u}^e\}^T[N]^T[N]\{\dot{u}^e\}dQ\\
&-\frac{1}{2}\int_{Q_s} z^2\,\{\delta u^e\}^T[B_u]^T[D_s][B_u]\{u^e\}dQ\\
&-\frac{1}{2}\int_{Q_s} z^2\,\{\delta u^e\}^T[B_u]^T[D_s][B_u]\{u^e\}dQ\\
&-\frac{1}{2}\int_{Q_p} z^2\{\delta u^e\}^T[B_u]^T\left[D_p\right][B_u]\{u^e\}\,dQ\\
&-\frac{1}{2}\int_{Q_p} z^2\{\delta u^e\}^T[B_u]^T\left[D_p\right][B_u]\{u^e\}\,dQ\\
&-\frac{1}{2}\int_{Q_p} zv\{\delta u^e\}^T[B_u]^T[e^T]^T[B_v]\,dQ\\
&-\frac{1}{2}\int_{Q_p} zv\{\delta u^e\}^T[B_u]^T[e^T][B_v]\,dQ\\
&+\int_{s1}\{\delta u^e\}^T[N]^T\{f_s\}\;ds) = 0
\end{aligned} \tag{3.37}$$

or,

$$\int_{t_0}^{t_1}\Bigg(\rho_s\int_{Q_s}\{\delta\ddot{u}^e\}^T[N]^T[N]\{\ddot{u}^e\}dQ+\rho_p\int_{Q_p}\{\delta\ddot{u}^e\}^T[N]^T[N]\{\ddot{u}^e\}dQ$$
$$-\int_{Q_s}z^2\{\delta u^e\}^T[B_u]^T[D_s][B_u]\{u^e\}dQ$$
$$-\int_{Q_p}z^2\{\delta u^e\}^T[B_u]^T\left[D_p\right][B_u]\{u^e\}\,dQ \qquad (3.38)$$
$$-\int_{Q_p}zv\{\delta u^e\}^T[B_u]^T[e^T]^T[B_v]\,dQ$$
$$+\int_{s1}\{\delta u^e\}^T[N]^T\{f_s\}\;ds\Bigg)dt=0$$

performing integration by parts of first two terms of equation (3.38):

$$\rho_s\int_{Q_s}(\{\delta u^e\}^T[N]^T[N]\{\dot{u}^e\})\,|_{t_0}^{t_1}dQ$$
$$-\rho_s\int_{t_0}^{t_1}\int_{Q_s}(\{\delta u^e\}^T[N]^T[N]\{\ddot{u}^e\})\,dQdt$$
$$+\rho_p\int_{Q_p}(\{\delta u^e\}^T[N]^T[N]\{\dot{u}^e\})\,|_{t_0}^{t_1}dQ$$
$$-\rho_p\int_{t_0}^{t_1}\int_{Q_p}(\{\delta u^e\}^T[N]^T[N]\{\ddot{u}^e\})\,dQdt$$
$$+\int_{t_0}^{t_1}\Bigg[-\int_{Q_s}(z^2\{\delta u^e\}^T[B_u]^T[D_s][B_u]\{u^e\})\,dQ \qquad (3.39)$$
$$-\int_{Q_p}\left(z^2\{\delta u^e\}^T[B_u]^T\left[D_p\right][B_u]\{u^e\}\right)dQ$$
$$-\int_{Q_p}(zv\{\delta u^e\}^T[B_u]^T[e^T]^T[B_v])\,dQ$$
$$+\int_{s1}(\{\delta u^e\}^T[N]^T\{f_s\})\;ds\Bigg]=0$$

or,

$$\begin{aligned}
&-\rho_s \int_{t_0}^{t_1} \int_{Q_s} (\{\delta u^e\}^T [N]^T [N] \{\ddot{u}^e\})\, dQ dt \\
&\quad - \rho_p \int_{t_0}^{t_1} \int_{Q_p} (\{\delta u^e\}^T [N]^T [N] \{\ddot{u}^e\})\, dQ dt \\
&\quad + \int_{t_0}^{t_1} \int_{Q_s} (z^2\, \{\delta u^e\}^T [B_u]^T [D_s] [B_u] \{u^e\})\, dQ dt \\
&\quad - \int_{t_0}^{t_1} \int_{Q_p} \left(z^2 \{\delta u^e\}^T [B_u]^T \left[D_p\right] [B_u] \{u^e\}\right) dQ dt \\
&\quad - \int_{t_0}^{t_1} \int_{Q_p} (z v \{\delta u^e\}^T [B_u]^T [e^T]^T [B_v])\, dQ dt \\
&\quad + \int_{t_0}^{t_1} \int_{s1} (\{\delta u^e\}^T [N]^T \{f_s\})\ ds\, dt = 0
\end{aligned} \tag{3.40}$$

by taking out common term $\{\delta u^e\}^T$ equation becomes:

$$\begin{aligned}
\{\delta u^e\}^T \int_{t_0}^{t_1} \Bigg[&-\rho_s \int_{Q_s} ([N]^T [N] \{\ddot{u}^e\})\, dQ - \rho_p \int_{Q_p} ([N]^T [N] \{\ddot{u}^e\})\, dQ \\
&- \int_{Q_s} (z^2 [B_u]^T [D_s] [B_u] \{u^e\})\, dQ \\
&- \int_{Q_p} \left(z^2 [B_u]^T \left[D_p\right] [B_u] \{u^e\}\right) dQ \\
&- \int_{Q_p} (z v [B_u]^T [e^T]^T [B_v])\, dQ + \int_{s1} ([N]^T \{f_s\})\ ds \Bigg] = 0
\end{aligned} \tag{3.41}$$

to satisfy above equation the terms inside the bracket must be equal to zero as:

$$\begin{aligned}
&-\rho_s \int_{Q_s} ([N]^T [N] \{\ddot{u}^e\})\, dQ - \rho_p \int_{Q_p} ([N]^T [N] \{\ddot{u}^e\})\, dQ \\
&- \int_{Q_s} (z^2 [B_u]^T [D_s] [B_u] \{u^e\})\, dQ \\
&+ \int_{Q_p} \left(z^2 [B_u]^T \left[D_p\right] [B_u] \{u^e\}\right) dQ
\end{aligned} \tag{3.42}$$

$$-\int_{Q_p}(zv[B_u]^T[e^T]^T[B_v])\,dQ+\int_{s1}([N]^T\{f_s\})\;ds=0$$

after rearranging we get:

$$\left[\rho_s\int_{Q_s}([N]^T[N])\,dQ+\rho_p\int_{Q_p}([N]^T[N])\,dQ\right]\{\ddot{u}^e\}$$
$$+\left[\int_{Q_s}(z^2[B_u]^T[D_s][B_u])\,dQ+\int_{Q_p}\left(z^2[B_u]^T\left[D_p\right][B_u]\right)dQ\right]\{u^e\}\qquad(3.43)$$
$$+\left[\int_{Q_p}(z[B_u]^T[e^T]^T[B_v])\,dQ\right]v=\int_{s1}([N]^T\{f_s\})\;ds$$

Equation (3.43) can be written as follows and is called as matrix equation of motion of one element:

$$\left(\left[m_p\right]+[m_s]\right)\{\ddot{u}^e\}+\left(\left[k_p\right]+[k_s]\right)\{u^e\}+[k_{uv}]v=\{F_s^e\}\qquad(3.44)$$

where,

$\left[m_p\right]=\rho_p\int_{Q_p}[N]^T[N]dQ$ is elemental mass matrix for piezoelectric

$[m_s]=\rho_s\int_{Q_s}[N]^T[N]dQ$ is elemental mass matrix for plate structure

$[k_s]=\int_{Q_s}z^2[B_u]^T[D_s][B_u]\,dQ$ is elemental stiffness matrix for plate structure

$\left[k_p\right]=\int_{Q_p}z^2[B_u]^T\left[D_p\right][B_u]dQ$ is elemental stiffness matrix for piezoelectric

$[k_{uv}]=\int_{Q_p}z[B_u]^T[e]^T[B_v]\,dQ$ is elemental electromechanical interaction matrix

$\{F_s^e\}=\int_{s1}[N]^T\{f_s\}\;ds$ is elemental external force acting on the structure

Similarly taking variation of equation (3.35) with respect to $'v'$ equation becomes:

$$\delta \int_{t_0}^{t_1} L dt = \int_{t_0}^{t_1} \left[-\frac{1}{2} \int_{Q_p} z\, \delta v\, [B_u]^T [e^T]^T [B_v] \{u^e\} dQ \right.$$

$$-\frac{1}{2} \int_{Q_p} \delta v\, [B_v]^T [e^T] z [B_u] \{u^e\} dQ \qquad (3.45)$$

$$\left. + \int_{Q_p} \delta v\, [B_v]^T [\zeta^T] [B_v] v dQ - \int_{s2} \delta v\, q\, ds \right] dt = 0$$

again taking out common term $'\delta v'$, above equation becomes:

$$\delta v \int_{t_0}^{t_1} \left[-\frac{1}{2} \int_{Q_p} z [B_v]^T [e^T] [B_u] \{u^e\} dQ \right.$$

$$-\frac{1}{2} \int_{Q_p} z [B_v]^T [e^T] [B_u] \{u^e\} dQ \qquad (3.46)$$

$$\left. + \int_{Q_p} v [B_v]^T [\zeta^T] [B_v] dQ - \int_{s2} q\, ds \right] dt = 0$$

after simplification we have:

$$\delta v \int_{t_0}^{t_1} \left[-\int_{Q_p} z [B_v]^T [e^T] [B_u] \{u^e\} dQ + \int_{Q_p} v [B_v]^T [\zeta^T] [B_v] dQ - \int_{s2} q\, ds \right] dt = 0 \qquad (3.47)$$

above equation will be satisfied if terms inside the bracket are equal to zero i.e:

$$-\int_{Q_p} z [B_v]^T [e^T] [B_u] \{u^e\} dQ + \int_{Q_p} v [B_v]^T [\zeta^T] [B_v] dQ - \int_{s2} q\, ds = 0 \qquad (3.48)$$

on further simplification we get:

$$-\int_{Q_p} (z [B_v]^T [e^T] [B_u] + v [B_v]^T [\zeta^T] [B_v]) \{u^e\} dQ = \int_{s2} q\, ds \qquad (3.49)$$

Equation (3.49) can be expressed in simple form as:

$$-[k_{vu}] \{u^e\} + [k_{vv}] v = \bar{q} \qquad (3.50)$$

The total voltage generated across piezoelectric patch is due to structural vibrations and externally applied charge. The voltage developed across piezoelectric patch can be expressed as:

$$v = \frac{\bar{q} + [k_{uv}] \{u^e\}}{[k_{vv}]} \qquad (3.51)$$

where,

$\bar{q} = \int_{s2} q ds$ is external charge applied on piezoelectric surface

$[k_{vv}] = \int_{Q_p} [B_v]^T [\zeta][B_v] v \, dQ$ is the capacitance of piezoelectric sensor

substituting equation (3.51) in equation (3.44) gives equation of motion as:

$$([m_p] + [m_s])\{\ddot{u}^e\} + ([k_s] + [k_p])\{u^e\} + [k_{uv}][k_{vv}]^{-1}(\bar{q} + [k_{vu}]\{u^e\}) = \{F_s^e\} \quad (3.52)$$

Following assembly procedure, mass matrices, stiffness matrices and force vectors of individual elements can be assembled to produce global matrix equation of motion of the two-dimensional smart cantilevered plate instrumented with piezoelectric sensor and actuator as:

$$[M]\{\ddot{u}\} + [K]\{u\} = \{F\} \quad (3.53)$$

where [M] & [K] are global mass & stiffness matrices respectively of the system and $\{F\}$ is vector of excitation forces. In figure (3.5) the finite element mesh of smart plate is shown, having 64 elements and 81 nodes. Each node has three degrees of freedom.

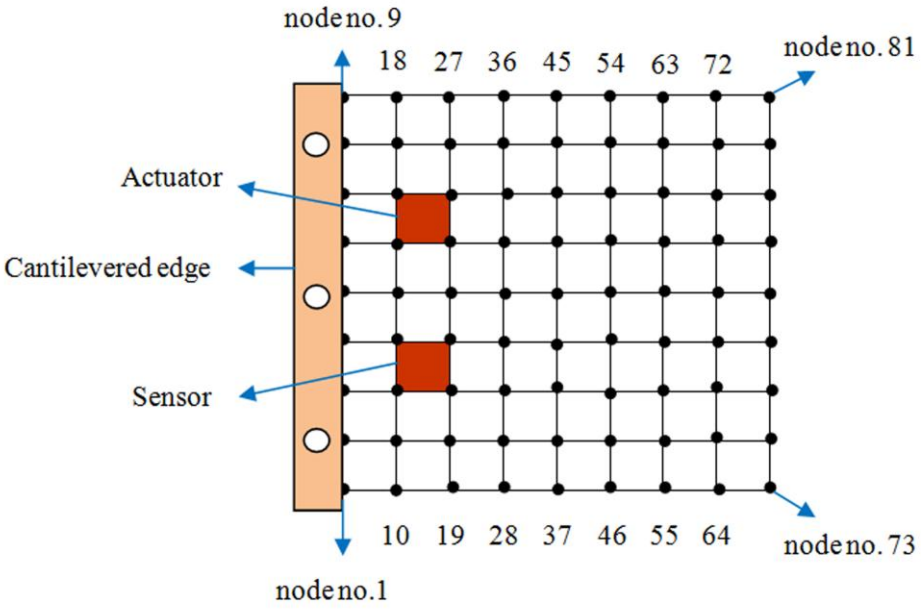

Figure 3.5 Finite element mesh on the smart plate

Therefore, global matrices of final equation of motion have order of 243×243 as:

$$[M]_{243\times243}\{\ddot{u}\}_{243\times1} + [K]_{243\times243}\{u\}_{243\times1} = \{F\}_{243\times1} \tag{3.54}$$

For cantilevered plate whose one side is fixed in mechanical clamp first 27 nodes are fixed to boundary. Therefore order of equation of motion of cantilevered plate is reduced as:

$$[M]_{216\times216}\{\ddot{u}\}_{216\times1} + [K]_{216\times216}\{u\}_{216\times1} = \{F\}_{216\times1} \tag{3.55}$$

$\{F\}$ is vector of excitation forces plus actuation forces applied by actuator to control the mechanical vibrations and can be shown as:

$$\{F\}_{216\times1} = [d]_{1\times216}\{f_a(t)\}_{216\times1} + \{f_d(t)\}_{216\times1} \tag{3.56}$$

where $[d]$ is matrix of actuator location, $\{f_d(t)\}$ is vector of disturbance force and $\{f_a(t)\}$ is actuator force vector. The elasticity matrix for intelligent structure (cantilevered plate instrumented with piezoelectric patches) is expressed as:

$$[D_s] = \frac{Y}{(1-v)^2}\begin{bmatrix} 1 & \mu & 0 \\ \mu & 1 & 0 \\ 0 & 0 & \dfrac{1-\mu}{2} \end{bmatrix} \tag{3.57}$$

where Y, μ are the Young's modulus & Poisson's ratio of the material of the base structure respectively.

3.5. Modal analysis

To analyse a multi-degree of freedom system, it can converted to a single degree of freedom system using modal analysis. Orthonormal modal transformation is given by

$$\{\mathrm{d}\}_{3\times1} = [\mathrm{U}]_{3\times216}\{\eta(\mathrm{t})\}_{216\times3} \tag{3.58}$$

where $[U]$ & η are orthonormal modal matrix & modal vector respectively. A damping matrix is considered according to following relation in equation of motion:

$$[C]_{216\times216} = 2\times\xi\times\omega_n\times[M] \tag{3.59}$$

where ξ is damping ratio such that $0.001 < \xi < 0.007$ and ω_n is natural frequency of the plate. Equation (3.54) can be written in modal domain as:

$$[M][U]\{\ddot{\eta}\} + [C][U]\{\dot{\eta}\} + [K][U]\{\eta\} = [D]\{f_a\} + \{f_e\} \tag{3.60}$$

where $[U]$ is orthonormal modal matrix. Pre-multiplying (3.60) by $[U]^T$, becomes:

$$[U]^T[M][U]\{\ddot{\eta}\} + [U]^T[C][U]\{\dot{\eta}\} + [U]^T[K][U]\{\eta\} = [U]^T[D]\{f_a\} + [U]^T\{f_e\} \tag{3.61}$$

after simplification we have:

$$[I]\{\ddot{\eta}\} + [c]\{\dot{\eta}\} + [\lambda^2]\{\eta\} = [U]^T[D]\{f_a\} + [U]^T\{f_e\} \tag{3.62}$$

Equation of motion of r^{th} mode is:

$$\ddot{\eta}_r + c_r\dot{\eta}_r + \lambda_r^2\eta_r = q_r(t) + y_r(t) \qquad r = 1, \dots, n \tag{3.63}$$

where η_r, q_r & y_r represent modal displacement, modal control force, modal excitation force & natural frequency of r^{th} mode respectively. For first three modes we can write:

$$\begin{aligned} \ddot{\eta}_1 + c_1\dot{\eta}_1 + \lambda_1^2\eta_1 &= q_1 \\ \ddot{\eta}_2 + c_2\dot{\eta}_2 + \lambda_2^2\eta_2 &= q_2 \\ \ddot{\eta}_3 + c_3\dot{\eta}_3 + \lambda_3^2\eta_3 &= q_3 \end{aligned} \tag{3.64}$$

The total modal external force, acting on intelligent structure is:

$$\{\mathrm{F}\} = \{f_a(t)\} + \{f_e(t)\} \tag{3.65}$$

where, $\{f_e(t)\}$ is vector of excitation force/disturbance force and $\{f_a(t)\}$ is actuator force vector. Actuator force vector can be expressed as:

$$\{f_a(t)\} = [U]^T[k_{uv}][k_{vv}]^{-1}\frac{\varepsilon_{33} \times a}{h_{piezo}} \tag{3.66}$$

where $'\varepsilon_{33}'$ is permittivity of piezoelectric patch, $'a'$ is area of piezoelectric patch and $'h_{piezo}'$ is the thickness of piezoelectric patch.

3.6. State-space model

A mathematical model which is required for optimal controller must be in state space format as:

$$\{\dot{\mathrm{x}}\} = [A]\{\mathrm{x}\} + [B]\{\mathrm{u}\} \tag{3.67}$$

where $\{x\}$ & $\{u\}$ are system state & control vector respectively, $[A]$ & $[B]$ are system state matrix & control matrix respectively. The output relation is given as:

$$\{y\} = [C]\{x\} \tag{3.68}$$

where $[C]$ is output matrix. In order to convert equation of motion to state-space let us take:

$$\dot{\eta_1} = x_1$$
$$\dot{\eta_2} = x_2$$
$$\dot{\eta_3} = x_3$$

Modal equations of first three modes can be re-written as:

$$\begin{aligned} \dot{x}_1 + c_1 x_1 + \lambda_1^2 \eta_1 &= q_1 \\ \dot{x}_2 + c_2 x_2 + \lambda_2^2 \eta_2 &= q_2 \\ \dot{x}_3 + c_3 x_3 + \lambda_3^2 \eta_3 &= q_3 \end{aligned} \tag{3.69}$$

These equations can be expressed in matrix form as:

$$\begin{bmatrix} 0 & 0 & 0 & 1 & 0 & 0 \\ 0 & 0 & 0 & 0 & 1 & 0 \\ 0 & 0 & 0 & 0 & 0 & 1 \\ 1 & 0 & 0 & 0 & 0 & 0 \\ 0 & 1 & 0 & 0 & 0 & 0 \\ 0 & 0 & 1 & 0 & 0 & 0 \end{bmatrix} \begin{Bmatrix} \dot{x}_1 \\ \dot{x}_2 \\ \dot{x}_3 \\ \dot{\eta}_1 \\ \dot{\eta}_2 \\ \dot{\eta}_3 \end{Bmatrix} + \begin{bmatrix} 0 & 0 & 0 & 1 & 0 & 0 \\ 0 & 0 & 0 & 0 & 1 & 0 \\ 0 & 0 & 0 & 0 & 0 & 1 \\ -\lambda_1^2 & 0 & 0 & c_1 & 0 & 0 \\ 0 & -\lambda_2^2 & 0 & 0 & c_2 & 0 \\ 0 & 0 & -\lambda_3^2 & 0 & 0 & c_3 \end{bmatrix} \begin{Bmatrix} x_1 \\ x_2 \\ x_3 \\ \eta_1 \\ \eta_2 \\ \eta_3 \end{Bmatrix} = \begin{Bmatrix} 0 \\ 0 \\ 0 \\ q_1 \\ q_2 \\ q_3 \end{Bmatrix} \tag{3.70}$$

Let

$$[m_{ss}] = \begin{bmatrix} 0 & 0 & 0 & 1 & 0 & 0 \\ 0 & 0 & 0 & 0 & 1 & 0 \\ 0 & 0 & 0 & 0 & 0 & 1 \\ 1 & 0 & 0 & 0 & 0 & 0 \\ 0 & 1 & 0 & 0 & 0 & 0 \\ 0 & 0 & 1 & 0 & 0 & 0 \end{bmatrix}, \qquad \{x\} = \begin{Bmatrix} x_1 \\ x_2 \\ x_3 \\ \eta_1 \\ \eta_2 \\ \eta_3 \end{Bmatrix}$$

$$[k_{ss}] = \begin{bmatrix} 0 & 0 & 0 & 1 & 0 & 0 \\ 0 & 0 & 0 & 0 & 1 & 0 \\ 0 & 0 & 0 & 0 & 0 & 1 \\ -\lambda_1^2 & 0 & 0 & c_1 & 0 & 0 \\ 0 & -\lambda_2^2 & 0 & 0 & c_2 & 0 \\ 0 & 0 & -\lambda_3^2 & 0 & 0 & c_3 \end{bmatrix}, \quad f = \begin{Bmatrix} 0 \\ 0 \\ 0 \\ q_1 \\ q_2 \\ q_3 \end{Bmatrix} \tag{3.71}$$

Equations (3.70) and (3.71) can be manipulated to write as:

$$\{\dot{x}\} = -[m_{ss}]^{-1}[k_{ss}]\{x\} + [m_{ss}]^{-1} f \tag{3.72}$$

Let $[A] = -[m_{ss}]^{-1}[k_{ss}]$ then we have:

$$\{\dot{x}\} = [A]\{x\} + [m_{ss}]^{-1} f \tag{3.73}$$

substituting equation (3.66) we have:

$$\{\dot{x}\} = [A]\{x\} + [m_{ss}]^{-1}[U]^T[k_{uv}][k_{vv}]^{-1}\frac{\varepsilon_{33} \times a}{h_{piezo}} \tag{3.74}$$

Let

$$[B] = [m_{ss}]^{-1}[U]^T[k_{uv}][k_{vv}]^{-1}\frac{\varepsilon_{33} \times a}{h_{piezo}} \tag{3.75}$$

therefore state-space model of cantilevered plate becomes:

$$\begin{gathered}\{\dot{x}\} = [A]\{x\} + [B]\{u\} \\ \{y\} = [C]v_{sen}\end{gathered} \tag{3.76}$$

where $[C]$ is output matrix and v_{sen} is voltage generated by piezoelectric sensor as:

$$v_{sen} = [k_{vu}][k_{vv}]^{-1}\{u\} \tag{3.77}$$

3.7. Conclusions

In this chapter mathematical model of a cantilevered plate instrumented with piezoelectric sensor and actuator patch is derived in detail. The finite element technique based on Hamilton's principle is employed to do so. The cantilevered plate is discretized into 64 elements and 81 nodes. The finite element has four nodes in the corner and each node has three degrees of freedom. The equation of motion of a cantilevered plate is expressed by using a global mass matrix, stiffness matrix and external force vector. The equations of motions are truncated to first three modes using modal truncation. Thereafter the model is converted into a state-space model to be used by the optimal controller eventually in following chapters.

Chapter 4: Discrete time Kalman estimator

4.1.Introduction

Man is interested in mechanical vibrations so as to design stable structures, monitor condition of dynamic structures, diagnose faults in machines, identify parameters of a structure and control vibrations (passively as well as actively). A typical vibration signal is summation of time responses of several modes of vibration. Fourier analysis of a vibration signal gives frequencies that are participating and individual extent of their participation. Time responses of individual modes of vibration can be computed theoretically using orthonormal modal transformation. Vibration modes can be experimentally measured using modal sensors. Many control laws require information of all variables of the state-space model. It is very difficult to measure all the state variables, particularly when measurement value contains uncertainty, random error or variation. Therefore, a program is required to estimate unknown states of the system based upon data available from a limited number of sensors. Researchers have given a lot of attention to state observers [116, 117, 118, 119]. State vector of linear system can be reconstructed from observation of single input-single output system [120] or multi input-multi output [121]. Kalman filter was proposed by Rudolf E. Kalman for estimation of states of linear discrete-time systems [122, 123]. Richard S. Bucy proposed Kalman-Bucy filter for continuous-time linear control systems [124]. There are many systems which cannot be presented in linear form, therefore Extended-Kalman filter was proposed to deal with nonlinear systems [125]. As figure (4.1) shows, a state observer is a mathematical technique, which can estimate unknown states of a system by comparing input and output.

There are two types of state estimators: full order state observer which estimates all states of a system regardless of whether some states are available for direct measurement and reduced order state observer which estimates only remaining states of system which are not measured. Kalman filter is widely used for robotic, navigation, GPS, control system etc.

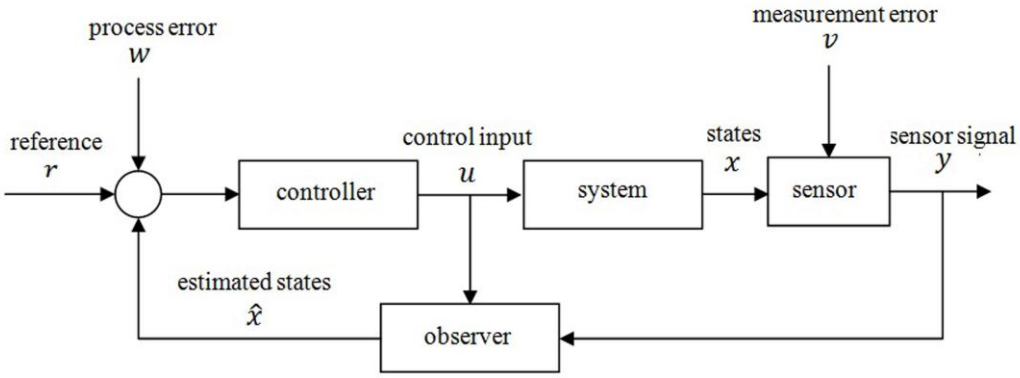

Figure 4.1 Control system with state observer

Following subsections discuss these two types of state observers. Thereafter, well known discrete Kalman observer which has been used in this work, is discussed. Kalman observer is illustrated in this chapter by applying it to estimate states of a test two degrees of freedom spring-mass-damper system.

4.2. Full order state observer

Consider a continuous system described by state space model as:

$$\begin{aligned} \dot{x}(t) &= Ax(t) + Bu(t) \\ y(t) &= Cx(t) \end{aligned} \tag{4.1}$$

where A, B & C are $n \times n$, $n \times 1$ & $1 \times n$ real constant matrices respectively and $x(t)$, $u(t)$ & $y(t)$ are state, control & output vectors respectively. In this approach, as it is shown in figure (4.2), a model of real plant is constructed and considered as estimator to predict states of the original system as:

$$\dot{\hat{x}}(t) = A\hat{x}(t) + Bu(t) \tag{4.2}$$

where $\hat{x}(t)$ is estimated vector of actual state vector $x(t)$; A, B & $u(t)$ are known and $\hat{x}(0) = x(0)$.

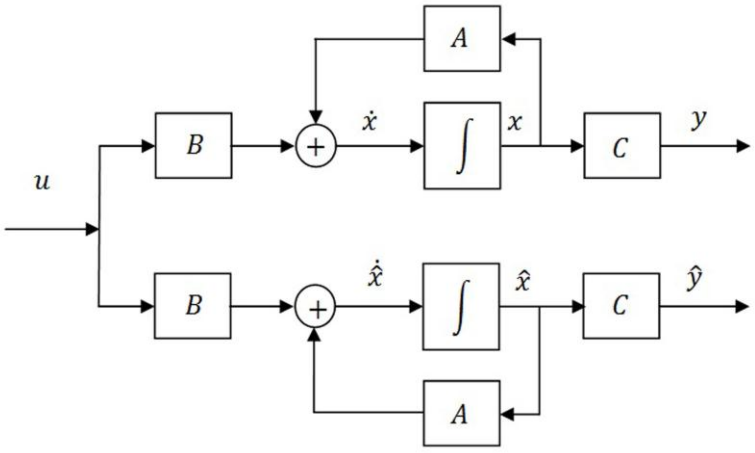

Figure 4.2 Full order state observer

System shown in figure (4.2) is an open loop system and therefore the error keeps on growing with time. To minimize error between estimated states and actual states, feedback control can be used. In order to increase the speed of full order state observer and correct the model, Luenberger proposed to add feedback of difference between actual output y and estimated output $\hat{y}$ (figure (4.3)).

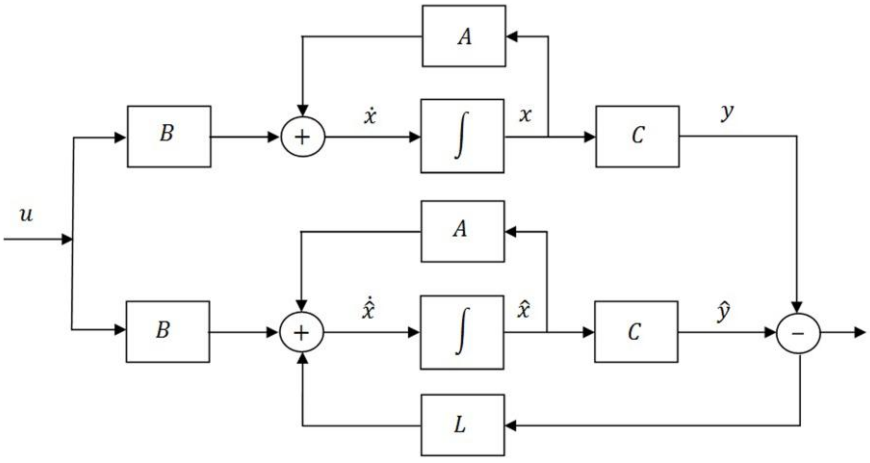

Figure 4.3 Luenberger state observer

Process equation of Luenberger state observer is expressed as:

$$\dot{\hat{x}}(t) = A\hat{x}(t) + L[y(t) - C\hat{x}(t)] + Bu(t) \tag{4.3}$$

where L is $n \times 1$ real constant gain matrix which can be calculated by following procedure. The state error vector is:

$$\tilde{x}(k) = x(k) - \hat{x}(k) \tag{4.4}$$

by differentiating both sides we have:

$$\dot{\tilde{x}}(t) = \dot{x}(t) - \dot{\hat{x}}(t) \tag{4.5}$$

substituting expressions from (4.1) and (4.3) in (4.5):

$$\begin{gathered} \dot{\tilde{x}}(t) = Ax(t) + Bu(t) - A\hat{x}(t) - Bu(t) - L[y(t) - C\hat{x}(t)] \\ \dot{\tilde{x}}(t) = (A - LC)\tilde{x}(t) \end{gathered} \tag{4.6}$$

The feedback gain L can be computed from Eigen values obtained from following equation:

$$|sI - (A - LC)| = 0 \tag{4.7}$$

4.3. Reduced order state observer

It is not reasonable to estimate all the states of a system when some of them are available. Also sometimes system contains a lot of noise which makes it difficult to estimate all the states of system using full order state observer. Therefore in such cases, an observer can be used to estimate only those states which cannot be measured. In order to use reduced order state observer system is divided into two parts (measurable part and estimated part) as:

$$\begin{gathered} \begin{bmatrix} \dot{x}_1 \\ \dot{x}_e \end{bmatrix} = \begin{bmatrix} a_{11} & a_{1e} \\ a_{e1} & A_{ee} \end{bmatrix} \begin{bmatrix} x_1 \\ x_e \end{bmatrix} + \begin{bmatrix} b_1 \\ b_e \end{bmatrix} u \\ y = \begin{bmatrix} 1 & 0 \end{bmatrix} \begin{bmatrix} x_1 \\ x_e \end{bmatrix} \end{gathered} \tag{4.8}$$

where x_1 is vector of direct measurable states and x_e is vector of estimated states. The equation of estimated states is:

$$\dot{x}_e = A_{ee}x_e + a_{e1}x_1 + b_e u \tag{4.9}$$

where $a_{e1}x_1$ & $b_e u$ are known already and can be considered as input to estimated part. On the other hand, measurable part can be expressed as:

$$\dot{x}_1 = a_{11}x_1 + a_{1e}x_e + b_1 u \tag{4.10}$$

Using output equation (4.8), equation (4.10) becomes:

$$\dot{y} - a_{11}y - b_1 u = a_{1e}x_e \tag{4.11}$$

Comparing equations (4.9) & (4.10) with process equation (4.3) of Luenberger observer we find that $'x_e'$, $'A_{ee}'$, $'a_{e1}x_1 + b_e u'$, $'\dot{y} - a_{11}y - b_1 u'$ & $'a_{1e}'$ represent $'\hat{x}'$, $'A'$, $'Bu'$, $'y'$ & $'C'$ respectively. Equation of the reduced order observer can therefore be written as:

$$\dot{\hat{x}} = A_{ee}\hat{x}_e + a_{e1}y + b_e u + m(\dot{y} - a_{11}y - b_1 u - a_{1e}\hat{x}_e) \tag{4.12}$$

the state error vector can be expressed as:

$$\tilde{x}_e = x_e - \hat{x}_e \tag{4.13}$$

Characteristic equation of the system is given by:

$$|sI - (A_{ee} - ma_{1e})| = 0 \tag{4.14}$$

The observer gain $'m'$ can be so selected that desired dynamic characteristics are obtained.

4.4. Kalman observer

Kalman filter was proposed by R. E. Kalman, the Hungarian scientist in 1960 to find a solution to improve city train schedule. Kalman filter is a world known mathematical tool which is being used as trajectory estimator in dynamic systems. For tracking first three modes of cantilevered plate, all states of the system need to be available. Since the measurement of all the states of the system is difficult, an observer is used to estimate

states of the system. Therefore in following subsections, concept of white noise is explained and subsequently Kalman observer is illustrated.

4.4.1. White noise

Kalman filter estimates the states of a system in presence of process noise and measurement noise. These noises are assumed to be white noise. The white noise has a distribution of Gaussian form with mean of zero and certain variance.

$$\mu = \frac{\sum w_i}{n} = 0 \tag{4.15}$$

where μ is mean, n is number of samples and w_i is measurement noise variable. Variance is calculated as:

$$\begin{aligned} \delta^2 &= \frac{\sum (w_i - \mu)}{n} \\ &= E(w_i^2) - [E(w_i)]^2 \\ &= E(w_i w_i^T) \end{aligned} \tag{4.16}$$

Where δ^2 is variance and E is expected value. The covariance matrix is calculated as:

$$\begin{aligned} Cov\big(w(k)\, w(k+n)\big) &= \begin{bmatrix} \delta_{w_1}^2 & \dots & 0 \\ \vdots & \ddots & \vdots \\ 0 & \dots & \delta_{w_n}^2 \end{bmatrix} \\ &= E(w(k)\, w(k)^T) \end{aligned} \tag{4.17}$$

4.4.2. Illustration of discrete Kalman filter

Kalman filter is used to estimate unknown states of discrete-time control system expressed by linear difference equation as:

$$x(k) = Ax(k-1) + Bu(k) + w(k-1) \tag{4.18}$$

with sensor measurement relation as:

$$y(k) = Cx(k) + v(k) \tag{4.19}$$

In a real process, A and B matrices may vary with time, but here they are assumed to be constant. Here $w(k)$ & $v(k)$ are process noise & measurement noise respectively which are assumed to be white noise, constant and independent of each other with normal probability distribution as:

$$\begin{aligned} P(w) &\sim N(0, Q) \\ Q &= E(ww^T) \end{aligned} \tag{4.20}$$

That means, process noise has a normal Gaussian probability distribution of zero-mean ($\mu = 0$) and covariance of Q. For measurement noise probability distribution is:

$$\begin{aligned} P(v) &\sim N(0, R) \\ R &= E(vv^T) \end{aligned} \tag{4.21}$$

where R is measurement noise covariance matrix. The error between actual measurement and estimated states is:

$$\begin{aligned} \bar{e}(k) &= x(k) - \bar{\hat{x}}(k) \\ e(k) &= x(k) - \hat{x}(k) \end{aligned} \tag{4.22}$$

where $\bar{e}(k)$ (with super minus) is defined priori error, $e(k)$ is posteriori estimate error, $\bar{\hat{x}}(k)$ is priori state and $\hat{x}(k)$ is posteriori state. Priori estimate error covariance and posteriori estimate error covariances are:

$$\begin{aligned} \bar{\Psi}(k) &= E[\bar{e}\ \bar{e}^T] \\ \Psi(k) &= E[e\ e^T] \end{aligned} \tag{4.23}$$

for finding the posteriori state estimate the following equation is considered:

$$\hat{x}(k) = \bar{\hat{x}}(k) + M(y(k) - C\bar{\hat{x}}(k)) \tag{4.24}$$

where new states (posteriori states) are estimated and corrected by multiplying some gain to the residual value. The term $(y(k) - C\bar{\hat{x}}(k))$ that is difference between actual value $y(k)$ & measurement prediction $C\bar{\hat{x}}(k)$ is called 'residual value' and M is real constant feedback gain matrix that is selected to minimize the posteriori error covariance. To satisfy equation (4.24), gain matrix M is given as:

$$M(k) = \bar{\Psi}(k)C^T(C\bar{\Psi}(k)C^T + R)^{-1} \tag{4.25}$$

after rearranging we get:

$$M(k) = \frac{\bar{\Psi}(k)C^T}{C\bar{\Psi}(k)C^T + R} \tag{4.26}$$

From equation (4.26) it is observed that if measurement error covariance R approaches zero, gain becomes:

$$\lim_{R(k)\to 0} M(k) = C^{-1} \tag{4.27}$$

In this condition, actual measurement $(y(k) = Cx(k))$ is trusted more. Similarly in equation (4.26) if priori estimate error covariance $\bar{\Psi}$ approaches zero we have:

$$\lim_{\bar{\Psi}(k)\to 0} M(k) = 0 \tag{4.28}$$

So now, predicted measurement $(\hat{y}(k) = C\hat{x}(k))$ is trusted more than actual measurement. Kalman filter estimates states of the system by using feedback control. Two steps are there in a Kalman filter: time update (predictor) and measurement update (corrector). In time update, current state and error covariance estimates are used to obtain the priori estimate for the next time step. In measurement update, a feedback is used with priori estimate to obtain an improved posteriori estimate. Working of Kalman filter is displayed in figure (4.4).

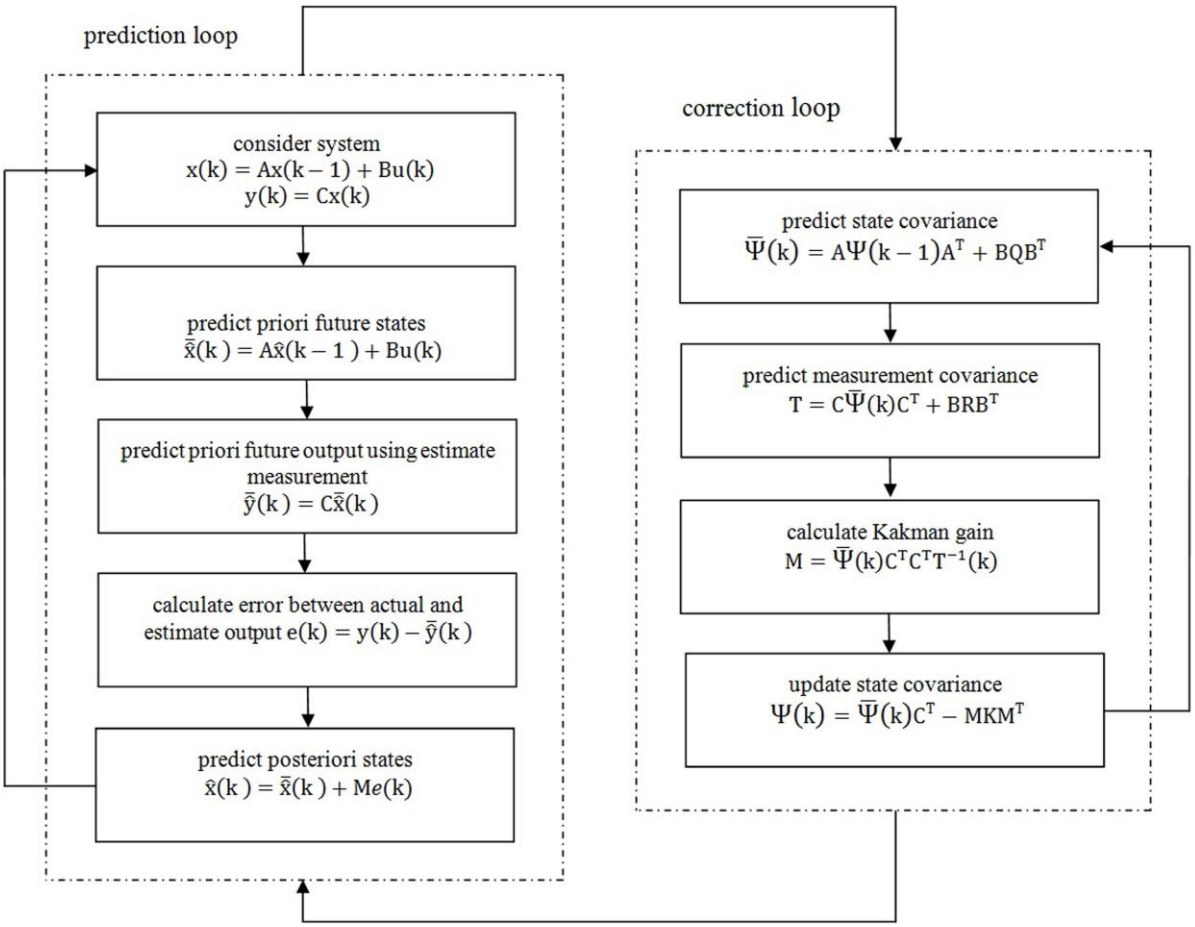

Figure 4.4 Flowchart of Kalman filter

Let us consider two degrees of freedom system described in section 1.4 of chapter 1. Kalman filter as detailed in present chapter, has been used to estimate displacement of two masses shown in figure (1.2). Figures (4.5) & (4.6) shows time response of actual displacements and estimated displacements of two masses. Good match is observed between displacements computed and estimated. Process noise covariance Q and measurement noise covariance R are considered as:

$$Q = 1, \qquad R = 0.01, \qquad N = [0.1] * 0.001$$

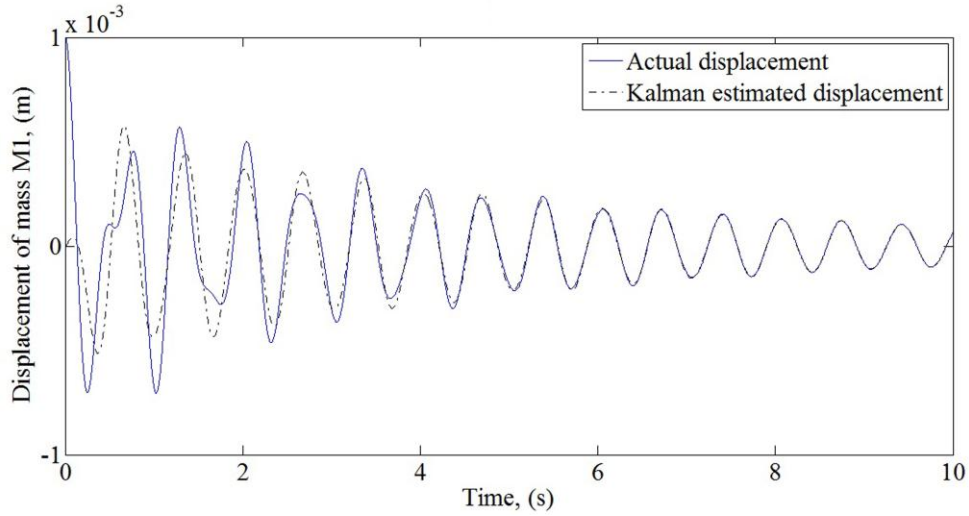

Figure 4.5 Actual/estimated displacements of two degrees of freedom system for mass M1

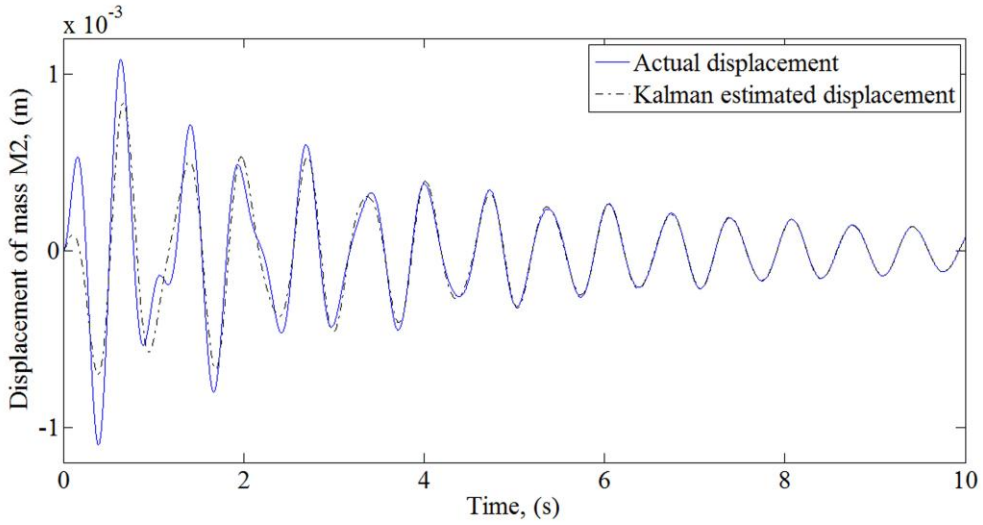

Figure 4.6 Actual/estimated displacements of two degrees of freedom system for mass M2

4.5. Conclusions

In this chapter concept of an observer has been introduced and Kalman filter is described in detail. To apply Kalman observer on a system, one has to execute two steps: first predict the states of system and then correct the predicted states using feedback control. Feedback gain can be defined to apply an appropriate correction on predicted states. The process of estimation and correction of states is continuously done in the Kalman observer to obtain time response of estimated states.

Chapter 5: Discrete time Linear Quadratic Tracking control

5.1. Introduction

A dynamic system varies from one state to another state with time depending on load, environmental conditions etc. There are numerous possible methods for controlling a dynamic system. Usually control laws are constructed that simultaneously minimize settling time and control effort. Optimal control law is derived by optimizing a performance index. Aim of an optimal control is to manipulate a sensor signal to satisfy a system such that a predecided performance index based on appropriate cost function is extremised. The concept of optimal control was proposed by L.S. Pontryagin, a soviet mathematician, in 1962 two decades after using modern control theories [126]. Optimal control has been extensively used in active vibration control. Optimal tracking control suggests optimal control gains which optimize a performance index depending on transient error and control effort [127]. Generally to derive an optimal control following steps are required:

- derive a mathematical model in state-space form of the system
- define a cost function or performance index to be extremised
- define a control law considering optimal value of performance index and boundary conditions

Linear Quadratic Regulator (LQR) controller and Linear Quadratic Gaussian (LQG) controller are two special types of the optimal controllers which have been used frequently in active vibration control. LQR and LQG are quadratic in control and regulation of error variable. The aim of the controller is to keep/regulate the state of the system close to zero. In Linear Quadratic Tracking (LQT) control, the output signal of the system is optimally maintained as close as possible to desired reference signals that keep on changing with time. In this chapter the mathematical background of LQT is discussed in detail.

5.2. Linear quadratic tracking control

In previous chapter finite element model of the smart plate is converted into state space model of following form:

$$\dot{x}(t) = Ax(t) + Bu(t) \tag{5.1}$$

in discrete form, state-space can be written as:

$$x(k+1) = Fx(k) + Gu(k) \tag{5.2}$$

with output relation as:

$$y(k) = Cx(k) \tag{5.3}$$

where $x(k)$, $u(k)$ & $y(k)$ are state, control & output vectors respectively. A, B & C are system matrix, control matrix & sensor vector respectively. F & G are discretised form of system matrix & control vector respectively. Aim of optimal control is to minimize cost function which includes integrals of the control effort and error between actual output & desired output. To track desired output with minimum expenditure of control effort error vector can be defined as:

$$e(k) = y(k) - z(k) \tag{5.4}$$

where $e(k)$ & $z(k)$ are error & desired input respectively. In this work, modes of vibration will be tracked by minimizing a performance index shown in equation (5.5), which is quadratic cost functional involving quadratic of error and control terms [128].

$$\begin{aligned} J = {} & \frac{1}{2}\left[Cx\left(k_f\right) - z\left(k_f\right)\right]^T F \left[Cx\left(k_f\right) - z\left(k_f\right)\right] \\ & + \frac{1}{2}\sum_{k=k_0}^{k_f-1} [Cx(k) - z(k)]^T Q \, [Cx(k) - z(k)] + u^T(k) R u(k) \end{aligned} \tag{5.5}$$

with boundary condition $x(k_0) = x_0$. Here F is symmetric positive semi-definite matrix, z is n dimensional desired reference vector, Q is $m \times m$ symmetric positive semi-defiinite

matrix to keep error small, C is sensor dynamic voltage, R is positive definite matrix and k_f represents final location of the vector. Mathematical solution of LQT can be described using following steps:

- derive Hamiltonian function
- derive state and costate system
- derive open-loop optimal control law
- derive nonlinear matrix Difference Riccati Equation (DRE)
- derive close loop optimal control

To minimize the performance index we need to define Hamiltonian function as:

$$\mathcal{H}[x(k), u(k), \lambda(k+1)] = V[x(k), u(k), k] + \lambda^T(k+1) f(x(k), u(k), k) \tag{5.6}$$

where V is a function consisting of performance index to be minimized subject to constraining function f and λ is co-state variable. In this work, Hamiltonian function is formulated as:

$$\begin{aligned}\mathcal{H}\big(x(k), u(k), \lambda(k+1)\big) &= \frac{1}{2}\sum_{k=k_0}^{k_f-1}\{[Cx(k) - z(k)]^T Q\,[Cx(k) - z(k)] \\ &+ u^T(k) R u(k)\} + \lambda^T(k+1)[Ax(k) + Bu(k)]\end{aligned} \tag{5.7}$$

To derive LQT controller, we have to take differentiation of Hamiltonian with respect x, λ and u to find optimal state, optimal co-state and optimal control voltage respectively. Partial differentiation of Hamiltonian function with respect to λ gives optimal state as:

$$x^*(k+1) = \frac{\partial \mathcal{H}}{\partial \lambda^*(k+1)} \tag{5.8}$$

where quantities with asterisk in superscript represent optimal quantities. Substituting Hamiltonian function in above equation gives:

$$\frac{\partial \mathcal{H}}{\partial \lambda^*(k+1)} = \frac{\partial}{\partial \lambda^*(k+1)}\left(\frac{1}{2}\sum_{k=k_0}^{k_f-1}\{[Cx(k)-z(k)]^T Q\,[Cx(k) - z(k)] + u^T(k)Ru(k)\} + \lambda^T(k+1)[Ax(k)+Bu(k)]\right) \tag{5.9}$$

after simplification equation becomes:

$$\frac{\partial \mathcal{H}}{\partial \lambda^*(k+1)} = \frac{\partial}{\partial \lambda^*(k+1)}\lambda^T(k+1)[Ax(k)+Bu(k)] \tag{5.10}$$

Optimal state equation can be written as:

$$x^*(k+1) = Ax^*(k) + Bu^*(k) \tag{5.11}$$

by taking partial differentiation of equation (5.7) with respect to $'x'$ discrete optimal co-state equation becomes:

$$\lambda^*(k) = \frac{\partial \mathcal{H}}{\partial x^*(k)} \tag{5.12}$$

substituting $\mathcal{H}$ we have:

$$\frac{\partial \mathcal{H}}{\partial x^*(k)} = \frac{\partial}{\partial x^*(k)}\left(\frac{1}{2}\sum_{k=k_0}^{k_f-1}\{[Cx(k)-z(k)]^T Q\,[Cx(k)-z(k)] + u^T(k)Ru(k)\} + \lambda^T(k+1)[Ax(k)+Bu(k)]\right) \tag{5.13}$$

After simplification equation becomes:

$$= \frac{\partial}{\partial x^*(k)}\left\{\frac{1}{2}[Cx(k)-z(k)]^T Q\,[Cx(k)-z(k)] + \lambda^T(k+1)Ax(k)\right\} \tag{5.14}$$

or,

$$= \frac{\partial}{\partial x^*(k)} \left[\frac{1}{2}\left(x(k)^T C^T Q C x(k) - x(k)^T C^T Q z(k) - z^T(k) Q C x(k) + z^T(k) Q C x(k)\right)\right] + \frac{\partial}{\partial x^*(k)}[\lambda^T(k+1) A x(k)] \tag{5.15}$$

then

$$= \frac{1}{2}[C^T Q C x(k) - C^T Q^T C x(k) - C^T Q C Z(k) - C^T Q^T C Z(k)] + [A^T \lambda(k+1)] \tag{5.16}$$

since $Q = Q^T$, the equation becomes:

$$\lambda^*(k) = [C^T Q C x^*(k) - C^T Q Z(k)] + [A^T \lambda^*(k+1)] \tag{5.17}$$

Let us consider following definitions:

$$V = C^T Q C \;\; \& \;\; W = C^T Q \tag{5.18}$$

substituting these terms equation (5.17) becomes:

$$\lambda^*(k) = V x^*(k) - W Z(k) + A^T \lambda^*(k+1) \tag{5.19}$$

after rewriting the above equation, discrete optimal co-state equation becomes:

$$\lambda^*(k) = V x^*(k) + A^T \lambda^*(k+1) - W Z(k) \tag{5.20}$$

similarly taking partial differentiation of Hamiltonian equation (5.7) with respect to $'u'$, setting result equal to zero, we have:

$$\frac{\partial \mathcal{H}}{\partial u^*(k)} = \frac{\partial}{\partial u^*(k)}\left(\frac{1}{2}\sum_{k=k_0}^{k_f-1}\{[Cx(k) - z(k)]^T Q\,[Cx(k) - z(k)] + u^T(k) R u(k)\} + \lambda^T(k+1)[Ax(k) + Bu(k)]\right) = 0 \tag{5.21}$$

only parts of Hamiltonian function which contain u terms will remain, as:

$$\frac{1}{2}\frac{\partial}{\partial u^*(k)}[u^T(k)Ru(k)] + \frac{\partial}{\partial u^*(k)}\lambda^T(k+1)Bu(k) = 0 \tag{5.22}$$

or,

$$\frac{1}{2}[Ru(k)R^Tu(k)] + [B^T\lambda(k+1)] = 0 \tag{5.23}$$

since $R^T = R$, above equation becomes:

$$\frac{1}{2}[Ru(k)Ru(k)] + [B^T\lambda(k+1)] = 0 \tag{5.24}$$

after simplification,

$$[Ru(k)] + [B^T\lambda(k+1)] = 0 \tag{5.25}$$

after rearranging as:

$$[Ru(k)] = -[B^T\lambda(k+1)] \tag{5.26}$$

pre-multiplying equation by R^{-1} gives:

$$[R^{-1}Ru(k)] = -[R^{-1}B^T\lambda(k+1)] \tag{5.27}$$

therefore open loop discrete optimal control input equation becomes:

$$u^*(k) = -[R^{-1}B^T\lambda^*(k+1)] \tag{5.28}$$

substituting optimal control value (5.28) in equation (5.11) gives optimal state as:

$$x^*(k+1) = Ax^*(k) - BR^{-1}B^T\lambda^*(k+1) \tag{5.29}$$

Let us define,

$$E = BR^{-1}B^T \tag{5.30}$$

then equation (5.29) becomes:

$$x^*(k+1) = Ax^*(k) - E\lambda^*(k+1) \tag{5.31}$$

after combining equation (5.19) and equation (5.31) in matrix form we have:

$$\begin{bmatrix} x^*(k+1) \\ \lambda^*(k) \end{bmatrix} = \begin{bmatrix} A & -E \\ V & A^T \end{bmatrix} \begin{bmatrix} x^*(k) \\ \lambda^*(k+1) \end{bmatrix} + \begin{bmatrix} 0 \\ -W \end{bmatrix} Z(k) \tag{5.32}$$

where the initial condition is $x(k_0) = \{0\}$. Fundamental theorem of the calculus of variations gives generalized boundary condition as:

$$\left[\mathcal{H}^* + \left(\frac{\partial s(x^*(k),k)}{\partial k}\right)\right]_{k_f} \delta k_f + \left[\left(\frac{\partial s(x^*(k),k)}{\partial x^*(k)}\right) - \lambda^*(k)\right]^T_{k_f} \delta x(k_f) = 0 \tag{5.33}$$

where s is entire terminal cost term in the performance index given by equation (5.7). For free final state system the variation represented by $\delta x(k_f)$ at final discrete time instant k_f becomes zero in equation (5.33). The final boundary condition on state equation in canonical system represented by equation (5.32) is given as:

$$\left[\lambda^*(k) - \left(\frac{\partial s(x^*(k),k)}{\partial x^*(k)}\right)\right]^T_{k_f} \delta x(k_f) = 0 \tag{5.34}$$

the above equation will be satisfied when terms inside the bracket become equal to zero, therefore:

$$\lambda^*(k_f) = \left(\frac{\partial s(x^*(k_f),k_f)}{\partial x^*(k_f)}\right) \tag{5.35}$$

by substituting term $'s'$ in above equation we have:

$$\lambda^*(k_f) = \frac{\partial[\frac{1}{2}e^T(k_f)CFe(k_f)]}{\partial x^*(k_f)} \tag{5.36}$$

substituting term $'e'$ in above equation gives:

$$\lambda^*(k_f) = \frac{\partial}{\partial x^*(k_f)}\{\frac{1}{2}\left[Cx^*(k_f) - Z(k_f)\right]^T F[Cx^*(k_f) - Z(k_f)]\} \tag{5.37}$$

after simplification we get:

$$\begin{aligned}\lambda^*(k_f) = \frac{\partial}{\partial x^*(k_f)}\{\frac{1}{2}\big[&x^{*T}(k_f)C^T FCx^*(k_f) \\ &- x^{*T}(k_f)C^T FZ(k_f) - Z^T(k_f)FCx^*(k_f)Z(k_f) \\ &+ Z^T(k_f)FZ(k_f)\big]\}\end{aligned} \tag{5.38}$$

or,

$$\begin{aligned}\lambda^*(k_f) = \frac{1}{2}\big[&C^T FCx^*(k_f) + C^T FCx^*(k_f) - C^T FZ(k_f) \\ &- C^T F^T Z(k_f)\big]\}\end{aligned} \tag{5.39}$$

since $F^T = F$, we get:

$$-\lambda^*(k_f) = C^T FCx^*(k_f) - C^T FZ(k_f) \tag{5.40}$$

Boundary condition on co-state in equation (5.40) and solution of the system of equation (5.32) indicate that state and co-state are linearly related as:

$$-\lambda^*(k) = P(k)x^*(k) - g(k) \tag{5.41}$$

where $P(k)$ is $n \times n$ matrix and $g(k)$ is $n \times 1$ vector. Using above equation, at instant $(k+1)$ as:

$$\lambda^*(k+1) = P(k+1)x^*(k+1) - g(k+1) \tag{5.42}$$

substituting equation (5.42) in equation (5.31), gives:

$$x^*(k+1) = Ax^*(k) - E[P(k+1)x^*(k+1) - g(k+1)] \tag{5.43}$$

after simplification as:

$$x^*(k+1) = Ax^*(k) - EP(k+1)x^*(k+1) - Eg(k+1) \tag{5.44}$$

rearranging above equation gives,

$$x^*(k+1) + EP(k+1)x^*(k+1) = Ax^*(k) + Eg(k+1) \tag{5.45}$$

or,

$$x^*(k+1)[I + EP(k+1)] = Ax^*(k) + Eg(k+1) \tag{5.46}$$

rearranging again:

$$x^*(k+1) = [I + EP(k+1)]^{-1}[\,Ax^*(k) + Eg(k+1)] \tag{5.47}$$

now substituting equations (5.41) and (5.42) in equation (5.20) gives:

$$\begin{aligned} &P(k)x^*(k) - g(k) = \\ &Vx^*(k) + A^T[\,P(k+1)x^*(k+1) - g(k+1)] - WZ(k) \end{aligned} \tag{5.48}$$

substituting equation (5.43) in equation (5.48) gives:

$$\begin{aligned} &P(k)x^*(k) - g(k) = Vx^*(k) + A^TP(k+1)[I + EP\,(k+1)]^{-1} \\ &[Ax^*(k) + Eg(k+1)][-g(k+1)] - A^Tg(k+1) - WZ(k) = 0 \end{aligned} \tag{5.49}$$

after simplification:

$$\begin{aligned} &-P(k)x^*(k) + g(k)Vx^*(k) + A^TP(k+1)[I + EP\,(k+1)]^{-1} \\ &A^TP(k+1)[I + EP(k+1)]^{-1}Eg(k+1) - A^Tg(k+1) - WZ(k) = 0 \end{aligned} \tag{5.50}$$

with further simplification as:

$$\begin{aligned} &\{-P(k) + A^TP(k+1)[I + EP\,(k+1)]^{-1}A + V\}x^*(k) \\ &+\{g(k)A^TP(k+1)[I + EP(k+1)]^{-1}E - A^Tg(k+1) - WZ(k)\} = 0 \end{aligned} \tag{5.51}$$

due to factor of $x^*(k)$, first part of above equation must be equal to zero as:

$$-P(k) + A^T P(k+1)[I + EP\,(k+1)]^{-1}A + V = 0 \tag{5.52}$$

or,

$$P(k) = A^T P(k+1)[I + EP\,(k+1)]^{-1}A + V \tag{5.53}$$

therefore, the nonlinear matrix difference Riccati equation becomes:

$$P(k) = A^T[P^{-1}(k+1) + E]^{-1}A + V \tag{5.54}$$

similarly for second part of equation (5.51)

$$g(k) + A^T P(k+1)[I + EP(k+1)]^{-1}Eg(k+1) - A^T g(k+1) - WZ(k) = 0 \tag{5.55}$$

after rearranging the equation becomes:

$$g(k) = -A^T[P^{-1}(k+1) + E]^{-1}Eg(k+1) + A^T g(k+1) + WZ(k) \tag{5.56}$$

or

$$g(k) = -A^T\{I - [P^{-1}(k+1) + E]^{-1}E\}g(k+1) + WZ(k) \tag{5.57}$$

therefore, the linear vector difference equation becomes:

$$g(k) = \{A^T - A^T P(k+1)[I + EP(k+1) + E]^{-1}E\}g(k+1) + WZ(k) \tag{5.58}$$

Final boundary condition for solving backward nonlinear difference matrix Riccati equation is obtained as:

$$P(k_f) = C^T FC \tag{5.59}$$

Final boundary condition for solving backward of linear vector difference equation (5.54) is obtained as:

$$g(k_f) = C^T F Z(k_f) \tag{5.60}$$

Once control gains are obtained offline the close-loop optimal control is obtained using co-state equation (5.36) as:

$$u^*(k) = -R^{-1}B^T[P(k+1)x^*(k+1) - g(k+1)] \tag{5.61}$$

rewriting as:

$$\begin{aligned} u^*(k) = & -R^{-1}B^T P(k+1)[Ax^*(k) + Bu^*(k)] \\ & + R^{-1}B^T g(k+1) \end{aligned} \tag{5.62}$$

premultiplying both sides by R gives:

$$\begin{aligned} Ru^*(k) = & -RR^{-1}B^T P(k+1)Ax^*(k) - RR^{-1}B^T P(k+1)Bu^*(k) \\ & + RR^{-1}B^T g(k+1) \end{aligned} \tag{5.63}$$

rearranging,

$$\begin{aligned} & Ru^*(k) + B^T P(k+1)Bu^*(k) \\ & = -B^T P(k+1)Ax^*(k) + B^T g(k+1) \end{aligned} \tag{5.64}$$

rearranging again,

$$\begin{aligned} & [R + B^T P(k+1)B]u^*(k) \\ & = -B^T P(k+1)Ax^*(k) + B^T g(k+1) \end{aligned} \tag{5.65}$$

Therefore optimal control that optimizes the performance index is given by:

$$u^*(k) = -L_b(k)\, x^*(k) - L_f(k) g(k+1) \tag{5.66}$$

where feedback control gain $L(k)$ and feed forward control gain $L_g(k)$ are given by:

$$\begin{aligned} L_b(k) &= [RB^T P(k+1)B]^{-1}\, B^T P(k+1)A \\ L_f(k) &= [R + B^T P(k+1)B]^{-1}\, B^T \end{aligned} \tag{5.67}$$

Block diagram shown in figure (5.1) demonstrates implementation of the discrete-time optimal tracker.

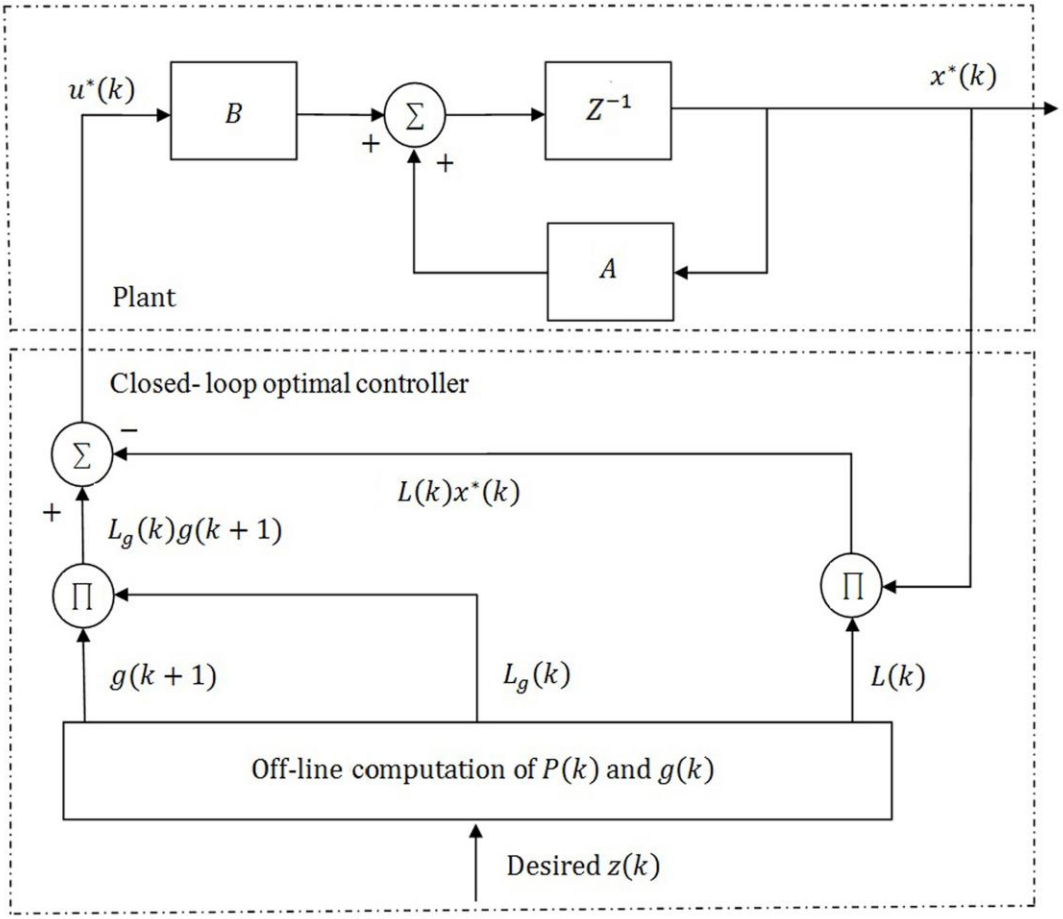

Figure 5.1 Block diagram of optimal tracking control

Substitution of optimal control law in equation of state gives optimal state x^* as:

$$\hat{x}^*(k+1) = [A - BL(k)]\hat{x}(k) + BL_g(k)g(k+1) \tag{5.68}$$

5.3. Conclusions

In this chapter, Linear Quadratic Tracking controller has been derived step by step. To make LQT controller track desired references a performance index minimizes the

error between desired output & actual output and the control effort. Generally, to develop LQT controller to track desired references following four steps have to be executed:

Step. 1. Formulate the appropriate Hamiltonian function based on the performance index.

Step. 2. Derive expressions for optimal state and co-state of system by taking differentiation of Hamiltonian with respect to co-state and state vector respectively.

Step. 3. Solve for the optimal state.

Step. 4. Derive optimal control voltages by taking differentiation of Hamiltonian function with respect to the control variable.

Chapter 6: Generating desired vibrations in a cantilevered plate: simulations

6.1. Introduction

A test structure can be dynamically tested very effectively if desired transient vibrations can be generated in the structure. Present work proposes to achieve this by using concept of 'active vibration control' with non-zero and time varying reference signals. In this chapter this proposed technique has been numerically applied on a cantilevered plate. Finite element model of structure discussed in chapter 3 and optimal tracking controller discussed in chapter 5 are used to perform numerical simulations.

6.2. LQT control based generation of desired vibrations

Consider a thin mild-steel cantilevered plate of size $160\ mm \times 160\ mm \times 0.51\ mm$. This plate is divided into $'64'$ equal quadrilateral elements of size $20\ mm \times 20\ mm$ as shown in figure (6.1). As can be observed, one PZT-5H piezoelectric patch is pasted at 11^{th} element to act as sensor and one PZT-5H piezoelectric patch is pasted at 14^{th} element to act as an actuator.

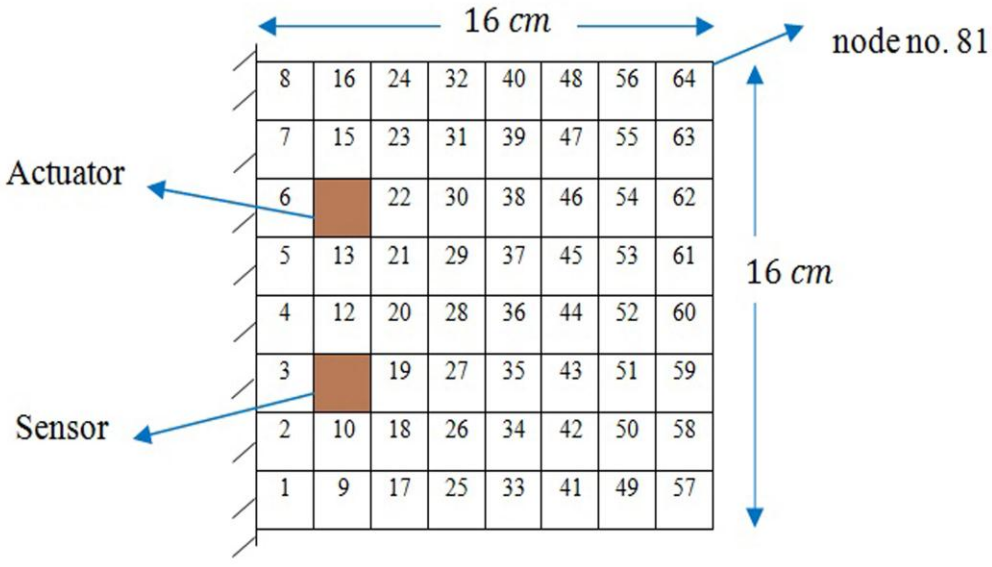

Figure 6. 1 Cantilevered plate

Piezoelectric patches have been located in regions where modal strains are large. Modal strains are high near the cantilevered edge of a cantilevered plate. Therefore piezoelectric patches have been located near the cantilevered edge of the plate. The properties of the SP-5H piezoelectric patch and mild-steel plate under test are tabulated in table (6.1).

Table 6.1 Properties of piezoelectric patches and plate under test

	length (mm)	width (mm)	thickness (mm)	density (Kg/m^3)	Young's modulus (N/m^2)	Poisson's ratio	d_{31} (m/volt)	relative dielectric constant
piezoelectric patch	20	20	1	7500	4.8 *e* 10	0.3	-285 *e* -12	3250
plate (mild-steel)	160	160	0.51	7800	2.07 *e* 11	0.3	-	-

The mathematical model of such a square plate with $'81'$ nodes and three degrees of freedom per node is coded in MATLAB software using finite element technique. Degrees of freedom corresponding to first $'9'$ nodes vanish due to fixed cantilevered boundary condition. The mathematical model is truncated to first three modes using orthonormal modal truncation. Thereafter the model is converted into a state-space form. Discrete form of corresponding state-space matrices of smart plate are as under (see equation (3.67)):

$$A = \begin{bmatrix} 0.98 & 9.20e^{-16} & 7.67e^{-16} & 0.002 & -1.95e^{-17} & -2.48e^{-18} \\ 1.79e^{-16} & 0.86 & 6.72e^{-16} & -2.34e^{-17} & 0.002 & -2.15e^{-17} \\ 2.98e^{-17} & 1.35e^{-16} & 0.25 & -3.72e^{-18} & -2.69e^{-18} & 0.001 \\ -22.27 & 1.36e^{-12} & 1.08e^{-12} & 0.97 & -1.89e^{-14} & -2.09e^{-15} \\ 2.65e^{-13} & -1.32e^{2} & 9.38e^{-13} & -2.27e^{-14} & 0.85 & -1.76e^{-15} \\ 4.19e^{-14} & 1.88e^{-13} & -6.37e^{+2} & -3.13e^{-15} & -2.20e^{-15} & 0.24 \end{bmatrix}$$

$$B = \begin{bmatrix} -7.59e^{-10} \\ -5.66e^{-10} \\ -7.68e^{-10} \\ -7.59e^{-7} \\ -5.52e^{-7} \\ -6.52e^{-7} \end{bmatrix}$$

In presented scheme, control voltage at a particular instant of time is dependent on all the modes. It is not that at a particular instant of time effort is explicitly made to track a particular mode (like in Independent Modal Space Control (IMSC) or Modified

Independent Modal Space Control (MIMSC)). All modes are simultaneously tracked at a particular instant of time. The flowchart of proposed technique is shown in figure (6.2)

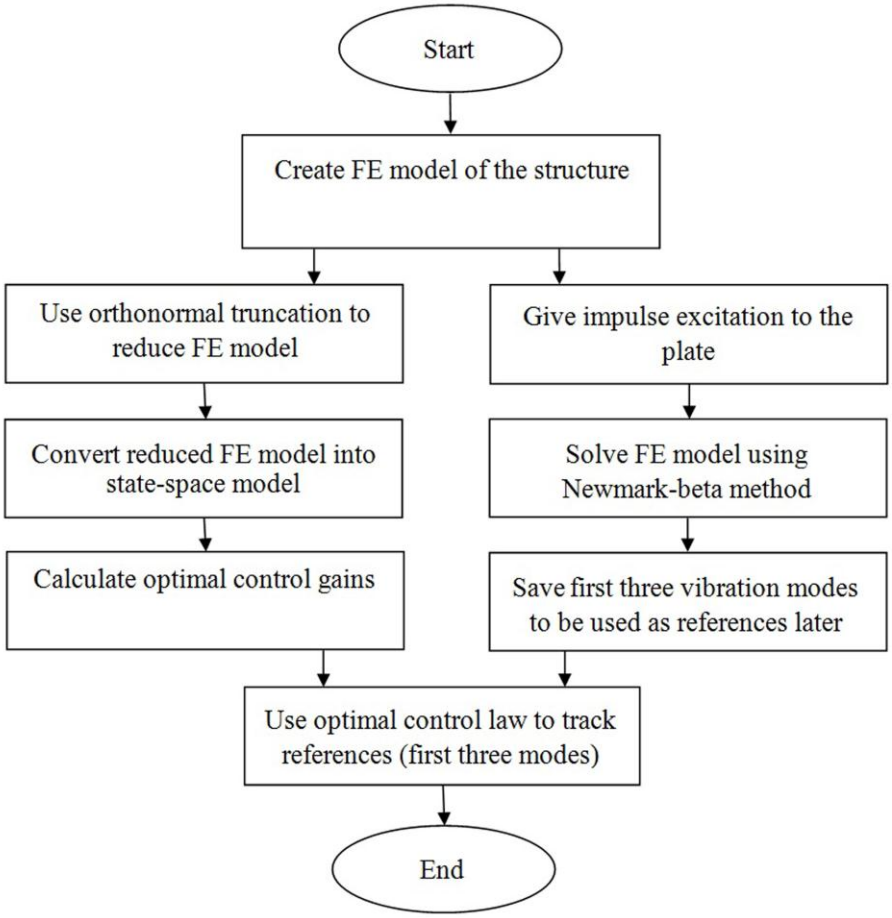

Figure 6. 2 Flowchart for theoretical simulations

Time response of vibrations of the plate contains several modes of vibration. Fourier transformation of transient response of the structure using FFT command of MATLAB gives frequency response of the signal as shown in figure (6.3). As can be seen in figure (6.3), first three natural frequencies are 18.59 , 44.57 and 105.45 hertz respectively. To generate transient response of individual modes, equation of motion (3.55) has been transformed into modal equation of motion by performing orthonormal modal transformation. Upon simplification, decoupled equations of motion of individual modes

are obtained in equation (3.63). Equation (3.63) is solved in time domain to generate transient response of individual modes.

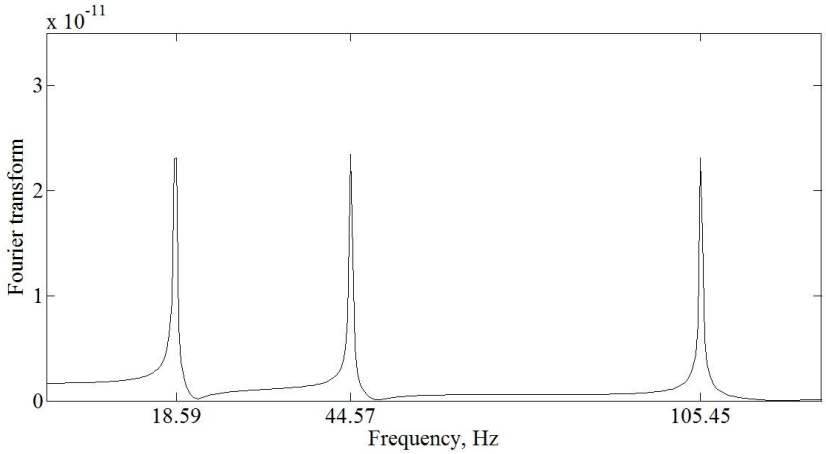

Figure 6. 3 First three natural frequencies of plate

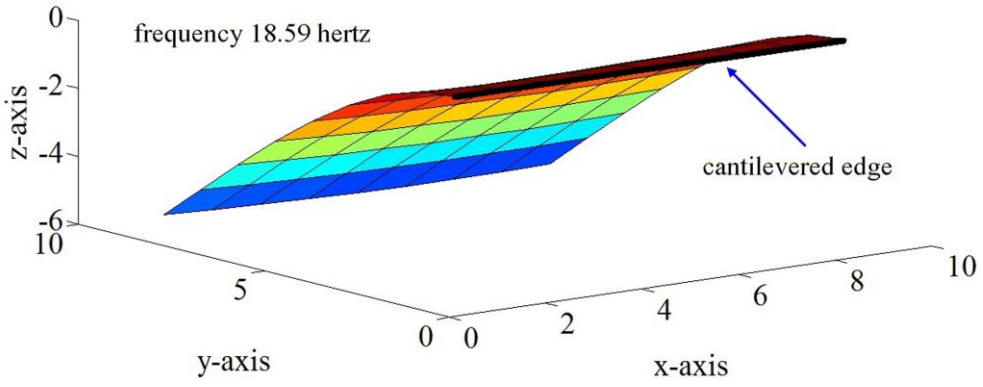

Figure 6. 4 Mode shape of first mode

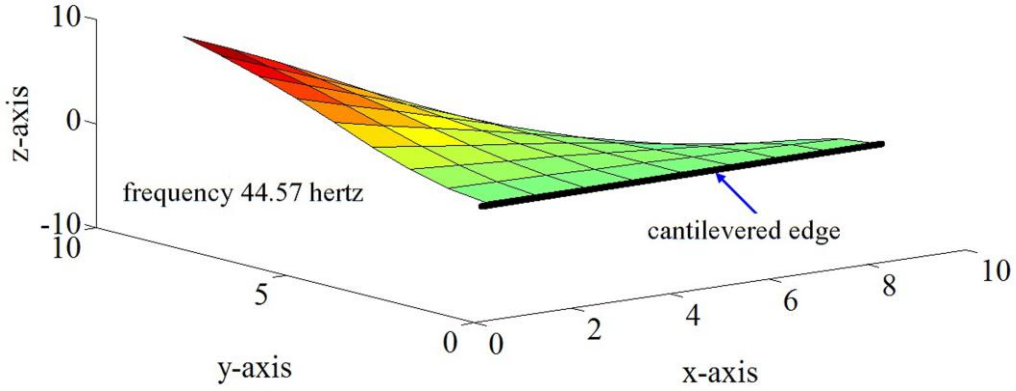

Figure 6. 5 Mode shape of second mode

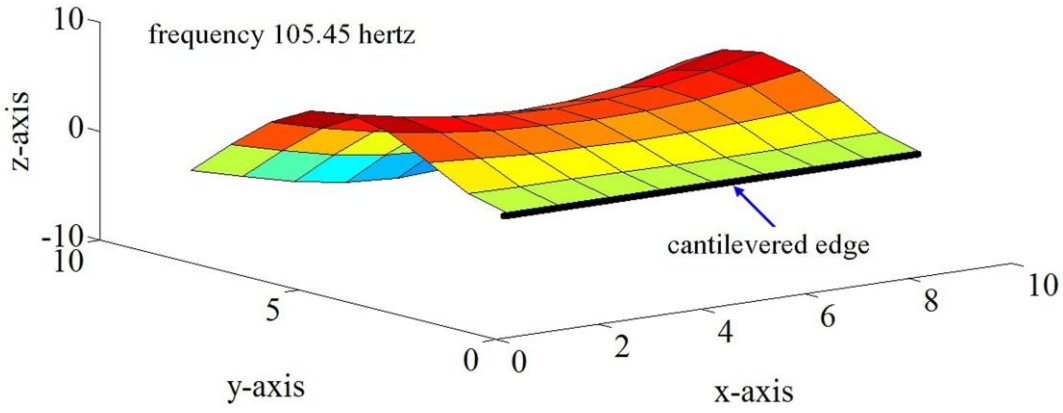

Figure 6. 6 Mode shape of third mode

Mode shapes of first three modes of cantilevered plate are shown in figures (6.4), (6.5) & (6.6). Figures (6.7), (6.8) & (6.9) show time response of first three modal displacments when edge opposite to cantilevered edge of the plate is disturbed by 2 mm. Time domain signals given in figures (6.7), (6.8) & (6.9) are taken as reference signals for first, second & third modal displacements respectively.

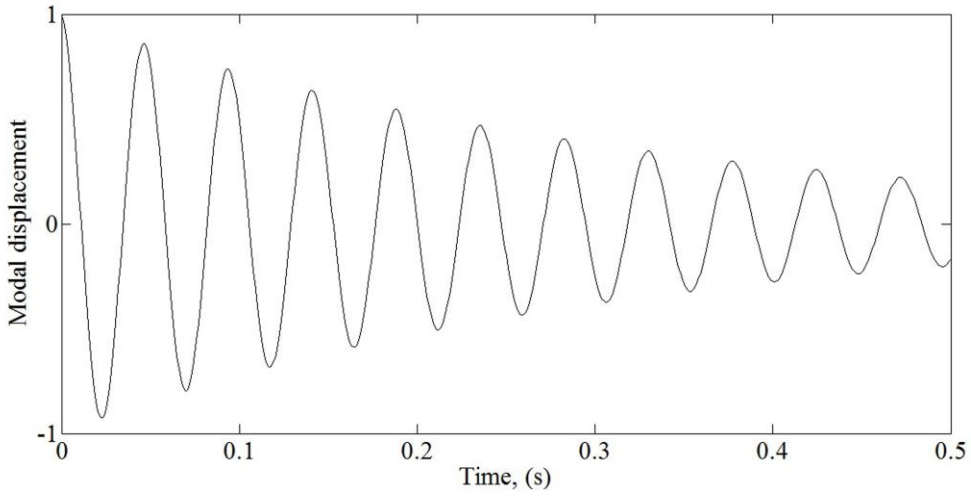

Figure 6. 7 Reference signal for first mode

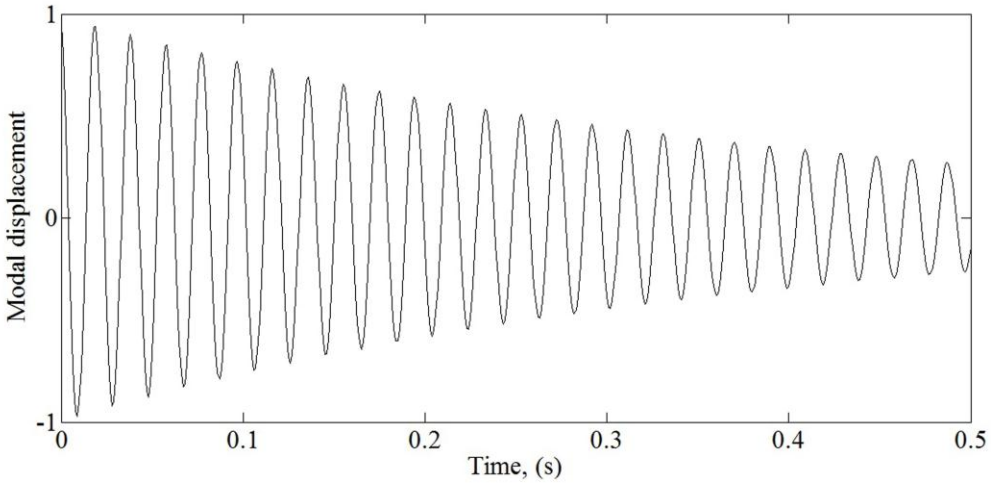

Figure 6. 8 Reference signals for second mode

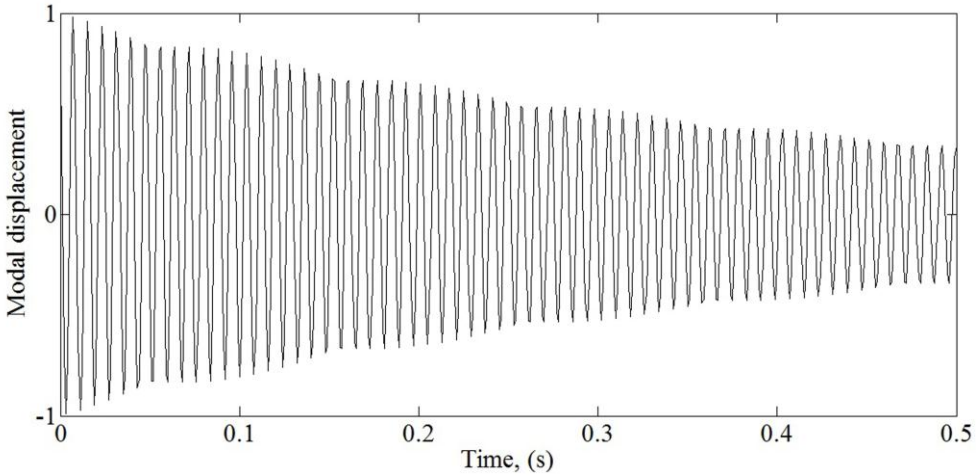

Figure 6. 9 Reference signals for third mode

Figures (6.10), (6.11) & (6.12) show time response of first three modal displacements of the plate when plate is controlled using optimal tracking control with references as displayed in figure (6.7), (6.8) & (6.9). It can be observed that with presented optimal tracking control, first three vibration modes of the plate can be made to simultaneously track reference signals effectively. Performance index used in the optimal tracking control is as expressed in equation (5.5). Weighting matrices F and Q matrices are taken as:

$$F = \begin{bmatrix} 1 & 0 & 0 & 0 & 0 & 0 \\ 0 & 1 & 0 & 0 & 0 & 0 \\ 0 & 0 & 1 & 0 & 0 & 0 \\ 0 & 0 & 0 & 1 & 0 & 0 \\ 0 & 0 & 0 & 0 & 1 & 0 \\ 0 & 0 & 0 & 0 & 0 & 1 \end{bmatrix}, \qquad Q = \begin{bmatrix} 1e^6 & 0 & 0 & 0 & 0 & 0 \\ 0 & 1e^6 & 0 & 0 & 0 & 0 \\ 0 & 0 & 1e^6 & 0 & 0 & 0 \\ 0 & 0 & 0 & 0 & 0 & 0 \\ 0 & 0 & 0 & 0 & 0 & 0 \\ 0 & 0 & 0 & 0 & 0 & 0 \end{bmatrix}$$

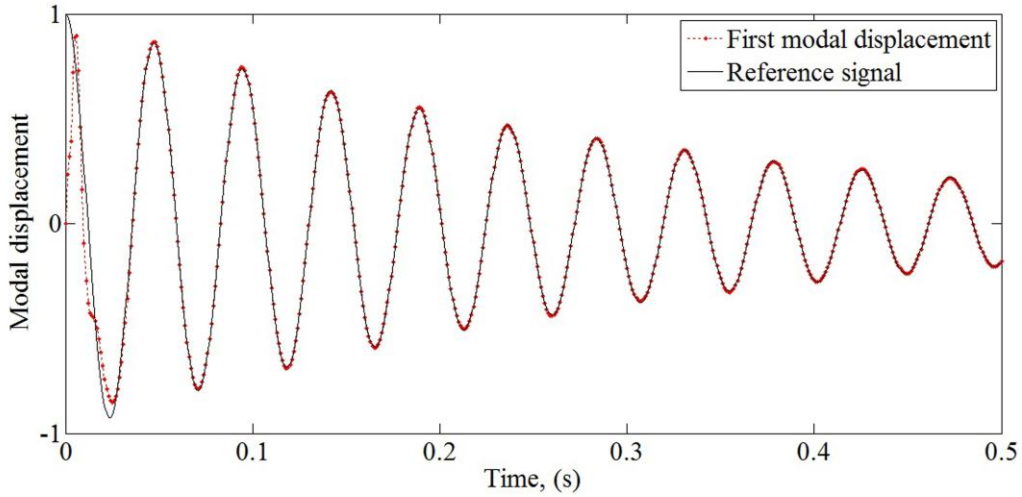

Figure 6. 10 Time response of first modal displacement

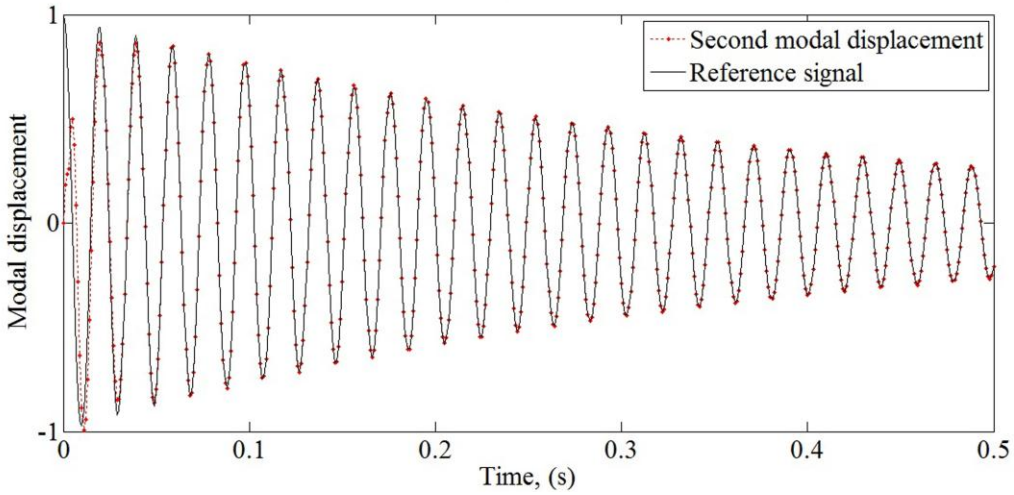

Figure 6. 11 Time response of second modal displacement

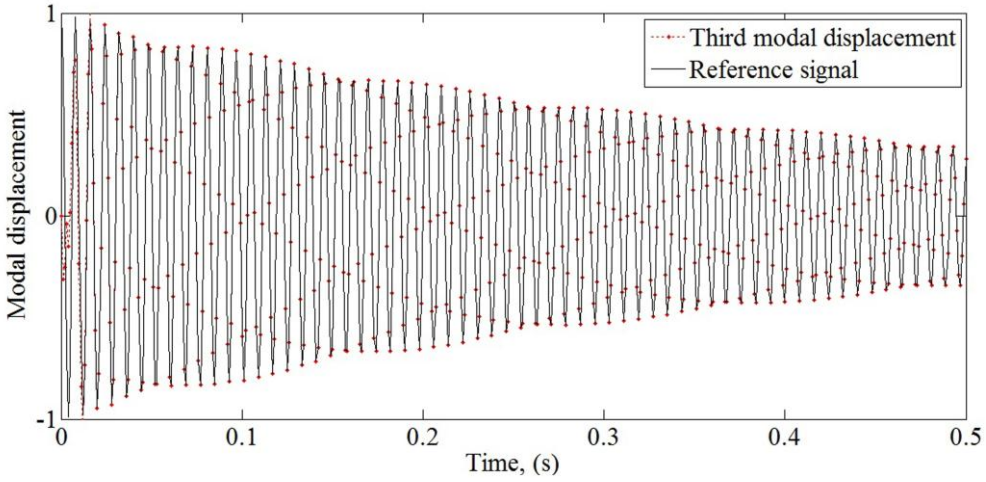

Figure 6. 12 Time response of third modal displacement

Figure (6.13) shows time response of impulse control voltage of duration 0.03 seconds and height 200 volts applied on piezoelectric actuator to excite/disturb the system.

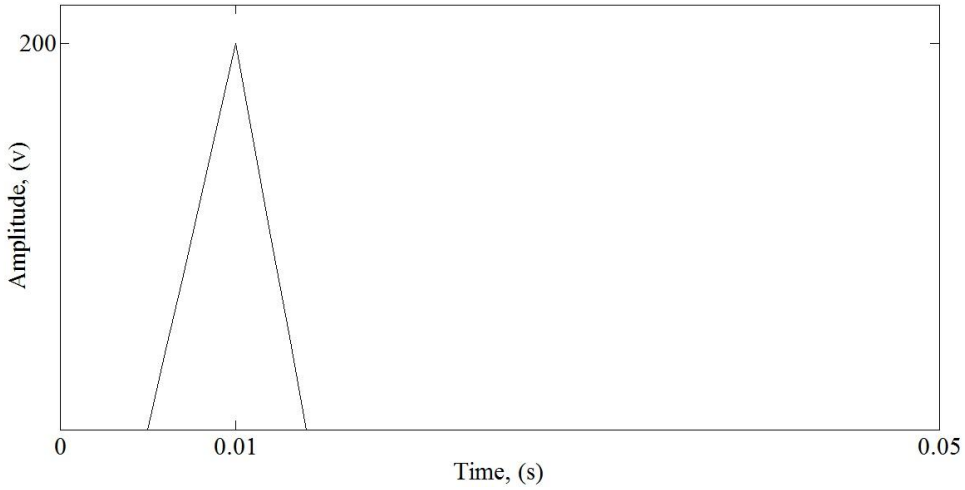

Figure 6. 13 Time response of impulse voltage used to excite the structure

Reference signals shown in figures (6.14) to (6.16) are modal displacements obtained by applying impulse control voltage shown in figure (6.13) of duration 0.03 seconds and height 200 volts on actuator patch. It can be observed in figures (6.14) to (6.16) that reference signals corresponding to impulse excitation are also being effectively tracked by the optimal controller.

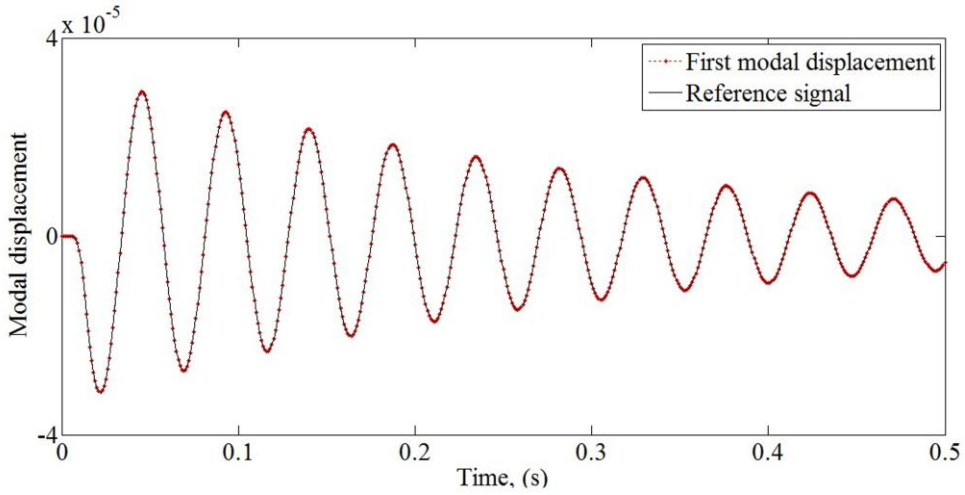

Figure 6. 14 Time response of first modal displacement

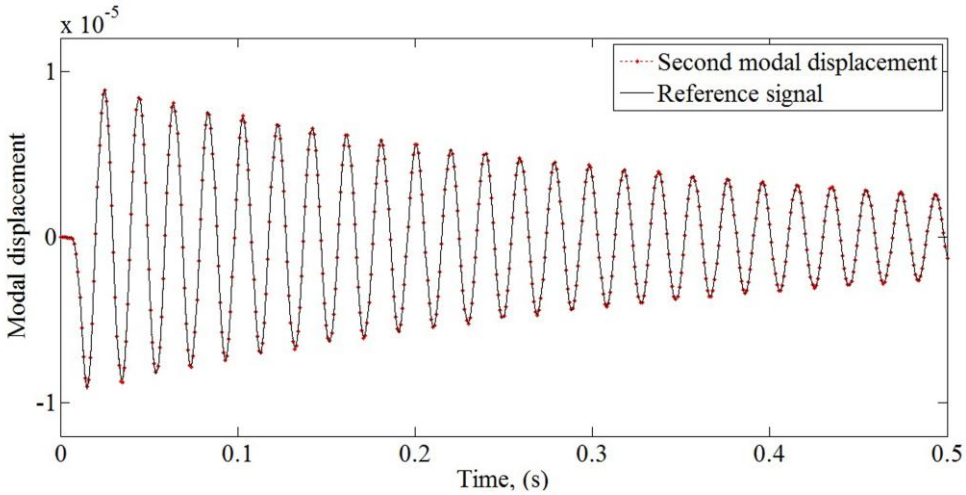

Figure 6. 15 Time response of second modal displacement

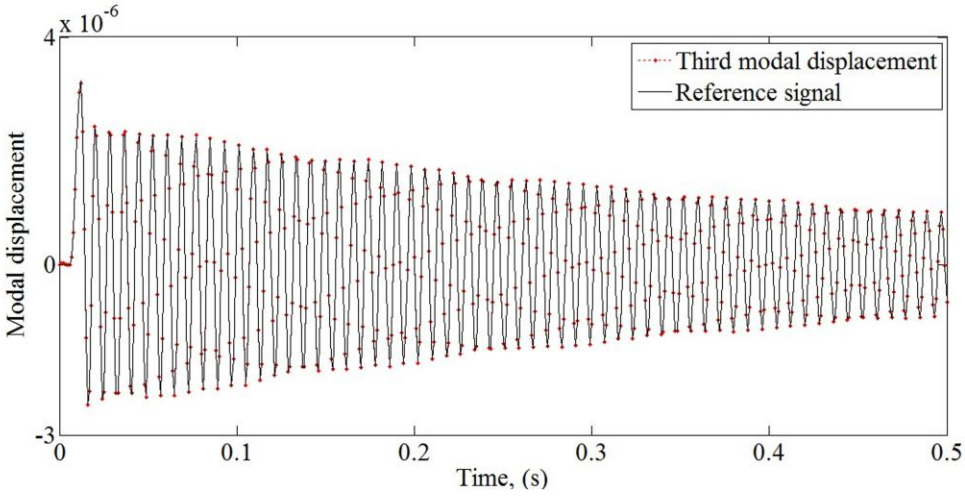

Figure 6. 16 Time response of third modal displacement

6.3. LQT control based suppression of vibrations

In all AVC works, control has been used as a regulator to suppress structural vibrations to mean position i.e. zero position. If desired transient decay curves are not given as reference then performance of an active structure may appreciably change if due to some reason there is gain/loss of mass or/and stiffness or/and damping of an active structure. This is a clear gap in the field of AVC which authors feel should be plugged to make performance of smart structures robust. There is a dire need to have an AVC strategy that enables the designer of active structures to design tailor-made transient response of a smart structure. This work will be of interest when it is desired to maintain a particular level of vibrations during journey of vibration decay so as to meet some functional requirement. There is no work in which optimal control has been used to simultaneously achieve desired transient decay curves of individual modes of vibration. In this section, optimal tracking control has been used to suppress structural vibrations of a cantilevered plate with desired transient decay curves of individual modes. AVC technique presented in this section allows to exercise more control on response of an active structure and allows to precisely dictate the vibratory response of a structure. The LQT technique is applied on a plate structure when it is disturbed and results are discussed in this section. First of all, zero references are given to all the states of the state-space model while applying LQT control law. In this simulation, test plate is disturbed by vertically displacing edge of plate opposite to the cantilevered edge of plate by 2 mm and then LQT controller is applied on smart plate system. All the three modes of vibration are given mean position i.e. zero references for tracking. Figures (6.17), (6.18) & (6.19) present time response of uncontrolled as well as controlled signals of first three modes. It can be observed that all the modes are getting suppressed and approaching towards the mean position.

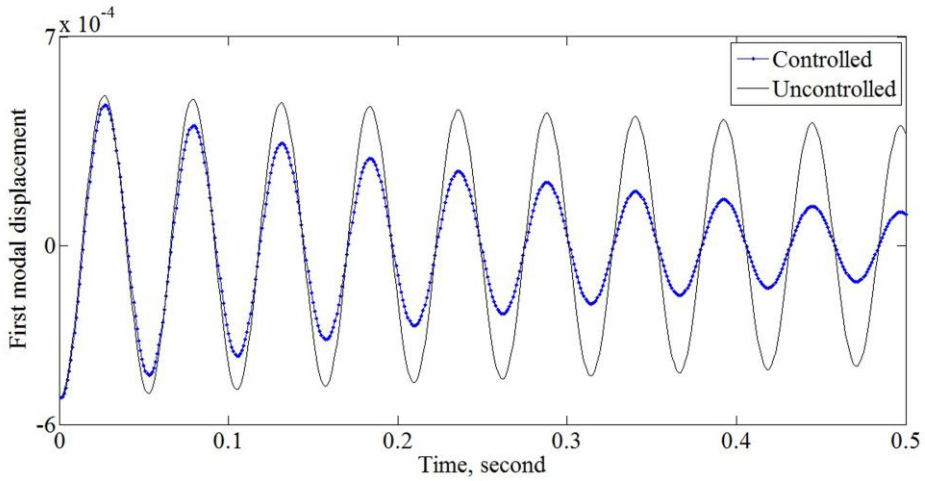

Figure 6. 17 Time response of uncontrolled, reference and LQT controlled vibration signal

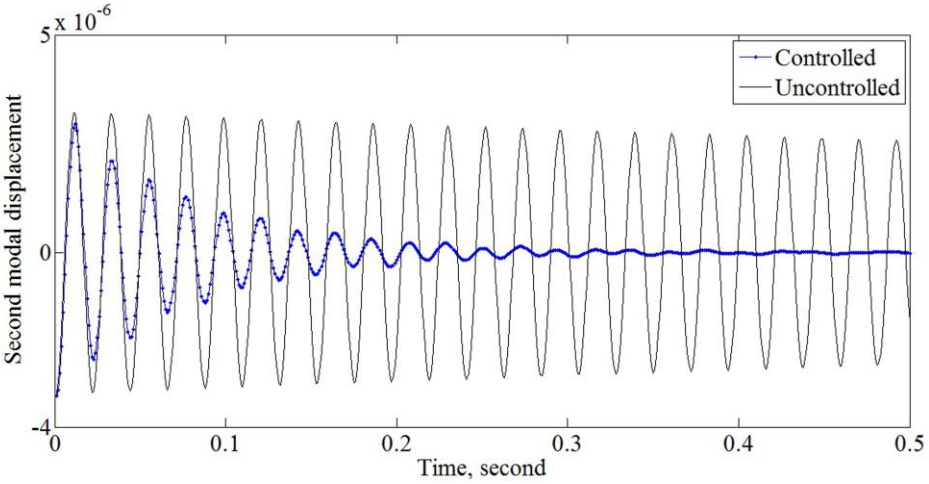

Figure 6. 18 Time response of uncontrolled, reference and LQT controlled vibration signal

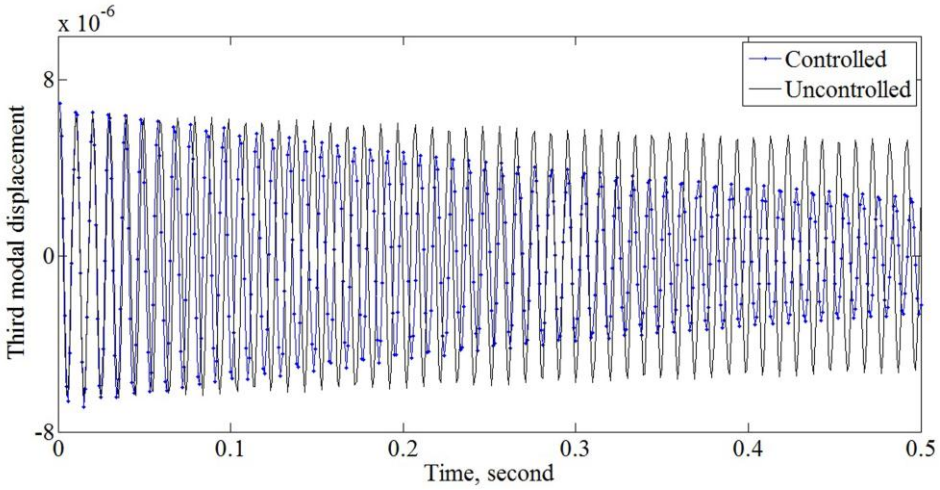

Figure 6. 19 Time response of uncontrolled, reference and LQT controlled vibration signal

Next, reference signals for first three modes of vibration are obtained by multiplying time responses of uncontrolled modal displacements shown in figures (6.20), (6.21) & (6.22) by a factor of 0.5. Figures (6.20) to (6.22) presents performance of LQT controller when these new time-varying references are taken. It can be clearly observed in figures (6.20) to (6.22) that all the three modes of vibration have successfully and impressively tracked their respective time-varying reference signals.

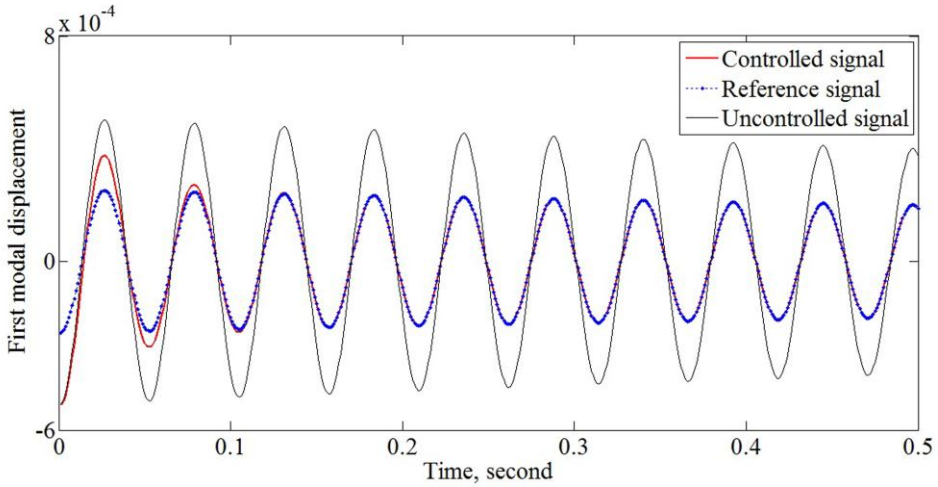

Figure 6. 20 Time response of uncontrolled, reference and LQT controlled vibration signal

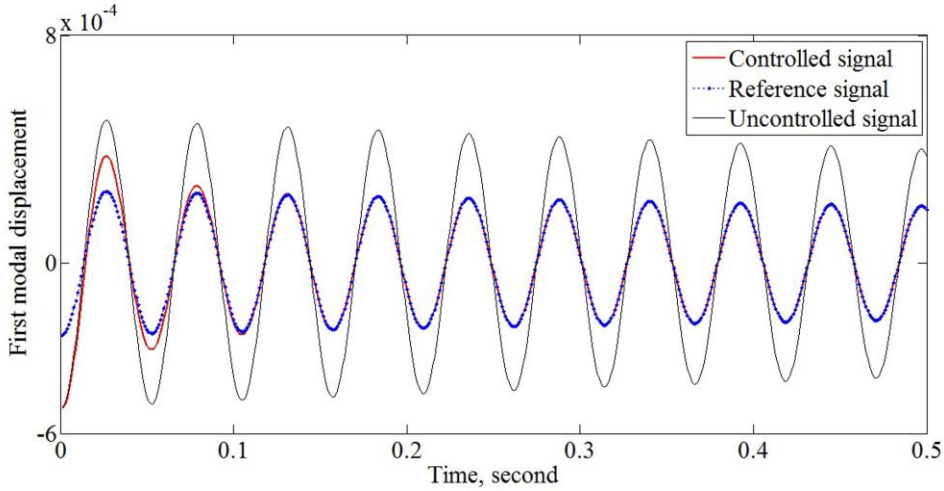

Figure 6. 21 Time response of uncontrolled, reference and LQT controlled vibration signal

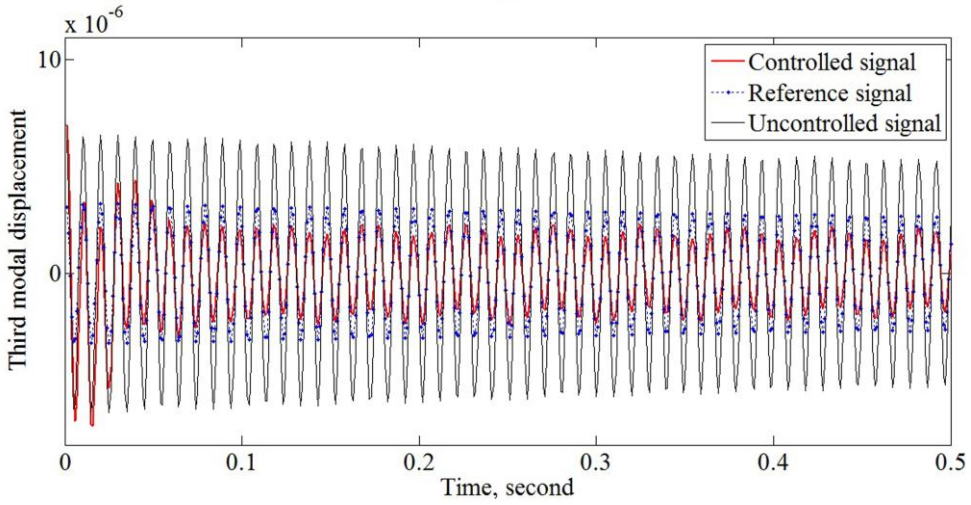

Figure 6. 22 Time response of uncontrolled, reference and LQT controlled vibration signal

Corresponding control voltages applied on the actuator is shown in figure (6.23). It can be confidently concluded that usage of LQT control in AVC application, allows to precisely dictate transient decay curves of individual modes simultaneously.

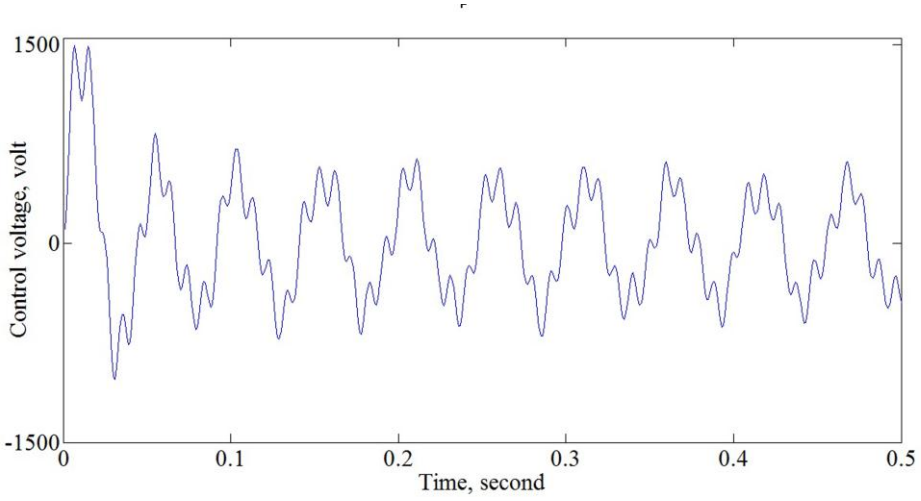

Figure 6. 23 Time response of control voltages applied on actuator

6.4. Conclusions

In this chapter two simulation tests are performed:

i) A cantilevered plate instrumented with piezoelectric sensor and actuator is taken as a test product. Reference decay curves are selected for first, second and third modal displacements. It is found that optimal tracking control is capable to simultaneously track these three reference signals simultaneously. Presented optimal controller is also able to efficiently track reference modal displacements obtained by exciting the plate by typical impulse signal. It is therefore concluded that optimal control strategy discussed in this work can be exploited to vibrate a test-product in the laboratory in the manner it would have vibrated in the real world.

ii) Optimal tracking control is employed to track zero references. Using this technique one can successfully suppress multiple modes of vibration simultaneously in a structure using a simple procedure. Active vibration control is also successfully performed when non-zero transient decay curves are taken as references while applying LQT control. Present work presents a simple strategy to dictate transient response of individual modes of vibration while suppressing structural vibrations of an active structure.

Chapter 7: Generating desired vibrations in a cantilevered plate: experiments

7.1. Introduction

The area of vibration control is evolving rapidly primarily due to the high demand of low weight automotive structures. To achieve desired vibration characteristics of the product in field, extensive vibration testing is required of the product in the laboratory. In previous chapter theoretical results show that the technique based on LQT control proposed for generating desired vibrations, can be applied on a test structure successfully. In this chapter, the proposed technique is verified through experiments. Labview software is used to interface the smart structure with a desktop computer. Kalman filter is used to estimate the states of the intelligent system. In following sections, experimental set-up, experimental results and conclusions are discussed.

7.2. Experimental set-up

Experimental set-up for this work is shown in figures (7.1) and (7.3). Experimental setup consists of:

1. Cantilevered plate instrumneted with piezoelectric patches
2. Signal conditioner
3. Band pass filter
4. PXI amplifier
5. CRO
6. SCB-68 connector box
7. Function generator
8. Labview software
9. Host computer

A cantilevered plate of mild-steel with average thickness of 0.51 mm and dimension of $160\ mm \times 160\ mm$ is selected as a test structure. The plate is divided into 64 equal

elements. The optimal place for sensor and actuator over plate is found using hit & trial method and is found to be near the cantilevered edge. A PZT-5H piezoelectric patch is selected as sensor/actuator and pasted carefully on element number 11 as sensor and element number 14 as actuator, using a thin layer of epoxy adhesive as shown in figure (7.1). Copper wires are soldered to both sides of piezoelectric patches in which negative side is pasted on the base plate. State space model of the test structure, Kalman filter & optimal tracking control algorithm are programmed in Labview software and loaded on to the PXI-system. Gains of the optimal controller and Kalman filter coefficients are calculated off-line for usage in Labview program.

As reported in chapter on simulation, we wish to track first three vibration modes experimentally. As shown in figures (7.1) and (7.3), sensor signal is amplified by signal conditioner. In order to have first three modes of the plate, the sensor signal is passed through a band-pass filter, which is set in the range of $0-120\,Hz$ to remove disturbances. The vibration signal enters PXI-controller through SCB-68 connector box. The output signal from the controller passes through SCB-68 connector and after amplification is applied on the actuator.

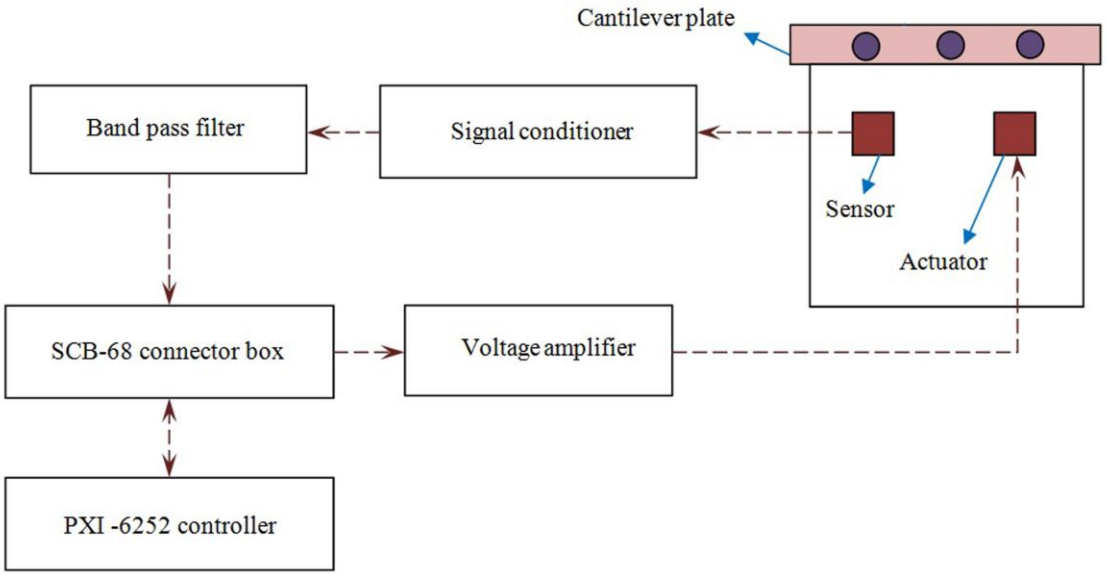

Figure 7.1 Block diagram of the experimental set up

7.3. Experimentation and experimental results

In current experiments, for generating desired vibrations, following steps are carried out:

- Excite test structure and store first three modes of vibration of the structure as estimated by the Kalman observer.
- Take first three modes of vibration of the structure as references and compute optimal control voltages using optimal tracking control.
- Apply optimal control voltages, as calculated above, on the actuator.

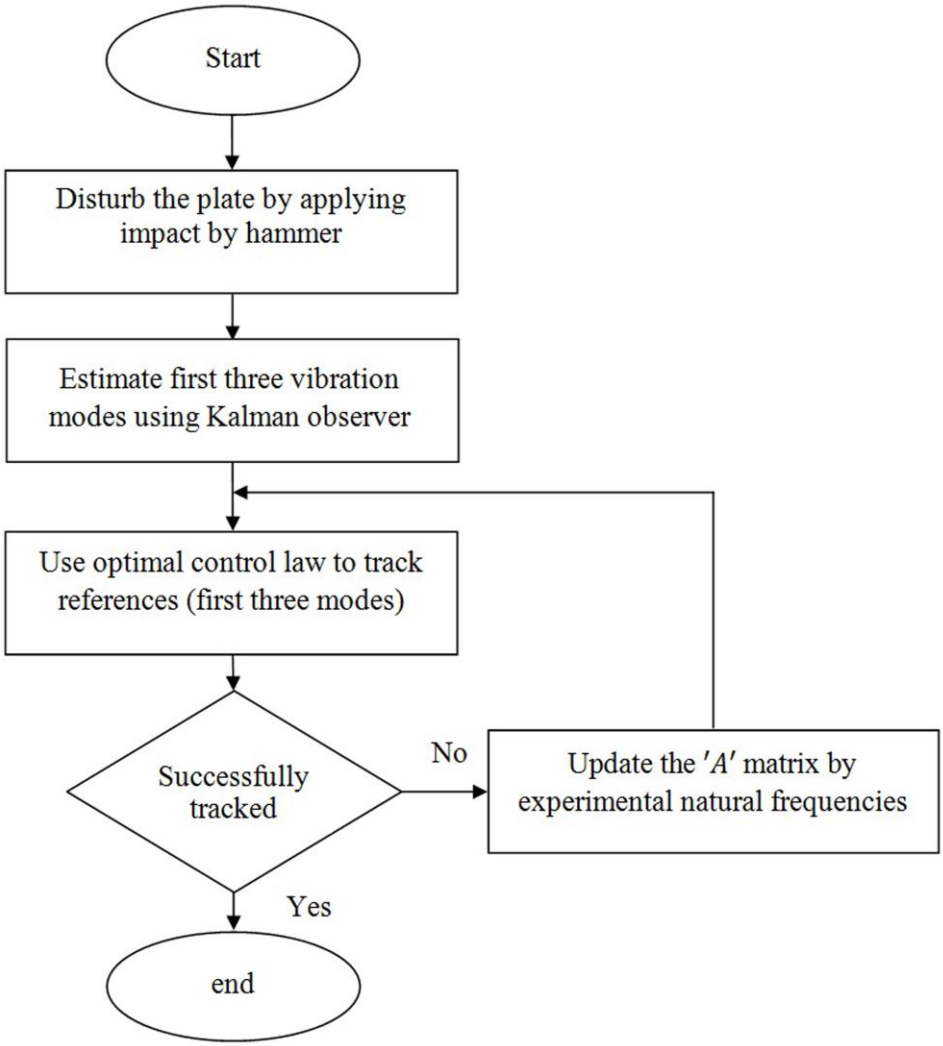

Figure 7.2 Flowchart of experimental work

All three modes of vibration get sufficiently excited simultaneously if the structure is hit by an impact hammer near the cantilevered edge around element number 12. The experimental and theoretical frequencies of the plate are tabulated in table (7.1).

Table 7.1 First three natural frequencies of plate

	experimental values (Hertz)	theoretical values (Hertz)
first mode	18.67	18.59
second mode	43.33	44.57
third mode	93	105.45

Vibration modes may not get tracked due to differences between theoretical and experimental frequencies, as shown in table (7.1). These differences may be due to error in material properties, variations in the thickness of the plate, poor modelling of boundary conditions etc. To resolve this problem, during experimentation, system matrix $'A'$ being used in the Kalman observer is updated using experimental natural frequencies. In figure (7.2) steps of proposed technique are shown through a flowchart.

Figure 7.3 Experimental set up

First of all controller is asked to simultaneously track only first two modes of vibration of the cantilevered plate. Figures (7.4) & (7.5) show time responses of reference as well as experimental modal displacements of first two modes when controller is tracking only first two modes simultaneously. Experimental time responses of first two modes is very effectively tracking corresponding references.

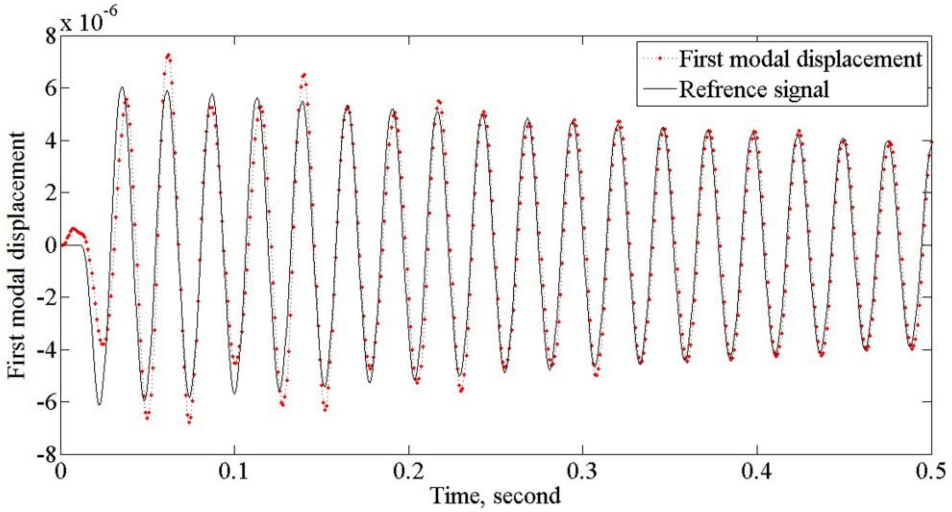

Figure 7.4 Experimental time response of first modal displacement

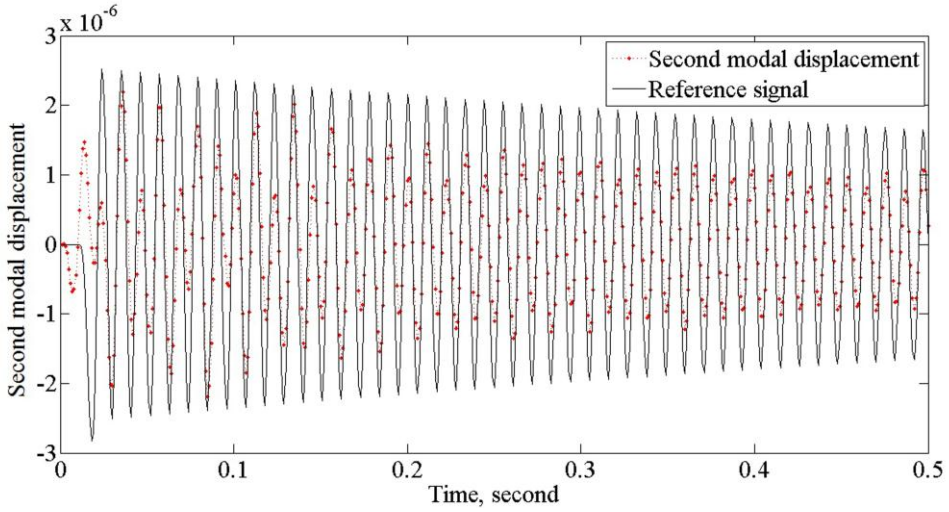

Figure 7.5 Experimental time response of second modal displacement

Next, controller is asked to simultaneously track first three modes of vibration of the cantilevered plate. Figures (7.6), (7.7) & (7.8) show time responses of theoretical as well

as experimental modal displacements. Experimental time responses of first three modes effectively track references. There is some mismatch between references and controlled time responses. This can be attributed to spillover effects that occur due to usage of truncated mathematical model. From figures (7.4) to (7.9) it can be seen that tracking is better when controller is tracking first two modes simultaneously compared to case when controller is tracking first three modes simultaneously. This is attributed to the fact that control effort is shared among only two modes in former case as against three modes latter case.

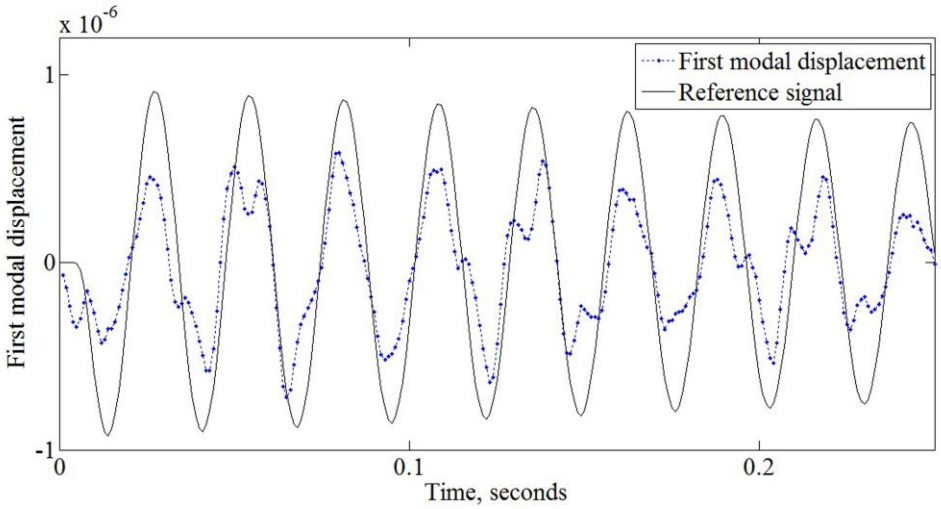

Figure 7.6 Experimental time response of (a) first modal displacement

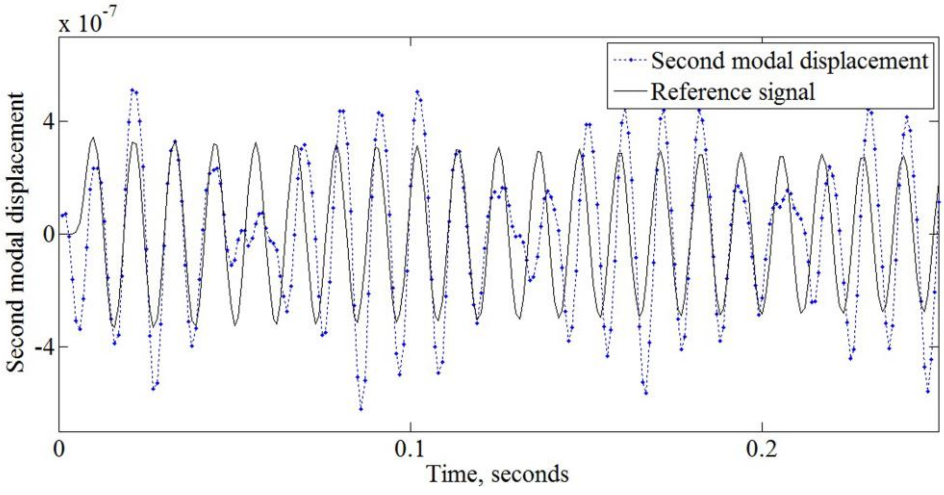

Figure 7.7 Experimental time response of second modal displacement

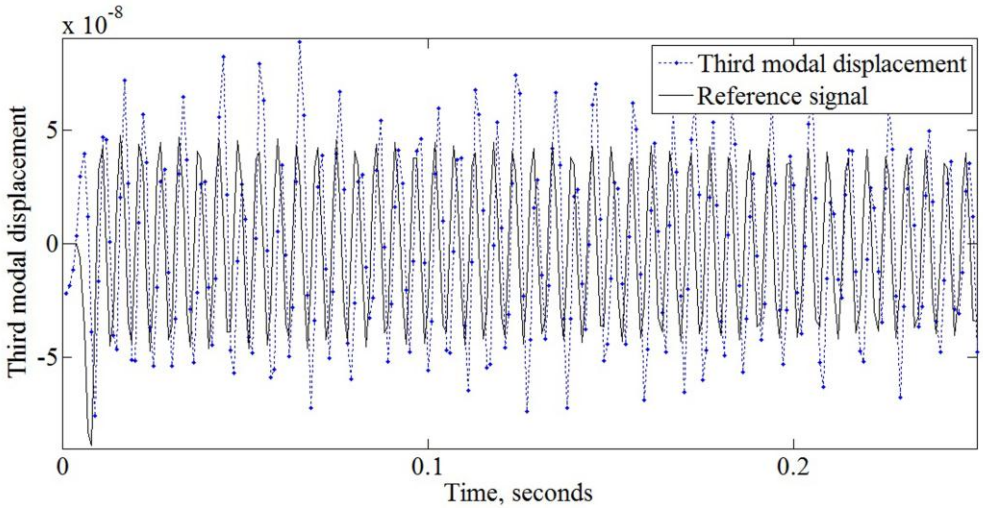

Figure 7.8 Experimental time response of third modal displacement

Experimental control voltages applied on the piezoelectric actuator patch are shown in figure 7.9, when controller is asked to control first three modes of vibration simultaneously .

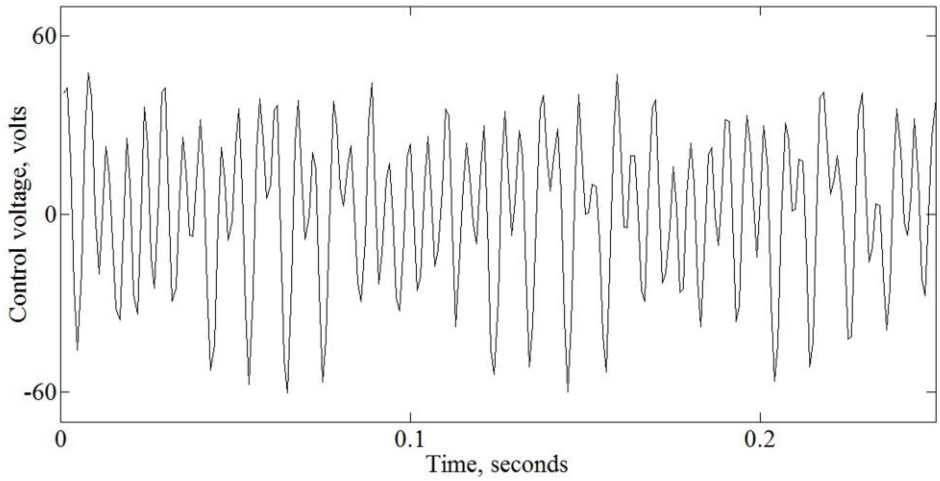

Figure 7.9 Experimental time response of control voltage

7.4. Conclusions

It is important to verify the performance of an intelligent structure through vibration tests in a laboratory before using it practically. It is desired to vibrate the test structure during testing phase exactly as it would actually vibrate during deployment in the field.

Present work has successfully demonstrated a technique to vibrate a test-structure in a laboratory in the manner it may vibrate in field. For this purpose, optimal tracking control has been successfully applied on state-space model of the test plate structure using Labview software and PXI system. This technique can be further exploited to generate desired vibrations even in complex shaped structures

.

Chapter 8: Conclusions and future scope

8.1. Conclusions

It is desirable to verify the performance of a structure through vibration tests in a laboratory before using it practically in field. This work presents a novel technique for vibration testing of a typical mechanical structure. In order to obtain this objective, in present work, a cantilevered plate instrumented with piezoelectric sensor and actuator is taken as a test product. Reference decay curves are selected for first, second and third modal displacements. Simulation and experimental results prove that using an optimal tracking control, desired vibration signals can be excited in a structure. To do this, mathematical model of the system is derived using finite element theory and then it is converted into a state-space model. An optimal tracking control is then employed to track desired references. Presented strategy can be used to do dynamic vibration testing of a product by forcing the product to experience same transient vibrations that it is expected to experience in field

Main contributions of this work are:

i. A novel technique is proposed for vibration testing of a structure in a laboratory. A cantilevered plate is made to experience transient vibrations which it may be expected to encounter in a real environment. This technique can also be used to dictate desired transient decay curves.
ii. First three modal displacements of the rectangular plate have been tracked simultaneously using optimal tracking controller both theoretically as well as experimentally.
iii. Presented strategy can be commercially used for dynamic vibration testing of a product.

8.2. Future scope

Probable directions for future work can be:

i. Illustration of vibration testing technique on actual products.

ii. Commercialization of vibration testing technique demonstrated in this thesis.

References

[1] A.C. Pisoni, C. Santolini, D.E. Hauf & S. Dubowsky, "Displacements in a vibrating body by strain gage measurements", *Inproceedings-Spie the International Society for Optical Engineering*, pp.119-119, 1995.

[2] Z.C. Qiu, X.M. Zhang, Y.C. Wang & Z.W. Wu, "Active vibration control of a flexible beam using a non-collocated acceleration sensor and piezoelectric patch actuator", *Journal of Sound and Vibration*, Vol. 326(3), pp.438-55, 2009.

[3] G. Carusoa, S. Galeanib & L. Meninib, "Active vibration control of an elastic plate using multiple piezoelectric sensors and actuators", *Simulation Modelling Practice and Theory*, Vol.11(5–6), pp.403–419, 2003.

[4] S. Kapuria & M.Y.Yasin, "Active vibration suppression of multilayered plates integrated with piezoelectric fiber reinforced composites using an efficient finite element model", *Journal of Sound and Vibration*, Vol.329, pp.3247-3265, 2010.

[5] Y. Gu, RL Clark, C.R. Fuller & A.C. Zander, "Experiments on active control of plate vibration using piezoelectric actuators and polyvinylidene fluoride (PVDF) modal sensors" *Journal of vibration and acoustics*. Vol.116 (3), pp.303-8, 1994.

[6] S. Shinya "Vibration control of a structure using Magneto-Rheological grease damper Front", *Mech. Eng.*, Vol. 8, pp.261-267, 2013.

[7] J. Li & W. A. Gruver, "An Electrorheological Fluid damper for Vibration Control", *IEEE* conference ICRA, pp.2476-2481, 1998.

[8] B. K. Sarabi, M. Sharma & D. Kaur, "Simulation of a New Technique for Vibration Tests, Based Upon Active Vibration Control", *IETE journal of research (Taylor & Francis),* Vol. 63(3), 2016.

[9] R.C. Simões, V. Steffen, J. Der Hagopian & J. Mahfoud, "Modal active vibration control of a rotor using piezoelectric stack actuators", Journal of Vibration and Control, Vol.13 (1), pp. 45-64, 2007.

[10] K. Khorshidi, E. Rezaei, A. A. Ghadimi, & M. Pagoli, "Active vibration control of circular plates coupled with piezoelectric layers excited by plane sound wave", *Applied Mathematical Modelling,* Vol. 39(3), pp.1217-1228, 2015.

[11] D. J. Inman, "Vibration with control", West Sessex: John Wiley & Sons, 2006.

[12] E. Crawley & de Luis J, "Use of piezoelectric actuators as elements of intelligent structures", *Journal AIAA,* Vol.25, pp. 1373-85, 1987.

[13] S. Raja, G. Prathap & PK. Sinha, "Active vibration control of composite sandwich beams with piezoelectric extension-bending and shear actuators", *Smart Materials and Structures,* Vol. 11(1), pp.63.

[14] K. Chandrashekhara & R. Tanneti, "Thermally induced vibration suppression of laminated plates with piezoelectric sensors and actuators", *Smart Mater. Struct.,* Vol.4, pp.281-290, 1995.

[15] B. K. Sarabi, M. Sharma & D. Kaur, "Techniques for creating mathematical model of structures for active vibration control*", IEEE conference RAECS_2014,* pp.1-6, 2014.

[16] T. Bailey & J.E. Ubbard "Distributed piezoelectric-polymer active vibration control of a cantilever beam", *Journal of Guidance, Control, and Dynamics*. Vol.8(5), pp.605-11, 1985.

[17] H. S. Tzou & C.I. Tseng, "Distributed piezoelectric sensor/actuator design for dynamic measurment/control of distributed parameter system: a piezoelectric finite element approach", *Journal of Sound and Vibration,* Vol.138, pp.17-34, 1990.

[18] B. P. Baillargeon & S. S. Vel, "Exact solution for the vibration and active damping of composite plates with piezoelectric shear actuators", *Journal of Sound and Vibration*, Vol.282, pp.781–804, 2005.

[19] B. K. Sarabi, D. K. Maghade & G. M. Malwatkar, "An empirical data driven based control loop performance assessment of multi-variate systems", *IEEE confreance INDICON*, pp. 70-74, 2012.

[20] B. Gou, "Optimal Placement of PMUs by Integer Linear Programming", *IEEE Transactions on Power Systems*, Vol. 23(3), pp.1525-1526, 2008.

[21] N.Theodorakatos, N. Manousakis & G. Korres, "Optimal Placement of Phasor Measurement Units with Linear and Non-linear Models", *Electric Power Components and Systems*, Vol.43(4), pp.357–373, 2015.

[22] B.Gou,"Generalized Integer Linear Programming Formulation for Optimal PMU Placement", *IEEE Transactions On Power Systems*, Vol. 23(3), 2008.

[23] M. Powell, "The convergence of variable metric methods for nonlinearly constrained optimization calculations," *Nonlinear Programming 3 Academic Press*, 1978.

[24] G. N. Vanderplaats, "An efficient feasible directions algorithm for design synthesis", *AIAA Journal*, Vol. 22(11), pp. 1633-1640, 1984.

[25] R. Dutta, R. Ganguli, & V.Mani, "Swarm intelligence algorithms for integrated optimization of piezoelectric actuator and sensor placement and feedback gains", *Smart Materials and Structures*, Vol.20(10), pp.105018, 2011.

[26] J. M. S. Moita, V. M. F. Correia, , P. G. Martins, C. M. M. Soares, & C. A. M. Soares, "Optimal design in vibration control of adaptive structures using a simulated annealing algorithm", *Composite Structures*, Vol.75(1), pp.79-87, 2006.

[27] J.H.Han & I. Lee, "Optimal placement of piezoelectric sensors and actuators for vibration control of a composite plate using genetic algorithms", *Smart Material and Structure*, Vol. 8 pp. 257-267, 1999.

[28] R. K. Kincaid & E. L. Keith, "Reactive Tabu Search and Sensor Selection in Active Structural Acoustic Control Problems", *Journal of Heuristics*, Vol.4, pp.199-220, 1998.

[29] L.Chen, C. Lin & C.Wang, "Dynamic stability analysis and control of a composite beam with piezoelectric layers, *Composite Structures*, Vol.56, pp.97–109, 2002.

[30] M.A. Beijen, J. van Dijk, W.B.J. Hakvoort & M.F. Heertjes, "Self-tuning Feedforward Control for Active Vibration Isolation of Precision Machines", *The International Federation of Automatic Preprints of the 19th World Congress Control Cape Town, South Africa*, 2014.

[31] M. M Jovanovic, A.M Simonovic, N. D Zoric, N. S Luki, S. N Stupar & S.S Ilic, "Experimental studies on active vibration control of a smart composite beam using a PID controller", *Smart Mater. Struct*, Vol.22, 2013.

[32] S.X.Xu & T.S.Koko, "Finite element analysis and design of actively controlled piezoelectric smart structures", *Finite Elements in Analysis and Design*, Vol.40 (3), pp.241–262, 2004.

[33] X.J.Dong, G.Meng & J.C.Peng, "Vibration control of piezoelectric smart structures based on system identification technique: numerical imulation and

experimental study", *Journal of Sound and Vibration*, Vol.297(3–5), pp.680–693, 2006.

[34] Y.R. Hu & A. Ng, "Active robust vibration control of flexible structures", *Journal of Sound and Vibration*, Vol.288(1–2), pp. 43–56, 2005.

[35] H. Gu, G. Song, "Active Vibration Suppression of a Smart Flexible Beam Using a Sliding Mode Based Controller", *Journal of Vibration and Control*, Vol.13, pp.1095-1107, 2007.

[36] Liu Lei & Wang Benli, "Multi Objective Robust Active Vibration Control for Flexure Jointed Struts of Stewart Platforms via H∞ and μ Synthesis", *Chinese Journal of Aeronautics*, Vol. 21(2), pp. 125–133, 2008.

[37] M. Sharma, S.P. Singh & B. L. Sachdeva, "Modal control of a plate using a fuzzy logic controllerSmart Materials and Structures", *Smart Materials and Structures*, 16(4), 2007.

[38] C. W. Chen, K. Yeh, W.L. Chiang, C.Y. Chen & D. J. Wu, Modeling, "H∞ Control and Stability Analysis for Structural Systems Using Takagi-Sugeno Fuzzy Model", *Journal of Vibration and Control*, Vol.13, pp.1519-1534, 2007.

[39] J. Tuma & J. Skutova, "Simulation of active vibration control of the cantilever beam" *In Carpathian Control Conference (ICCC)*, Vol. 13, pp. 744-747, 2012.

[40] M. A. Elshafei & F. Alraiess, "Modeling and analysis of smart piezoelectric beams using simple higher order shear deformation theory", *Smart Mater. Struct*. Vol 22 (3), pp.035006, 2013.

[41] H. Abramovich & A. Livshits, "flexural vibrations of piezolaminated slender beams: a balanced model", *Journal of Vibration and Control*, 8, pp.1105, 2012.

[42] W.S.P. Heyliger, "A discrete-layer model of laminated hygrothermopiezoelectric plates", *Mechanics of Composite Materials and Structures*, Vol.7(1), pp.79-104, 2000.

[43] O. Barannyk, B.J. Buckham & P. Oshkai, "On the methodology for evaluation of dynamic effects of a surface bonded piezoelectric patch for active vibration control", *Journal of Vibration and Control*, Vol.19(2), pp.204-218, 2013.

[44] S. Kapuria & M. Y. Yasin, "Active vibration control of piezoelectric laminated beams with electroded actuators and sensors using an efficient finite

element involving an electric node", *Smart Mater. Struct*. Vol. 19(4), pp.045019, 2010.

[45] D. Biswas & M. C. Ray, "Active constrained layer damping of geometrically nonlinear vibration of rotating composite beams using 1-3 piezoelectric composite", *Int Journal Mech Mater*, Vol. 9, pp.83-104, 2013.

[46] M.R. Kermani, R.V. Patel & M. Moallem, "April. Active vibration control in a macro-manipulator using strengthened piezoelectric actuators", *International Conference on Robotics and Automation*, Vol. 5, pp. 5232-5237, 2004.

[47] M.S. Saad, H. Jamaluddin & I.Z.M. Darus, "April. Active vibration control of flexible beam system using proportional control scheme in finite difference simulation platform", *International Conference on Modeling, Simulation and Applied Optimization*, Vol. 4, pp. 1-5, 2011.

[48] J. Wei, Z. Qiu, J. Han & Y. Wang, "Experimental comparison research on active vibration control for flexible piezoelectric manipulator using fuzzy controller", *J Intell Robot Syst* , Vol. 59, pp.31-56, 2010.

[49] H. Hongsheng, W. Juan, Q. Suxiang, & Q. Linfang, "August. Active vibration control by piezoelectric self-sensing actuator for beam under a moving mass" *International Conference on Electronic Measurement and Instruments*, Vol.8, pp. 3-600, 2007.

[50] D. Bandopadhya, & J.Njuguna, "A study on the effects of Kalman filter on performance of IPMC-based active vibration control scheme*" IEEE Transactions on Control Systems Technology* , Vol.18(6), pp.1315-1324, 2010.

[51] M. S. Rechdaoui, L. Azrar, S. Belouettar, E. M. Daya & M. P. Ferry, Active vibration Control of piezoelectric sandwich beam at large amplitudes, Mechanics of Advanced Materials and Structures, (2009),16,98-109.

[52] J. C. Collinger, W. C. Messner & J. A. Wickert, "An investigation into using magnetically attached piezoelectric elements for vibration control", *Journal of Vibration and Acoustics*, Vol.134(6), pp.061008, 2012.

[53] Z.Qiu, J. Han, X. Zhang, Y. Wang & Z. Wu, "Active vibration control of a flexible beam using a non-collocated acceleration sensor and piezoelectric patch actuator", *Journal of Sound and Vibration*, Vol.326(3), pp.438-455, 2009.

[54] K.Takagi, H. Sato & M. Saigo, "Vibration control of a smart structure embedded with metal-core piezoelectric fibers", *Advanced Composite Materials*, Vol.15(4), pp. 403-417, 2012.

[55] Y. M. Huang & S.C. Hung, "Analytical study of an active piezoelectric absorber on vibration attenuation of a plate", *Journal of Sound and Vibration*, Vol. 330(3), pp. 361-373, 2011.

[56] S. E. Miller, H. Abramovich & Y. Oshman, "Active distributed vibration control of anisotropic piezoelectric laminated plates", *Journal of Sound And Vibration*, Vol.183(5), pp.797-817, 1995.

[57] Y.H. Zhang, & X.N. Zhang. "Active vibration control of a stiffened plate with a piezoelectric actuator". *Symposium on Piezoelectricity, Acoustic Waves and Device Applications*, pp. 264-268, 2011.

[58] V. Gupta, M. Sharma, N. Thakur & S P Singh, "Active vibration control of a smart plate using a piezoelectric sensor–actuator pair at elevated temperatures", *Smart Mater. Struct.* Vol.20, pp.105023, 2011.

[59] Z. Qiu, X. Zhang, H. Wu, H.Zhang, "Optimal placement and active vibration control for piezoelectric smart flexible cantilever plate", *Journal of Sound and Vibration*, Vol.301(3), pp. 521-543, 2007.

[60] J. H. Han & I. Lee, "Analysis of composite plates with piezoelectric actuators for vibration control using layerwise displacement theory", *Composites Part B: Engineering* , Vol. 29(5), pp.621-632, 1998.

[61] P. A. Jadhav & K. M. Bajoria, "Free and forced vibration control of piezoelectric FGM plate subjected to electro-mechanical loading", *Smart Mater. Struct*. Vol.22(6), 2013.

[62] A.B.H.I.J.I.T. Mukherjee, S.P. Joshi & A. Ganguli, "Active vibration control of piezolaminated stiffened plates", *Composite structures*, Vol.55(4), pp.435-443, 2002.

[63] S. Kapuria & M.Y. Yasin, "Active vibration suppression of multilayered plates integrated with piezoelectric fiber reinforced composites using an efficient finite element model", *Journal of Sound and Vibration*, Vol.329(16), pp.3247-3265, 2010.

[64] H. S. Tzou & C. I. Tseng, "distributed piezoelectric sensor/actuator design for dynamic measurement/control of distributed parameter systems: a piezoelectric finite element approach", *Journal of Sound and Vibration*, Vol.138(1), pp.17-34, 1990.

[65] B.P. Baillargeon & S.S. Vel, "Exact solution for the vibration and active damping of composite plates with piezoelectric shear actuators", *Journal of Sound and Vibration*, Vol.282(3), pp.781-8042005, 2005.

[66] Y. Luo, S. Xie & X. Zhang, "The actuated performance of multi-layer piezoelectric actuator in active vibration control of honeycomb sandwich panel", *Journal of Sound and Vibration*, Vol.317(3), pp.496–513, 2008.

[67] M. K. Kwak & D. H. Yang, "Active vibration control of a ring-stiffened cylindrical shell in contact with unbounded external fluid and subjected to harmonic disturbance by piezoelectric sensor and actuator", *Journal of Sound and* Vibration, Vol.332(20), pp.4775-4797, 2013.

[68] B. Robu, L. Baudouin & C. Prieur, "Active vibration control of a fluid/plate system using a pole placement controller*"*, *International Journal of Control*, Vol.85(6), pp.684-694, 2012.

[69] T. Kamada, T. Fujita, T. Hatayama,T. Arikabe, N. Murai, S. Aizawa & K. Tohyama, "Active vibration control of frame structures with smart structures using piezoelectric actuators", *Smart Mater. Struct*. Vol.6, pp.448-456, 1997.

[70] A. Bahrami, M. Tafaoli-Masoule & M.N. Bahrami, "Active vibration control of piezoelectric Stewart platform based on fuzzy control", *International Journal of Material and Mechanical Engineering*, Vol.2(1), pp.17-22, 2013.

[71] A. H. Daraji & J. M. Hale, "Active vibration reduction of a flexible structure bonded with optimised piezoelectric pairs using half and quarter chromosomes in genetic algorithms", *Journal of Physics* Vol.382, 2012.

[72] J. H. Han & I. Lee, "Optimal placement of piezoelectric sensors and actuators for vibration control of a composite plate using genetic algorithms", *Smart Mater. Struct*. Vol.8, pp.257–267, 1999.

[73] K. R. Kumar & S. Narayanan, "Active vibration control of beams with optimal placement of piezoelectric sensor/actuator pairs", *Smart Mater. Struct.* Vol.17(5), 2008.

[74] Y.Y. Li & L. Cheng, "Controllability assessment of plate-like structures with uncertainties under piezoelectric actuation", *Journal of Sound and vibration*, Vol.280(1), pp.379-400, 2005.

[75] E.Pereira, I. M.Díaz, E. J. Hudson, & P. Reynolds, "Optimal control-based methodology for active vibration control of pedestrian structures", *Engineering Structures*, Vol.80, pp.153-162, 2014.

[76] S. S. Rao, T. S. Pan & V.B. Venkayya, "Optimal placement of actuators in actively controlled structures using genetic algorithms", *AIAA journal*, Vol. 29.6, pp.942-943, 1991.

[77] V. Gupta, M. Sharma & N. Thakur, "Optimization criteria for optimal placement of piezoelectric sensors and actuators on a smart structure: a technical review", *Journal of Intelligent Material Systems and Structures*, Vol.21(12), pp.1227-1243, 2010.

[78] A.R. Damanpack, M. Bodaghi, M.M. Aghdam & M. Shakeri, "Active control of geometrically non-linear transient response of sandwich beams with a flexible core using piezoelectric patches", *Composite Structures*, Vol.100, pp.517–531, 2010.

[79] S. Raja, P.K.Sinha, G. Prathap & D. Dwarakanathan, "Thermally induced vibration control of composite plates and shells with piezoelectric active damping", *Smart materials and structures*, Vol.13(4), pp.939, 2004.

[80] V. Gupta, M. Sharma, N. Thakur, "Active structural vibration control: Robust to temperature variations", *Mechanical Systems and Signal Processing*, Vol.33, pp.167-180, 2012.

[81] A. J. Connolly, M. Green, J. F. Chicharo & R. R. Bitmead, "The Design of LQG & H∞ Controllers for use in active Vibration Control & Narrow Band Disturbance Rejection", *Conference on Decision & Control*, Vol.34,1995.

[82] J.C. Lee & J.C. Chen, "Active control of sound radiation from a rectangular plate excited by a line moment", *Journal of sound and vibration* , Vol.220(1), 99-115, 1999.

[83] C. Shin, C. Hong & W.B. Jeong, "Active vibration control of beams using filtered-velocity feedback controllers with moment pair actuators", *Journal of Sound and Vibration*, Vol.332(12), pp.2910-2922, 2013.

[84] Z. Wang & W. Zhang, "Adaptive active vibration control for a piezoelectric stewart platform" *International Conference Intelligent Computing and Intelligent Systems*, Vol.2, pp.752-756, 2009.

[85] A. R. Tavakolpour, M. Mailah, I. Z. M. Darus & O. Tokhi, "Self-learning active vibration control of a flexible plate structure with piezoelectric actuator", *Simulation Modelling Practice and Theory* Vol.18, pp.516–532, 2010.

[86] J.M. Rodriguez-Fortun, J. Orus, J. Alfonso & J.A. Castellanos, "Nonlinear active vibration control using piezoelectric actuators", *IEEE American Control Conference*, pp. 744-749, 2010.

[87] X. J. Dong, G. Meng, J. C. Peng, "Vibration control of piezoelectric smart structures based on system identification technique: Numerical simulation and experimental study", *Journal of Sound and Vibration*, Vol.297, pp.680–693, 2006.

[88] G. L. Abreu, S. M. D. Conceição, V. Lopes Jr, M.J. Brennan, & M.T.S. Alves, "System identification and active vibration control of a flexible structure", *Journal of the Brazilian Society of Mechanical Sciences and Engineering*, 34(SPE), pp.386-392, 2012.

[89] Y.Cao, H. Sun, F. An & X. Li, "Virtual absorbed energy in decentralized velocity feedback control of a plate with piezoelectric patch actuators", *Applied Acoustics*, Vol.74, pp.909-919, 2013.

[90] C.S. Park, S. Kim, G.G. Park & J.K. Seok, "Active Mechanical Vibration Control of Rotary Compressors for Air-conditioning Systems" *Journal of Power Electronics*, Vol.12(6), pp.1003-1010, 2012.

[91] H.W. Kim, J.H. Kim, "Effect of piezoelectric damping layers on the dynamic stability of plate under a thrust", *Journal of Sound and Vibration*, Vol.284, pp. 597-612, 2005.

[92] X. Ojeda, M. Gabsi, M. Lecrivain & X. Mininger, "Noise reduction using piezoelectric active control on high speeds switched reluctance drives", *Conference onIndustry Applications*,Vol.42,. 2204-2209, 2007.

[93] M. Sharma, S. P. Singh & B. L. Sachdeva, "Modal control of a plate using a fuzzy logic Controller", *Smart Mater. Struct*. Vol.16, pp.1331-1341, 2007.

[94] N. Zoric, A. Simonovic, Z. Mitrovic, S. Stupar, "Active vibration control of smart composite beams using PSO-optimized self-tuning fuzzy logic controller", *Journal Of Theoretical and Applied Mechanics*, Vol.51(2), pp.275-286, 2013.

[95] A. D. Muradova & G. E. Stavroulakis, "Fuzzy Vibration Control of a Smart Plate", *International Journal for Computational Methods in Engineering Science and Mechanics*, Vol.4, pp.212-220, 2013.

[96] H. Li, J.Yu, C. Hilton & H. Liu, "Adaptive sliding-mode control for nonlinear active suspension vehicle systems using T–S fuzzy approach". *IEEE Transactions on Industrial Electronics*, Vol.60(8), pp.3328-3338, 2013.

[97] A. Benjeddou, "Advances in piezoelectric finite element modeling of adaptive structural elements: a survey", *Computers and Structures* , Vol.76, pp. 347-363, 2000.

[98] R. J. Allemang, "Experimental modal analysis for vibrating structures", 1983.

[99] J.M. Simoes Moita, C.M. Mota Soares & C.A. Mota Soares, "Geometrically Non-Linear Analysis of Composite Structures with Integrated Piezoelectricv Sensors and Actuators", *Composite Structures,* Vol. 57, pp. 253–261,2002.

[100] J. N. Reddy, "Theory and Analysis of Elastic Plates and Shells 2nd ed (Boca Raton, FL: CRC Press), 2007.

[101] S. K. Park, & X. L. Gao, ""Bernoulli–Euler beam model based on a modified couple stress theory", *Journal of Micromechanics and Microengineering*,Vol.16(11), pp.2355, 2006.

[102] K. Umesh, R. Ganguli, "Shape and vibration control of a smart composite plate with matrix cracks", *Smart Materials and Structures* Vol.18, pp.1–13, 2009.

[103] F. Heidary, & M. Reza Eslami "Dynamic analysis of distributed piezothermoelastic composite plate using first-order shear deformation theory", *Journal of Thermal Stresses*, Vol.27(7), pp.587-605, 2004.

[104] X. Q. Peng, K. Y. Lam & G. R. Liu "Active vibration control of composite beams with piezoelectrics: a finite element model with third order theory", *Journal of Sound and Vibration*, Vol.209(4), pp.635-650, 1998.

[105] S. A. Kulkarni & K. M. Bajoria "Finite element modeling of smart plates/shells using higher order shear deformation theory", *Composite Structures*, Vol.62(1), pp.41-50, 2003.

[106] D. H. Robbins & J. N. Reddy, "Analysis of piezoelecrically actuated beams using a layer-wise displacement theory", *Computers and Structures*, Vol.41, pp.265-279, 1991.

[107] J.N. Reddy, "On laminated composite plate with integrated sensors and actuators", *Eng. Struct.* , Vol.21, pp.568–593, 1999.

[108] M. Petyt, "Introduction to finite element vibration analysis", 2nd ed (New York: Cambridge University Press, 1990.

[109] S. Acharjee & N. Zabaras, "A non-intrusive stochastic Galerkin approach for modeling uncertainty propagation in deformation processes" Computers & structures 85.5 (2007): 244-254.

[110] K. K. Pradhan & S. Chakraverty, "Free vibration of Euler and Timoshenko functionally graded beams by Rayleigh–Ritz method", *Composites Part B: Engineering* , Vol.51, pp.175-184, 2013.

[111] K. Dovstam, "Augmented Hooke's law in frequency domain. A three dimensional, material damping formulation", *International Journal of Solids and Structures*, Vol.32(19), pp.2835-2852, 1995.

[112] H. S. Tzou & R. V. Howard, "A piezothermoelastic shell theory applied to active structure ASME Transactions", *Journal of Vibration and Acoustics*, Vol.116, pp.295-302, 1994.

[113] S. Sharma, R. Vig & N. Kumar, "Active vibration control: considering effect of electric field on coefficients of PZT patches", *Smart Structures and Systems*, Vol.16(6), pp.1091-1105, 2015.

[114] W. Smittakorn & P. R. Heyliger, "A discrete-layer model of laminated hygrothermopiezoelectric plates, *Mechanics of Composite Materials and Structures* Vol.7, pp.79-104, 2000.

[115] S. J. Dyke, et al. "Modeling and control of magnetorheological dampers for seismic response reduction", *Smart materials and structures*, Vol.5(5), pp.565, 1996.

[116] S. Y. Chen, "Kalman filter for robot vision: a survey", *IEEE Transactions on Industrial Electronics*, Vol.59(11), pp.4409-4420, 2012.

[117] G. Welch & G. Bishop, "An introduction to the Kalman filter", Department of Computer Science, University of North Carolina, 2006.

[118] I. Rhodes, "A tutorial introduction to estimation and filtering", *IEEE Transactions on Automatic Control*, Vol.16(6), pp.688-706, 1971.

[119] D. Simon, "Kalman filtering with state constraints: a survey of linear and nonlinear algorithms", *IET Control Theory & Applications*, Vol.4(8), pp.1303-1318, 2010.

[120] D. G. Luenberger, "Observing the state of a linear system", *IEEE transactions on military electronics*, Vol.8(2), pp.74-80, 1964.

[121] D. Luenberger, "Observers for multivariable systems", *IEEE Transactions on Automatic Control* , Vol.11(2), pp.190-197, 1966.

[122] R. E. Kalman, "A new approach to linear filtering and prediction problems", *Journal of basic Engineering*, Vol.82(1), pp.35-45, 1960.

[123] R. E. Kalman, "Contributions to the theory of optimal control", Bol. Soc. Mat. Mexicana, Vol.5(2), pp.102-119, 1960.

[124] R. S. Bucy, "Optimal filtering for correlated noise", *Journal of Mathematical Analysis and Applications*, Vol.20(1), pp.1-8, 1967.

[125] R. E. Kalman & R. S. Bucy, " New results in linear filtering and prediction theory", *Journal of basic engineering*, Vol.83(1), pp.95-108, 1961.

[126] L.S. Pontryagin, V.G. Boltyanskii, R.V..Gamkrelidze & E.F. Mishchenko. The Mathematical Theory of optimal Processes, Wiley-Interscience, New York, NK, 1962.

[127] J.C. Doyle, K.Glover, P.P. Khargonekar & B.A. Francis, "State-space soulotions to standard H_2 and H_∞ control problems", *IEEE Transactions on Automatic Control*, Vol. 34, pp. 831-847, 1989.

[128] D. S. Naidu, "Optimal Control Systems. CRC Press", 2003, Chennai Micro Print (P) Ltd., Chennai- 600029.